

Norwegian University
of Life Sciences

Master's Thesis 2024 60 ECTS

Faculty of Environmental Sciences and Natural Resource Management

Understanding dissolved organic matter dynamics in a boreal forest lake: stratification, oxygen conditions, and DOM variability

Eline Elvira Brouwer

MSc Ecology

Acknowledgments

This master's thesis marks the final step toward accomplishing my degree in Ecology at the Norwegian University of Life Sciences. I would express my gratitude to my supervisors Gunnhild Riise and Thomas Rohrlack. Their help throughout the sampling period, laboratory analysis, and overall guidance has contributed massively to this thesis. I am grateful for all the things I learned during this journey.

Also, many thanks to the laboratory technicians who performed part of the analysis for this thesis. Finally, I would like to express my gratitude to my beloved family, friends, and my dog Daya. Their support and presence have helped me enormously during this one-year thesis.

Abstract

In recent decades, lakes have been observed to increase in color, also known as brownification. Increases in dissolved organic matter (DOM) concentrations in lakes, or more specifically chromophoric DOM (CDOM), caused this increase. In addition to terrestrial DOM, lakes have also been shown to release DOM from the sediment, mostly DOM that was previously bound to iron (Fe). However, only a few studies included non-terrestrial sources of DOM, and the general dynamics of DOM within lake ecosystems are still poorly understood.

This research aimed to examine the internal DOM dynamics in Lake Solbergvann, Norway, focusing on the role of stratification and prevalence of oxygen. The research objectives were to investigate (1) DOM cycling under different oxygen conditions (oxic layer, transition zone, anoxic layer) during a spring/summer period (May-September) in a lake that is subject to browning, (2) the seasonal variation in DOM molecular weight (MW) across different depth layers to provide a better understanding of environmental conditions that influence DOM dynamics. The results revealed complex DOM dynamics that do not always result in linear relationships. Nevertheless, an attempt was made to clarify these interactions to enhance the understanding of DOM dynamics.

In the oxic water layers, the DOM concentrations nearly doubled due to high runoff conditions, and the strong thermal stratification created barriers for oxygen diffusion and DOM transport to deeper layers. CDOM was strongly correlated to dissolved organic carbon (DOC). Minimal variability in DOM dynamics was observed. However, the overall MW of CDOM increased in this oxic layer due to increased DOM runoff from terrestrial sources. While maintaining stable CDOM and DOC concentrations, the transition zone – at the oxic-anoxic boundary – exhibited the greatest variability in the relationships across DOC and CDOM fractions. Mechanisms from oxic and anoxic waters concurrently govern the DOM dynamics in this zone (e.g., redox conditions, diffusion barriers, and decomposition), which likely resulted in increased diversity in their DOM dynamics. The anoxic water layers showed increasing concentrations of CDOM, DOC, Fe, manganese, and phosphorus despite major influxes from shallower waters. Stratification isolated these water layers, suggesting influences beyond dilution impacting these concentrations. The results indicate that Fe-bound DOM, identified as CDOM3 (3 – 10 kDa), was released from the sediment due to Fe reduction: This fraction made up a large proportion of the entire DOM pool, thus severely affecting DOM dynamics. Key factors restricting DOM release from the sediment were also identified; e.g., sulfate presence increases the competition for electron acceptors, thus reduces Fe reduction potential. Furthermore, pH governs various processes that impact DOM dynamics, but this study demonstrated that redox reacts may impact pH, but a low pH contribute to DOM release through enhanced Fe dissolution, thus creating feedback loops. However, more data is needed to draw strong statistically significant conclusions.

Table of Contents

<i>Acknowledgments</i>	<i>iii</i>
<i>Abstract</i>	<i>iv</i>
<i>Abbreviations</i>	<i>vii</i>
<i>Figures</i>	<i>viii</i>
<i>Tables</i>	<i>ix</i>
<i>Appendices</i>	<i>ix</i>
1. Introduction	1
1.1 Background	1
1.2 Drivers of Increased DOM	2
1.3 Molecular Weight of DOM	3
1.4 Research Aim and Objectives	5
1.5 Research Objectives	5
1.6 Overview of the Thesis	5
2. Materials and Methods	6
2.1 Study Area	6
2.2 Data Collection	7
2.2.1 Sampling Site Selection.....	7
2.2.2 Remote Electronic Sensing	7
2.2.3 On-site Measurements	8
2.2.4 Water Samples.....	8
2.2.5 Weather Data.....	9
2.3 Laboratory Analysis	9
2.3.1 Unfiltered Samples	9
2.3.2 Filtered Samples	10
2.4 Data Processing and Statistical Analysis	12
2.5 Limitations	13
3. Results	15
3.1 Weather	15
3.1 General Lake Measurements	18
3.1.1 Temperature.....	18
3.1.2 Oxygen Saturation	20
3.1.3 pH	20
3.1.4 Conductivity	21
3.1.5 Secchi depth	21
3.1.6 Phosphorus	22
3.1.7 Iron	23
3.1.8 Manganese.....	23
3.1.9 Sulfur and Sulfate	24

3.1.10	Additional measurements	24
3.2	Dissolved organic matter	25
3.2.1	Dissolved Organic Carbon	25
3.2.2	Chromophoric Dissolved Organic Matter	25
3.3	Statistical Analysis.....	28
3.3.1	Fractioning of CDOM	28
3.3.2	Principal Component Analysis and Pearson's Correlation Coefficient	30
4.	<i>Discussion</i>.....	36
4.1	Oxic conditions	36
4.1.1	Weather changes impacting DOM dynamics	36
4.1.2	Other potential drivers impacting DOM dynamics	39
4.1.3	Isolation of Oxic Waters by Thermal Stratification	39
4.1.4	Oxygen Dynamics	40
4.2	Transition Zone	41
4.2.1	A Complex Interplay of Processes as a Source for DOM Variability.....	41
4.2.2	Oxygen Dynamics	42
4.3	Anoxic conditions	43
4.3.1	Isolated anoxic waters, yet increasing DOM concentrations	43
4.3.2	Oxygen Dynamics	45
4.3.3	pH as a mediator for Fe, DOM and P release.....	47
5.	<i>Conclusion</i>.....	50
6.	<i>References</i>	52
7.	<i>Appendices</i>.....	60
	Appendix A: Raw Data of the Measurements in Lake Solbergvann.....	60
	Appendix B: Contour plots of NH₄⁺, Tot N, Al, Cl⁻, BChl, and Chl a	62
	Appendix C: Table of Molecular Weight and Signal Peak	63
	Appendix D: P-values and Pearson correlation coefficient at 0.75m	64
	Appendix E: P-values and Pearson correlation coefficient at 1.75m.....	65
	Appendix F: P-values and Pearson correlation coefficient at 2.75m.....	66
	Appendix G: P-values and Pearson correlation coefficient at 3.75m	67
	Appendix H: P-values and Pearson correlation coefficient at 4.25m	68
	Appendix I: P-values and Pearson correlation coefficient at 4.75m.....	69

Abbreviations

DOM	Dissolved Organic Matter
DOC	Dissolved Organic Carbon
CDOM	Chromophoric Dissolved Organic Carbon
CDOM1	CDOM of molecular weight < 1 kDa
CDOM2	CDOM of molecular weight 1 – 3 kDa
CDOM3	CDOM of molecular weight 3 - 10 kDa
CDOM4	CDOM of molecular weight > 10 kDa
O₂	Oxygen
P	Phosphorus
Fe	Iron
Mn	Manganese
S	Sulfur
SO₄²⁻	Sulfate
N	Nitrogen
NO₂	Nitrite
NO₃⁻	Nitrate
Al	Aluminum
Cl⁻	Chloride
BChl	Bacteriochlorophyll
Chl a	Chlorophyll a
PCA	Principal Component Analysis
PCC	Pearson Correlation Coefficient
kDa	Kilodalton
mAU	Milli Absorption Units
Nm	nanometer

Figures

Figure 1. Diagram illustrating the relationships between dissolved organic matter, dissolved organic carbon, and chromophoric dissolved organic matter.....	1
Figure 2. Location of Lake Solbergvann in Oslo, Southeast Norway.....	6
Figure 3. Sampling location within Lake Solbergvann.....	7
Figure 4. Daily mean temperature (°C) from May-September 2023.....	16
Figure 5. Daily total precipitation (mm) in May-September 2023.....	17
Figure 6. Graph of the seasonal variation in water temperature (°C).....	18
Figure 7. Contour plot of the seasonal variation in water temperature (°C).....	19
Figure 8. Contour plot of the seasonal variation in oxygen saturation (%).....	20
Figure 9. Contour plot of the seasonal variation in pH.....	20
Figure 10. Contour plot of the seasonal variation in conductivity.....	21
Figure 11. Bar plot of the seasonal variation in Secchi depth.....	21
Figure 12. Contour plot of the seasonal variation in dissolved phosphorus.....	22
Figure 13. Contour plot of the seasonal variation in total phosphorus.....	22
Figure 14. Contour plot of the seasonal variation in iron.....	23
Figure 15. Contour plot of the seasonal variation in manganese.....	23
Figure 16. Contour plot of the seasonal variation in sulfur.....	24
Figure 17. Contour plot of the seasonal variation in sulfate.....	24
Figure 18. Contour plot of the seasonal variation dissolved organic carbon.....	25
Figure 19. Contour plot of chromophoric dissolved organic matter.....	26
Figure 20. Graph CDOM molecular weight distribution.....	27
Figure 21. Bar chart of the distribution of CDOM of four molecular weight fractions.....	29
Figure 22. Principal component analysis at a depth of 0.75m (22a) and 1.75m (22b).....	31
Figure 23. Principal component analysis at a depth of 2.75m.....	32
Figure 24. Principal component analysis at a depth of 3.75m.....	33
Figure 25. Principal component analysis at a depth of 4.25m.....	34
Figure 26. Principal component analysis at a depth of 4.75m.....	35
Figure 27. Key mechanisms behind internal DOM release.....	48

Tables

Table 1. Comparison of average monthly air temperatures.....	15
Table 2. Comparison of average monthly precipitation.....	17

Appendices

Appendix A. Raw data of the measurements in Lake Solbergvann.....	60
Appendix B. Contour plots of NH_4^+ , Total N, Al, Cl ⁻ , BChl, and chlorophyll a.....	62
Appendix C. Table of Molecular Weight and Signal Peak.....	63
Appendix D. P-values and Pearson correlation coefficient at 0.75m.....	64
Appendix E. P-values and Pearson correlation coefficient at 1.75m.....	65
Appendix F. P-values and Pearson correlation coefficient at 2.75m.....	66
Appendix G. P-values and Pearson correlation coefficient at 3.75m.....	67
Appendix H. P-values and Pearson correlation coefficient at 4.25m.....	68
Appendix I. P-values and Pearson correlation coefficient at 4.75.....	69

1. Introduction

1.1 Background

Lakes are important ecosystems for carbon sequestration (Chmiel et al., 2015; Tranvik et al., 2009). In these ecosystems, both organic and inorganic substances can accumulate through influxes from terrestrial sources or benthic releases (Björnerås et al., 2017; Chmiel et al., 2015; Peter et al., 2016). Their accumulation can have considerable impacts on both biogeochemical processes in lakes, such as the behavior and transportation of organic and inorganic compounds (Knorr, 2013; O'Loughlin & Chin, 2004). Increases in organic compounds in lakes may contribute to an increase in lake color, which can be referred to as brownification (Solomon et al., 2015). Brownification is particularly prevalent in the northern hemisphere and more pronounced in Scandinavia (Solomon et al., 2015). This change in watercolor is largely attributed to increased concentrations of chromophoric dissolved organic matter (CDOM) (Fasching et al., 2014; Solomon et al., 2015; Williamson et al., 2015).

DOM is separated from particulate organic matter through filtering, usually at a pore size of 0.45µm. DOM is an overarching group that consists of organic molecules, proteins, carbohydrates, and humic acids (Figure 1) (Wetzel, 2001). DOM can stem from a wide range of sources, including external sources such as runoff of terrestrial organic matter (McKnight & Aiken, 1998), but also internal sources such as photosynthesis (Lepane et al., 2004) and leaching DOM from sediments

(Brothers et al., 2014). DOC represents the amount of carbon in the DOM-complex (Wetzel, 2001). CDOM is the fraction of DOM that absorbs solar radiation at specific wavelengths and emits it as color (Wetzel, 2001). DOC and CDOM are often highly correlated (Juetten et al., 2022). However, DOC can also contain colorless

substances, such as terpenes,

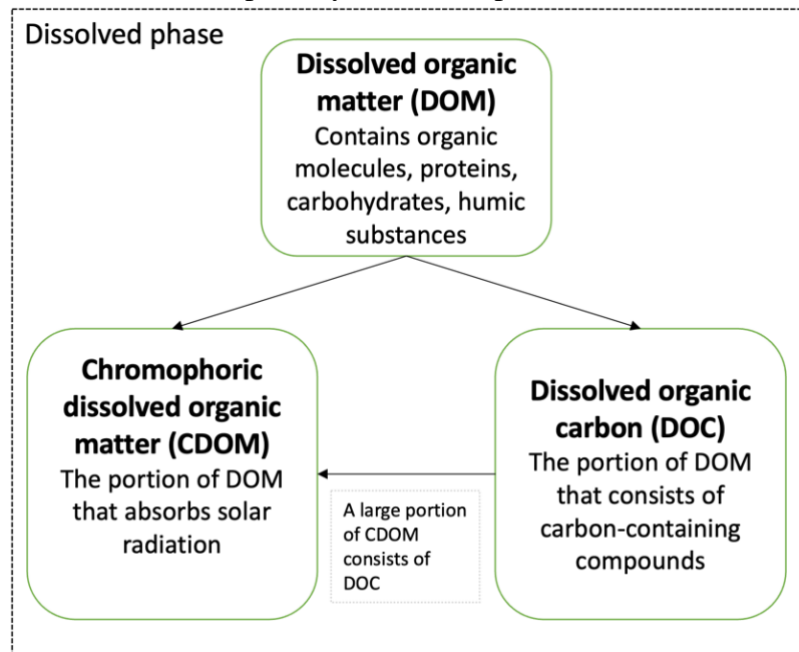


Figure 1. Diagram illustrating the relationships between dissolved organic matter (DOM), dissolved organic carbon (DOC), and chromophoric dissolved organic matter (CDOM).

that do not contribute to increasing watercolor (Rostad et al., 2011). The light-absorbing properties of CDOM influence the light attenuation in a lake. Thus, high levels of CDOM can result in water bodies that often have a darker appearance (Blanchet et al., 2022; Cooper et al., 1989). CDOM predominantly absorbs light at shorter wavelengths, depleting purple and blue colors, resulting in waters that show a red and yellow color (longer wavelengths).

1.2 Drivers of Increased DOM

Studies that seek explanations for increasing DOM concentrations in lakes are often limited to changes that affect terrestrial DOM, for example in Blanchet et al., 2022; Kritzberg et al., 2020; Woolway et al., 2020 and Monteith et al., 2007. Climatic drivers include temperature and precipitation changes, which both have increased in Scandinavia in recent decades (Lutz et al., 2024; Nikulin et al., 2011). Elevated temperatures contribute to a longer growing season, enhancing terrestrial organic carbon production (Finstad et al., 2016). Increased precipitation affects the transportation and microbial decomposition of DOM, as well as the redox reactions that impact the cycling of inorganic substances (de Wit et al., 2016; Knorr, 2013). Other external drivers often used to explain increases in DOM involve the recovery from acidification by reduced atmospheric sulfur emission (Monteith et al., 2007) and changes in land use (Juetten et al., 2022; Kritzberg, 2017).

Although brownification has far-ranging consequences for biodiversity, biogeochemical processes, and drinking water treatment (Kritzberg et al., 2020), only limited studies included the internal DOM dynamics that affect the DOM concentrations in water bodies (Brothers et al., 2014; Peter et al., 2016; Skoog & Arias-Esquivel, 2009). These studies observe that DOM can leach out of the sediment, particularly under anoxic conditions. The initial increase in DOM in water bodies could be triggered by high precipitation that increases DOM runoff from terrestrial sources (Brothers et al., 2014; Hongve et al., 2004). These elevated DOM concentrations can enhance respiration rates while restricting benthic primary production by shading (Jones, 1992; Williamson et al., 1999). Furthermore, high DOM concentrations can restrict the mixing of water layers and increase the surface water temperature while decreasing the overall average water temperature due to a steeper thermocline (Fee et al., 1996; Read & Rose, 2013). These processes collectively create or maintain anoxic conditions in the deeper water layers by depleting oxygen through DOM decomposition or impeding oxygen diffusion from surface waters (Brothers et al., 2014; Elçi, 2008).

Anoxic conditions in the hypolimnion can promote the release of phosphorus (P), DOM, and iron (Fe) from the sediment (Brothers et al., 2014; Peter et al., 2016; Skoog & Arias-Esquivel, 2009). This release is primarily driven by redox-sensitive substances, such as Fe, which is particularly relevant considering the observed increase in Fe concentrations in the northern hemisphere (Björnerås et al., 2017). Under anoxic conditions, Fe(III) is reduced to Fe(II), and this process may also release adsorbed DOM and P from the sediment (Knorr, 2013). The redox reactions of Fe are also governed by pH and the presence of substances such as nitrate, sulfate, and manganese that influence its redox potential (Björnerås et al., 2019; Grybos et al., 2009; Musolff et al., 2017). However, anoxic conditions near the sediment severely contribute to the release of Fe and DOM, making the Fe-bound DOM bioavailable for microbial degradation, consequently intensifying oxygen consumption from microorganisms (Brothers et al., 2014; Lau et al., 2024; Peter et al., 2016; Skoog & Arias-Esquivel, 2009). This process eventually results in a positive feedback loop between increased DOM concentrations and anoxia. The released DOM and Fe contribute to increased watercolor (Kritzberg & Ekström, 2012; Xiao & Riise, 2021), and DOM may eventually be mineralized, leading to increased CO₂ emissions from a lake, possibly turning the lake into a carbon source (Brothers et al., 2014; Lau et al., 2024).

1.3 Molecular Weight of DOM

Photochemical, physical, and biological processes shape the molecular properties of DOM, while these properties also influence these processes (Benner & Amon, 2015; Lanxiu et al., 2004; Lepane et al., 2004). These processes can contribute to the breakdown of DOM into smaller compounds. This change in DOM properties, for example, from higher molecular weight (MW) to lower MW compounds. This shift in MW can then impact the rate of the photochemical, physical, and biological processes, thus creating a feedback loop.

The MW of DOM and its concentration MW can be investigated using a combination of chromophoric and spectroscopic methods. First, the MW of DOM can be examined using size-exclusion chromatography, which excludes molecules based on their size (see section 2.3.2 for further details). This step provides information about the retention time of these particles, which can be converted to the MW of DOM. Then, spectroscopic methods, for example a UV spectrometer, are used to determine the concentration DOM based on its absorbance properties. However, as this involves the absorbance properties of DOM, these methods are limited to examining the portion of DOM that is visible at a specific wavelength,

also known as CDOM (Jaffé et al., 2008). Nevertheless, since CDOM is often correlated to DOC, particularly in lakes that receive most of its DOM from terrestrial sources, it can still provide valuable information about DOM dynamics (Griffin et al., 2018; Juetten et al., 2022).

It has been reported that the MW influences the binding capacity of organic matter to other substances, such as Fe (Benedetti et al., 2002; Y. Li et al., 2022), with DOM of higher MW binding stronger to Fe (Zhou et al., 2000). Furthermore, the properties of DOM can also provide information about the sources of this DOM. DOM in freshwater bodies usually stems from allochthonous sources, which are typically higher in MW than DOM which derives from the production of autochthonous material (Meili, 1992).

Previous studies have reported the MW distribution from allochthonous sources (Juetten et al., 2022; Lanxiu et al., 2004; Lepane et al., 2003; Repeta et al., 2002). In addition, other studies investigated the MW distribution of sediments in lakes (Lepane et al., 2003; O'Loughlin & Chin, 2004), but little is known about the MW distribution of DOM that includes both DOM from terrestrial sources and DOM that is being leached from the sediment and their dynamics. A recent study observed that the molecular composition of DOM showed increased heterogeneity under anoxic conditions with relatively higher MW while under oxic conditions DOM displayed less variability (Lau et al., 2024). However, differences in the onset of anoxia in the bottom waters and other environmental and regional conditions in this study can provide additional insights into the DOM dynamics.

To the best of my knowledge, this study is the first to investigate the DOM concentrations and their corresponding MW across different depths in a Norwegian lake. This lake, Lake Solbergvann, is characterized by oxic conditions on the surface layers but shows persistent anoxia in its bottom waters. Lake Solbergvann is a small and shallow lake in Norway and has been subject to browning over the last three decades (Isidorova et al., 2016). I combined electronic sensors, on-site measurements, and water samples that measured organic and inorganic substances in this study. I determined the MW of DOM and its concentrations using size-exclusion chromatography with UV spectroscopy.

1.4 Research Aim and Objectives

This research aims to examine the internal dissolved organic matter (DOM) dynamics by analyzing the role of stratification and prevalence of oxygen on DOM dynamics in Lake Solbergvann, Norway. Based on this research aim, the following research question was formulated: How do internal DOM dynamics change under a summer stratification period with different oxygen conditions?

1.5 Research Objectives

1. To investigate DOM cycling under different oxygen conditions (oxic layer, transition zone, anoxic layer) during a spring/summer period (May-September) in a lake that is subject to browning
2. To investigate the seasonal variation in DOM molecular weight across different depth layers (oxic layer, transition zone, anoxic layer) in Lake Solbergvann to provide a better understanding of environmental conditions that influence DOM dynamics

1.6 Overview of the Thesis

This thesis investigates the dynamics of DOM in Lake Solbergvann during a summer stratification period. **Chapter 2** describes this study's methods, including laboratory procedures, statistical analysis, and limitations. **Chapter 3** contains the results of this study. This chapter begins by describing external factors such as short-term (2023) and long-term (1991-2020) weather patterns. This section is followed by the measurements taken in Lake Solbergvann, including temperature, oxygen, pH, and other variables. This chapter also contains a separate section for organic matter, with the results of dissolved organic carbon described in section 3.2.1 and chromophoric dissolved organic matter in section 3.2.2. **Chapter 4** is divided into three sections: oxic conditions, a transition zone between oxic and anoxic conditions, and anoxic conditions. The discussion section begins by exploring what variables impacted the DOM concentrations and the corresponding molecular weight distribution. Then, it dives into the role of oxygen and how this governs the DOM dynamics at each layer. Finally, **Chapter 5** concludes my findings and recommendations for further research.

2. Materials and Methods

2.1 Study Area

Lake Solbergvann is a small (1.25 ha) lake located around 7 kilometers from the center of Oslo, Norway (Figure 2). The lake has a maximum depth of approximately five meters and is surrounded by a coniferous forest that covers around 90 percent of its catchment area (Xiao & Riise, 2021). It is at an elevation of 235 meters and serves as a headwater that drains into Lake Nøklevann, although the outflow is limited. The lake has an estimated water retention time of 0.5 years (Xiao & Riise, 2021). The color of Lake Solbergvann has increased significantly from 1996 to 2011, when it tripled from 60 to 192 mg Pt L⁻¹ (Isidorova et al., 2016). Increases in color can be explained by increases in total organic carbon and iron (Xiao & Riise, 2021). The lake is supposed to lack complete mixing in the spring, which strongly influences the oxygen condition, with extensive periods of anoxic conditions frequently observed (Isidorova et al., 2016).

The climate in the area is classified as a humid continental climate with a hemiboreal subtype (Climate.data.org, n.d.). This implies relatively large temperature differences occur between seasons and considerable precipitation throughout the year. Oslo has an average annual temperature of 6.9°C with 834mm of precipitation (normal period from 1991 to 2020) (Verstat.no, n.d.). The hottest average temperature is in July (17.6°C). Meanwhile, the coldest average temperature is in January (-2.3°C). The summer months in Oslo are typically the wettest months of the year, with 103mm on average in August.

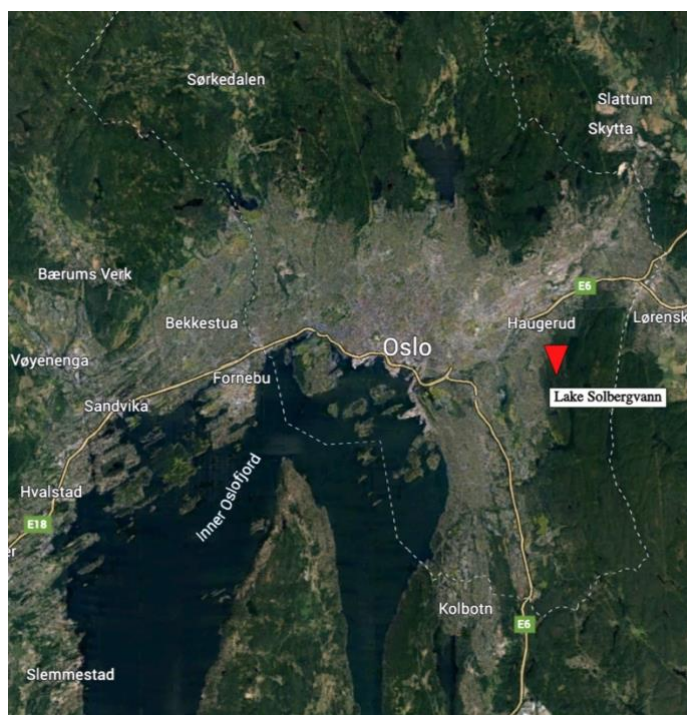


Figure 2. Location of Lake Solbergvann in Oslo, Southeast Norway.

2.2 Data Collection

2.2.1 Sampling Site Selection

The primary data collection involved three distinct methods, which are elaborated in the following section. Prior to data collection, one sampling site was selected (GPS coordinates: 59.899537°N, 10.866225°E) in Lake Solbergvann as a fixed point for my measurements (Figure 3), which exhibited a depth of approximately five meters. A rubber boat was used to access the sampling site.

A buoy was used to locate the precise spot in the lake for the repeated measurement. This buoy was attached to a rope with an eight-kilogram dumbbell secured at the opposite end of the rope. Selecting one sampling site aimed to enhance the consistency and accuracy of the measurements.

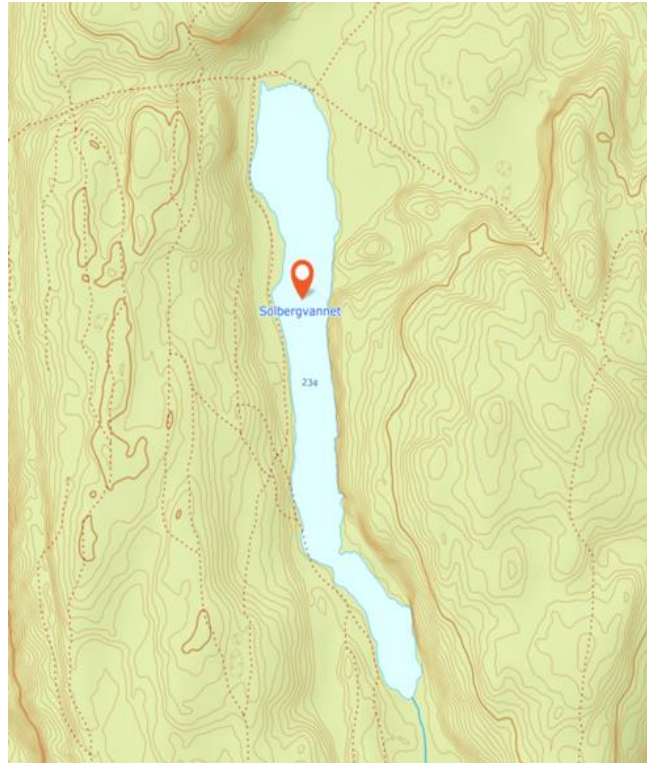


Figure 3. Sampling location within Lake Solbergvann (59.899537°N, 10.866225°E)

2.2.2 Remote Electronic Sensing

HOBO Pendant MX Temperature/Light Data Loggers were used to continuously track temperature changes at different depths in Lake Solbergvann. Six sensors were attached to a rope at one-meter intervals. These loggers are able to record the temperatures from -20° to 50°C with an accuracy of $\pm 0.5^\circ\text{C}$, recording data every 10 minutes.

The loggers were deployed in the lake on 11 May 2023. I retrieved data from the loggers on four occasions to assess their performance: 14 June, 9 August, and 9 September. The final retrieval of the data from these loggers occurred on 1 December. This timeframe was based on the seasonal relevance related to the onset of stratification and restrictions related to ice cover during the spring.

2.2.3 On-site Measurements

I conducted on-site measurements every 14 days from 31 May 2023 until 6 September 2023, resulting in eight measurements. These measurements included water transparency, water temperature, and oxygen levels.

A Secchi disk was used to measure the water transparency. The disk was slowly immersed into the water column until it disappeared, then raised until it reappeared. This process was reiterated until the precise depth at which the disk was no longer visible was established. Afterward, the length of the rope attached to the Secchi disk was measured, and this number was used to indicate water transparency.

Temperature ($^{\circ}\text{C}$), oxygen saturation (%), and oxygen concentration (mg/L) were measured using a ProODO YSI (YSI ProQuatro Multiparameter). The initial measurements only included measurements at depths of 0.5m, 1m, 1.5m, 2m, 2.5m, and 3m, as measurements deeper than the oxycline were overlooked. On two occasions, the decision was made to expand the dataset to obtain a more comprehensive data set. Firstly, measurements up to 5 meters were included with intervals of 0.5 meters starting from the second sampling day. On the third sampling day, measurements at 0.1 meters were also included. Each depth was measured twice, once by moving the instrument downward through the water column and once by moving it upward. This was carried out in order to cross-verify the measurements for consistency and accuracy of the readings.

2.2.4 Water Samples

The water samples were collected in the same period as the on-site measurements. Samples were collected at depths of 0.75m, 1.75m, 2.75m, 3.75m, 4.25m, and 4.75m. Each sampling day included samples from each depth except for samples on 4.75m. The decision was made to add samples at 4.75m to enhance data completeness. In total, 45 samples were collected.

Each sample was stored in a 500ml bottle, which had been rinsed three times prior with water from the corresponding depth to minimize contaminating the samples with other substances. The bottles were emptied of air as much as possible to minimize the offset of biological processes, thus enhancing the stability of the samples for analysis. These samples were immediately transported to the laboratory for (the preparation of) analysis.

2.2.5 Weather Data

Weather observations were also included in this study (available at <https://seklima.met.no>). The included weather elements were daily mean air temperature and daily precipitation. For 2023, observations were collected from 1 May to 30 September. Additionally, long-term trends were included for comparison, which consisted of observations from 1991 to 2020.

Two weather stations were selected. Blindern (SN18700) was selected based on the available long-term air temperature and precipitation records. Trasop (SN18180) was chosen because of its close proximity to Lake Solbergvann. This station was only used to describe the variation in local precipitation in 2023. This dataset had fourteen missing measurements for precipitation and temperature from 1991 to 2020.

2.3 Laboratory Analysis

The water samples were filtered using a glass microfiber filter of 0.8 μm to obtain a dissolved sample for analysis. The unfiltered samples were put in 10 ml vials and placed in the freezer. The filtered samples were divided into one 50 ml and two 10 ml vials and frozen for later analysis. One 10 ml vial was acidified with ultrapure HNO_3 and used for metal analysis. For each analysis, six blank samples containing only distilled water were included to measure the presence of background substances.

2.3.1 Unfiltered Samples

pH and conductivity

The pH and conductivity of the samples were measured upon arrival in the laboratory. A VWR MU 6100 H was utilized to measure the pH (on a pH scale of 1-14) and conductivity (in $\mu\text{s}/\text{cm}$) of the samples. The instrument was calibrated using two pH buffer solutions before measuring the pH to ensure accurate measurements.

Total phosphorus

The total phosphorus (Tot-P) was measured according to Norwegian standards (NS-EN 1189) by adding reagents to the samples. Five samples with known $\text{PO}_4\text{-P}$ concentrations were included for calibration. After defrosting the samples, 5 ml was taken from the samples and put into a vial. Ascorbic acid (0.2 ml) and molybdate (0.2 ml) were added to the vials. The IKA Vortex Genius 3 shaker was used to shake the samples after the addition of each of the reagents. The samples were autoclaved for 30 minutes at 121°C at 1 ATM. Ascorbic acid and molybdate

cause a reduction that leads to the formation of a color reaction, which can be quantified using a spectrophotometer. This instrument (SHIMADZU UV-1201) measured the color at a wavelength of 880 nm with a 2 cm cuvette. Tot-P concentrations were calculated using a calibration curve.

Total nitrogen

Total nitrogen (Tot-N) was measured by Norwegian standards (NS 4743). Potassium persulfate (5 ml) was added to 5 ml of the samples. The samples were autoclaved at 121°C at 1 ATM for 30 minutes. This process converts all nitrogen to nitrate (NO₃-), which was quantified using a Flow Injection Analysis (FIAstar 5000 analyzer) that runs a color reaction mediated through the conversion to nitrite (NO₂) via a reduction process. Consequently, the color reaction from NO₂ gives a red color and is inspected at a wavelength of 540 nm using a spectrophotometer. A laboratory technician carried out the ion chromatography measurements.

2.3.2 Filtered Samples

Dissolved phosphorus

The dissolved phosphorus (Dis P) measurements followed the same procedure as total phosphorus (NS-EN 1189) described in section 2.3.1, except the dissolved samples were not autoclaved. Ascorbic acid (0.2ml) and molybdate (0.2ml) were added to 5 ml samples while using the Vortex shaker after adding each substance. The spectrophotometer (SHIMADZU UV-1201) was used to measure the color after 30 minutes. The instrument was used at a wavelength of 880 nm using a two cm cuvette. The blanks contain an average of 0.0077mg/l of Dis P, which was subtracted from the results of the water samples. A calibration curve was used to calculate the Dis P concentrations.

Ammonium

Ammonium (NH₄-N) was measured according to Norwegian standards (NS 4746). The samples were pipetted into 3 ml tubes. Hypochlorite (0.5 ml) and salicylate (0.5 ml) were added to the tubes. An IKA Vortex Genius 3 shaker was used to shake after each substance was added. After one hour, the spectrophotometer (SHIMADZU UV-1201) was used at a wavelength of 655 nm using a two cm cuvette to measure the color. NH₄-N concentrations were calculated based on the calibration curve.

Nitrate, chlorite, and sulfate

Nitrate (NO_3^-), chlorite (Cl^-), and sulfate (SO_4^{2-} -S) were measured according to Norwegian standards (NS-EN ISO 10304-1) by using ion chromatography (DIONEX ICS-6000 DC). NO_3^- was below the detection limit ($5\mu\text{g}$ of NO_3^-) in all the samples. This analysis was conducted by a technician at the laboratory.

Iron, manganese, aluminum, and sulfur

Iron (Fe), manganese (Mn), aluminum (Al), and sulfur (S) were analyzed using an Inductively Coupled Plasma Mass Spectroscopy (ICP-MS) to determine their concentrations. Nitric acid (HNO_3) was added to the samples before they were analyzed. None of the samples were below the detection or quantification limit. A laboratory technician carried out this analysis.

Dissolved organic carbon

Dissolved organic carbon (DOC) was analyzed according to the Norwegian standard (NS-EN 1484) by using a total organic carbon analyzer (Shimadzu TOC-V CPN). HCL was added to the samples as a substance that removes inorganic carbon. This step was followed by burning the samples and measuring the CO_2 present using an infrared detector. A laboratory technician carried out the DOC analysis.

Chromophoric dissolved organic matter

To estimate the molecular weight distribution of the chromophoric dissolved organic matter (CDOM), size-exclusion chromatography (Thermo Scientific HPLC system 3000) with a size exclusion column SEC-300 was used. This instrument separates the molecules based on their size. The HPLC was calibrated for distribution from 200 to 50,000 Dalton using Sigma-Aldrich PEG standard ReadyCal 200-50,000 Da. Samples from 0.75m to 4.25m were included in this analysis. Unfortunately, one sample (9 August at 1.75m) was accidentally omitted from the analysis, resulting in one missing data point for CDOM.

A volume of $20\mu\text{l}$ was extracted from each sample, and 10 mM ammonium bicarbonate was added to stabilize the pH. This first step provides information regarding the retention time of the molecules. The retention time has an inverse correlation with size, where smaller compounds have a longer retention time due to their prolonged passage through the SEC column because they can access smaller pores. Twelve samples were included to establish a calibration curve between retention time and molecular weight (in Dalton).

The second step occurs after the samples have flown through the column. Then, they are pumped through a UV spectrometer at a UV absorbance of 254 nm to measure the CDOM abundance (expressed in milli Absorption Units (mAU)). This method is in line with previous studies (Grybos et al., 2009; Leenheer & Croue, 2003; Lepane et al., 2004; Perminova et al., 2003), where they often measured CDOM at a wavelength of 254 nm due to the occurrence of charge electron transfer at this wavelength. Mrkva (1983) also reported that around this wavelength, the maximum absorbance of aromatic compounds occurs. Combining these two steps provides a dataset that includes the molecular weight (in Dalton) and signal strength (mAU) for each sample. A laboratory technician also conducted this analysis.

Chlorophyll a and bacteriochlorophylls

A glass fiber filter was used to capture chlorophyll a and bacteriochlorophyll in the samples (using 200 ml of the samples). These filters were freeze-dried to remove residual water. Thereafter, acetone (3 ml) was added to stimulate pigments to dissolve into solution. The concentrations were quantified using high-performance liquid chromatography (HPLC) on an Ultimate 3000 system, with absorbance measured by a photometer across different wavelengths (400-700 nm). The retention time of the pigment and the wavelength resulted in a calibration curve that could quantify the concentration of chlorophyll a and bacteriochlorophyll present. A laboratory technician conducted the HPLC analysis.

2.4 Data Processing and Statistical Analysis

Minor corrections were needed to make comparisons between depths in this study. A minor correction was made to the temperature measurements of the HOBO loggers due to sensor misplacement after reading out the loggers. The sensors were unintentionally positioned deeper in the lake, leading to a decrease in temperature of approximately nine percent. Thus, the temperature data after 9 August was adjusted by adding nine percent to its values.

Interpolation of the oxygen levels and water temperature was necessary for statistical analysis. These measurements were taken at depth intervals of 0.5m, which did not precisely align with the depths of other measurements (taken from 0.75m at one-meter intervals). Thus, oxygen and temperature data were interpolated to match the depths of the other measurements. In addition, another interpolation involved CDOM. One CDOM measurement (9 August at 1.75m) was accidentally omitted. To estimate the Total CDOM on this day, the CDOM data at

1.75m on 9 August was interpolated. This interpolation was based on trends of CDOM at 1.75m on other sampling days and how CDOM behaved on 9 August at 0.75m.

The extensive CDOM dataset was divided into subsets for analysis using the kmeans function in RStudio. This function determined that the optimal number of clusters was four based on the molecular size distribution and signal strength. The molecular weight fractions were chosen based on a combination of previous studies (Lepane et al., 2004; O'Loughlin & Chin, 2004; Riise et al., 1994) and how specific fractions correlated with substances that are known to interact with organic matter, such as iron and manganese (Brothers et al., 2014; Kritzberg & Ekström, 2012; Peter et al., 2016; Skoog & Arias-Esquivel, 2009).

The data was organized using Microsoft Excel (version 16.83). RStudio (version 2023.12.0+369) was used to visualize temporal and depth-related interactions of variables by using contour plots. RStudio was also used to conduct the statistical analysis. In this study, Principal component analyses (PCA) and Pearson correlation coefficients (PCC) were used to analyze the data. The PCA is an unsupervised explorative analysis that captures the maximum variability and can be used to visualize correlations among variables in the principal components. The PCC was used to statistically examine the strength, direction, and significance between variables.

2.5 Limitations

This study included multiple limitations associated with specific methods. Firstly, there was a slight discrepancy in the sampling location when the buoy used to locate the sampling site was removed from the lake on three occasions to assess the performance of the HOBO loggers. Despite efforts to reposition the buoy as close to the original location, minor deviations occurred during this relocation, potentially affecting the measurements' accuracy and consistency. Secondly, another limitation arises from the method used to establish the Secchi depth, which includes the subjectivity of the readings of the Secchi depth, as individuals can interpret the disappearance of the Secchi disk differently. Furthermore, sharp gradients with depth might be difficult to uncover, as the water sampler was approximately 60 centimeters long. Additionally, despite the efforts made to minimize the offset of biochemical processes in the water samples, this offset cannot be completely eliminated.

Multiple limitations are also associated with the CDOM measurement method. Firstly, CDOM data needed to be interpolated on 9 August at 1.75m. However, this date was an exceptional sampling data due to extreme rainfall on the previous day, thus the accuracy of the

interpolation cannot be fully assured. Other limitations related to CDOM arise from using a single wavelength at 254 nm; this may result in a bias towards aromatic groups because non-aromatic groups usually reach their absorption maxima at shorter wavelengths (McKnight et al., 2001). Therefore, not all CDOM may be detected at this wavelength. Moreover, using molecular weight fractions for analysis may limit the precision of the analysis by overlooking the full complexity of CDOM molecular weight distribution.

In addition, dynamic changes occurring between the sampling days (taken every 14 days) had not been measured. However, continuous measurements in temperature estimate the position of the thermocline, which indicates the depth of water masses that circulate and are in contact with the atmosphere. Lastly, this study was constrained by limitations in time and resources, resulting in a sampling size of only eight measurements. As a consequence, the statistical power and representativeness of the results may be compromised.

3. Results

3.1 Weather

Weather data were collected from two weather stations in Oslo: Blindern (SN18700) and Trasop (SN18180). Trasop, the closest station to Lake Solbergvann, recorded only short-term precipitation but not long-term precipitation or air temperature trends. Thus, this station will only be used to describe variations in local precipitation in 2023. Blindern recorded both long-term precipitation and air temperature trends, thus functions as a comprehensive source of weather data while local variations in precipitation are retrieved from Trasop.

Air temperature

The air temperature in 2023 deviated substantially from the long-term trends (Table 1). In June and September 2023, the air temperature was notably higher than the average long-term trend, while July and August were slightly cooler. Figure 4 illustrates the daily mean temperature (°C) from May to September 2023. The lowest mean temperature occurred in early May, occurring before the start of the sampling period. The temperature rose considerably in the subsequent week, peaking in June (24.8°C).

Table 3. Comparison of average monthly air temperatures at Blindern (SN18700) from 1991 to 2020 with the average monthly temperatures in 2023 and their deviations.

	Average temperature (°C) 1991-2020	Average temperature (°C) 2023	Deviation (°C)
May	11.4	11.9	+0.6
June	15.4	19.0	+3.6
July	17.7	16.3	-1.4
August	16.5	16.2	-0.3
September	12.1	14.4	+2.3

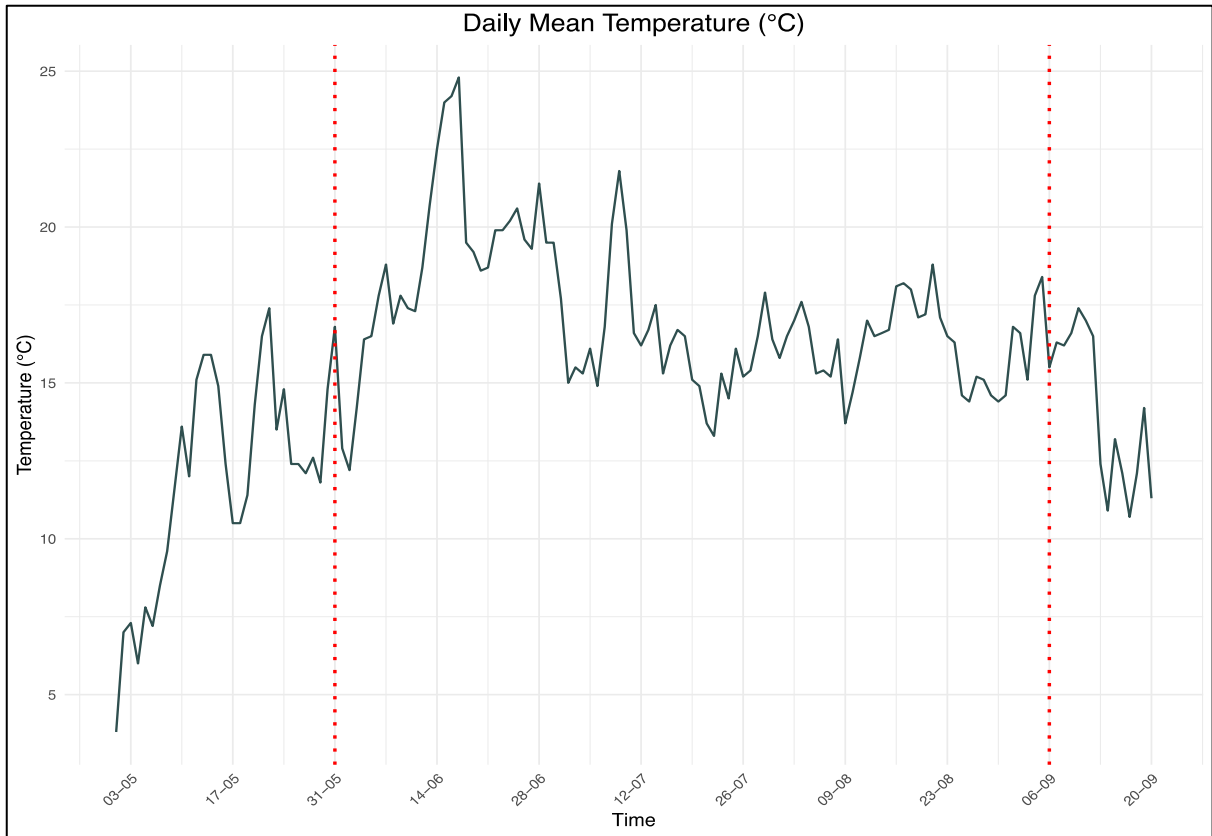


Figure 4. Daily mean temperature (°C) from May to September 2023. Red dotted lines indicate the first (31st of May) and last (6th of September) sampling day at Lake Solbergvann. The dates falling between the 31st of May and the 6th of September correspond to the sampling days. Data retrieved from the Norwegian Centre for Climate Services (2023).

Precipitation

Table 2 presents the precipitation trends from 1993 to 2023 at Blindern and precipitation records at Trasop in 2023. Notable differences were found in the precipitation recorded at Blindern and Trasop (see columns 4 and 5). Thus, data from Blindern was also included to ensure comparability with long-term trends, while Trasop accurately represents local variation. May and June 2023 received low precipitation compared to long-term trends, 20 mm and 31 mm, respectively (Table 2 at Trasop). On the contrary, July and August were relatively wetter than recorded in long-term trends. These months included three outstanding rainfall events: 8 August (49 mm), 20 August (42 mm), and 27 August (73 mm), resulting in a relatively high total precipitation in August (Figure 5).

Table 4. Comparison of average monthly precipitation at Blindern (SN18700) from 1991 to 2020 with the average monthly precipitation in 2023 at both Blindern and Trasop (SN18180) and their deviations.

	Average monthly precipitation 1993-2022 (Blindern)	Monthly precipitation 2023 (Blindern)	Monthly precipitation 2023 (Trasop)	Deviation Blindern - Blindern	Deviation Blindern - Trasop
May	65.0	17.4	20.1	-47.6	-44.9
June	84.8	39.9	31	-44.9	-53.8
July	92.8	146.9	100.6	+54.1	+7.6
August	106.1	259.8	245	+153.7	+138.9
September	86.1	105.8	86.1	+19.7	0

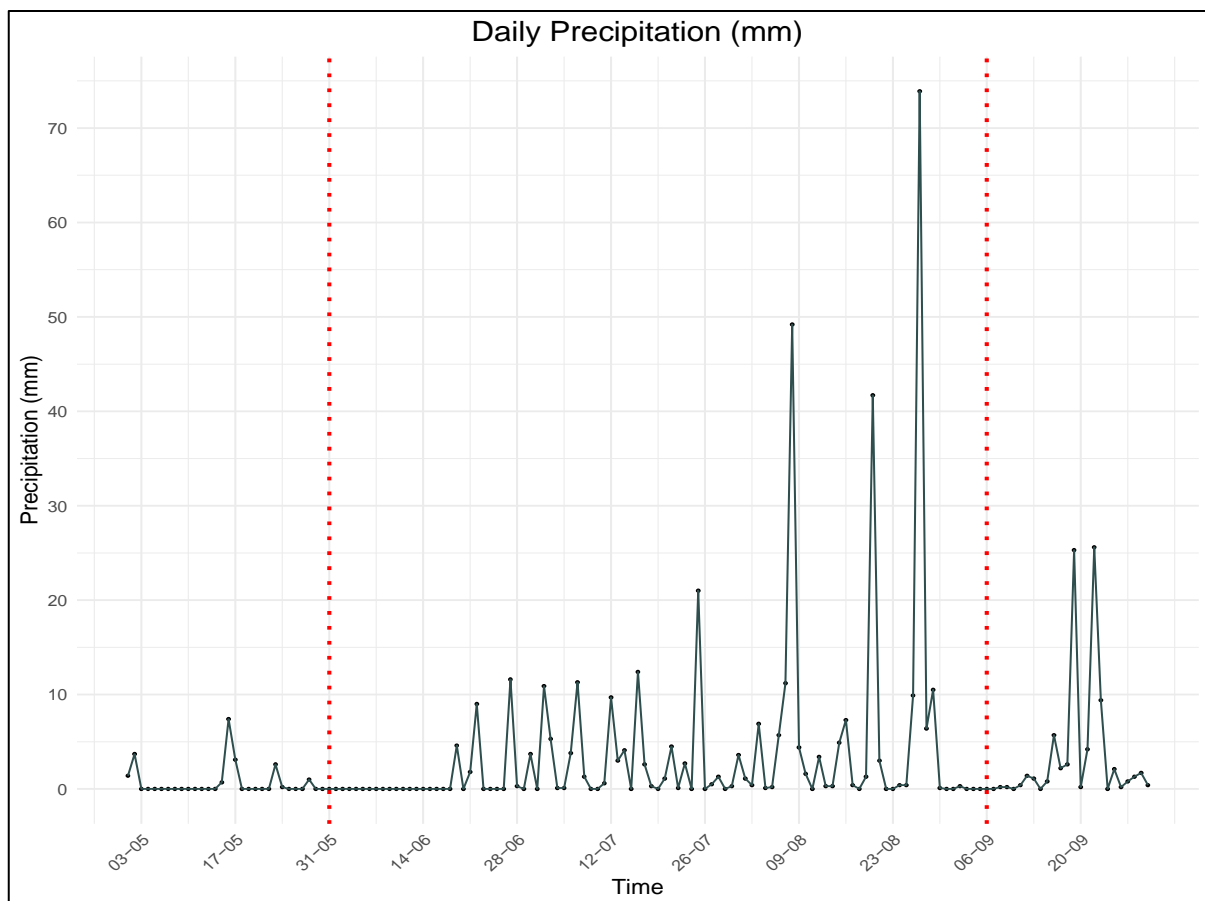


Figure 5. Daily total precipitation (mm) in May-September 2023 at Trasop weather station. Red dotted lines indicate the first (31st of May) and last (6th of September) sampling day at Lake Solbergvann. The dates falling between the 31st of May and the 6th of September correspond to the sampling days. Data retrieved from the Norwegian Centre for Climate Services (2023).

3.1 General Lake Measurements

3.1.1 Temperature

Water temperature (°C) in Lake Solbergvann was measured using a combination of HOBO loggers and on-site measurements, measuring at different depths and durations. The HOBO loggers continuously recorded the water temperature starting at a depth of 1.20m from 11 May until 1 December, though only measurements from May to September are displayed in Figure 6 for study relevance. On-site measurements included depths as shallow as 0.1m and were taken from 31 May until 6 September (Figure 7). The raw data can be found in Appendix A.

The coldest surface water temperatures were recorded on 13 May (HOBO loggers: 6.7°C at 1.20m) and 31 May (on-site: 14.5°C at 0.5m). The water temperature steadily increased until the end of June (on-site) or early July (HOBO loggers), reaching its peak on 28 June (on-site: 20.8°C at 0.1m) and 1 July (HOBO loggers: 18.7°C at 1.20m). These peaks concur with peaks in daily mean air temperatures (see Figure 4). These peak temperatures were followed by a period with moderate fluctuations and a general decreasing trend in water temperatures.

Substantial rainfall on 8 August (49 mm) and 27 August (73 mm) led to a large reduction in surface water temperatures, while the temperature of the deeper water layers remained relatively stable (see Figures 6 and 7). The water temperature gradually increased in these deeper water layers, with slower changes at deeper depths. Thus, this variation in water temperature was less extreme than on the surface layers, possibly attributed to the limited mixing of water layers.

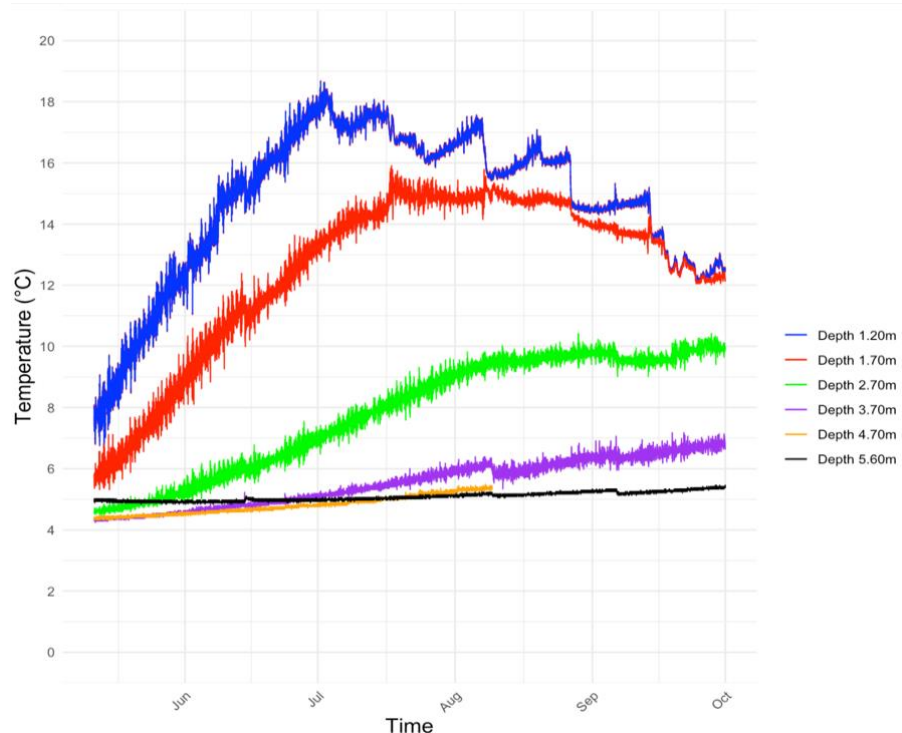


Figure 6. Graph of the seasonal variation in water temperature (°C) at different depths (1.20m, 1.70m, 2.70m, 3.70m, 4.70m, and 5.60m) recorded by the HOBO loggers in Lake Solbergvann from May to October.

Stratification

Figure 6 illustrates slight thermal stratification during the initial employment of the HOBO loggers, with a minimal temperature difference of 2.9°C between the surface and bottom water layers. However, since the HOBO loggers only recorded temperatures from a depth of 1.20m, they captured less thermal stratification than the on-site measurements, which started at 0.1m (Figure 7). These measurements recorded the largest temperature difference between surface and bottom waters on 28 June, with a difference of 14.1°C . After this period, the strong thermal stratification subsided due to declining air temperatures and increased precipitation. Nevertheless, the lake remained thermally stratified until the end of the sampling period.

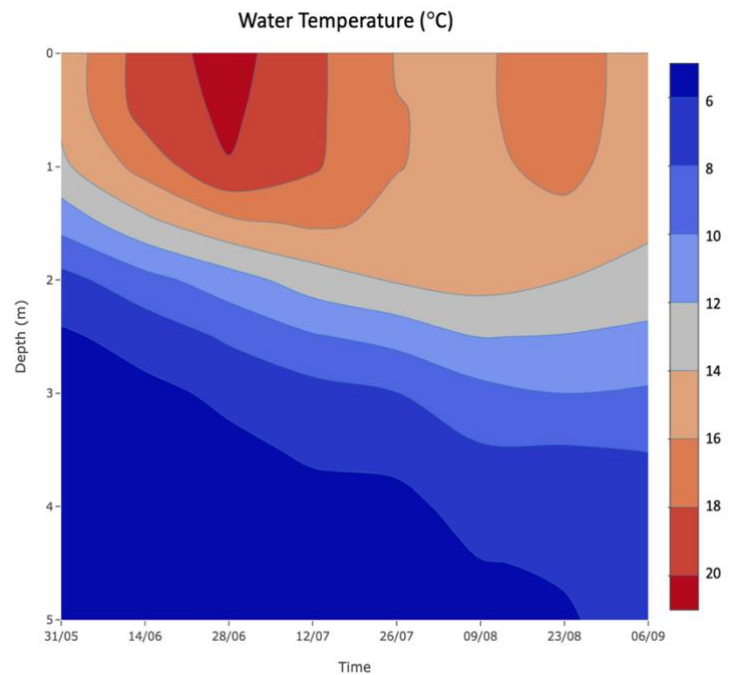


Figure 7. Contour plot of the seasonal variation in water temperature ($^{\circ}\text{C}$) at different depths (0.1m, 0.75m, 1.75m, 2.75m, 3.75m, 4.25m, 4.75m) in Lake Solbergvann on the sampling days from May to September.

3.1.2 Oxygen Saturation

Oxygen (O₂) saturation (%) and concentration (mg/L) were measured on the eight sampling days. O₂ saturation depends on temperature, while O₂ concentrations are not. Thus, only O₂ saturation is included in this description.

The O₂ saturation (Figure 8) ranged from 0% (at all depths below 3m) to 91.5% (0.1m on 23 August). A strong O₂ saturation gradient can be observed. The oxic-anoxic boundary occurred around 2.75m, where oxygen saturation was low, but the waters were never fully anoxic. The oxycline moved slightly upward throughout the sampling period. On 9 August, substantially more O₂ was present at 2.0m (44.4%) compared to the 26 July (1%) and the 23 August (2.3%). This event occurred after the heavy rainfall on 8 August, possibly diffusing O₂ into deeper water layers.

3.1.3 pH

The pH (Figure 9) in Lake Solbergvann ranged from 4.6 (0.75m on 6 September) to 6.8 (0.75m on 31 May). The pH was notably higher during periods of low precipitation (May until mid-July), followed by a consistent decrease in pH, particularly at depths shallower than 3 meters. Interestingly, the pH between 2.5m and 3m was mainly lower than that of other depths.

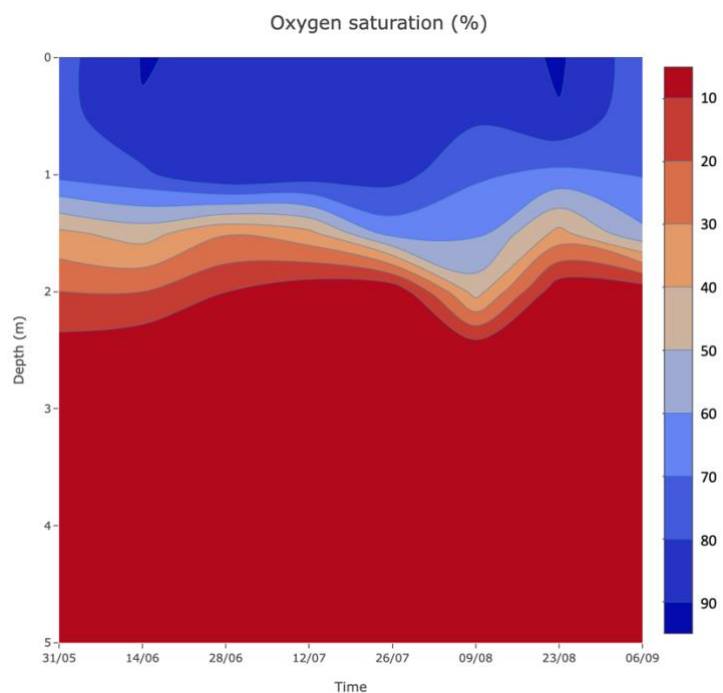


Figure 8. Contour plot of the seasonal variation in oxygen saturation (%) at different depths (0.1m, 0.75m, 1.75m, 2.75m, 3.75m, 4.25m, 4.75m) in Lake Solbergvann on sampling days from May to September. Note that the color scheme in Figures 8 and 9 deviates from the color scheme used in the rest of the figures.

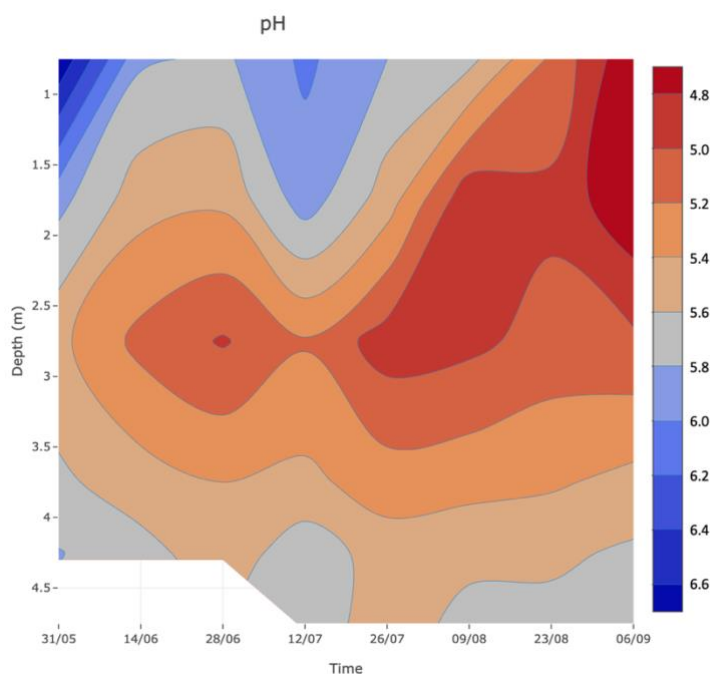


Figure 9. Contour plot of the seasonal variation in pH at different depths (0.75m, 1.75m, 2.75m, 3.75m, 4.25m, 4.75m) in Lake Solbergvann on sampling days from May to September. Note that the color scheme in Figures 8 and 9 deviates from the color scheme used in the rest of the figures.

3.1.4 Conductivity

The conductivity (Figure 10) ranged from 22.3 $\mu\text{s/cm}$ (0.75m on 26 July) to 55.2 $\mu\text{s/cm}$ (4.75m on 12 July). Surface waters generally had a lower conductivity, contrasting with higher conductivity in the deeper water layers. On 9 August, the conductivity in the upper part of the water column was substantially higher compared to other sampling days, which aligns with the high precipitation observed on 8 August.

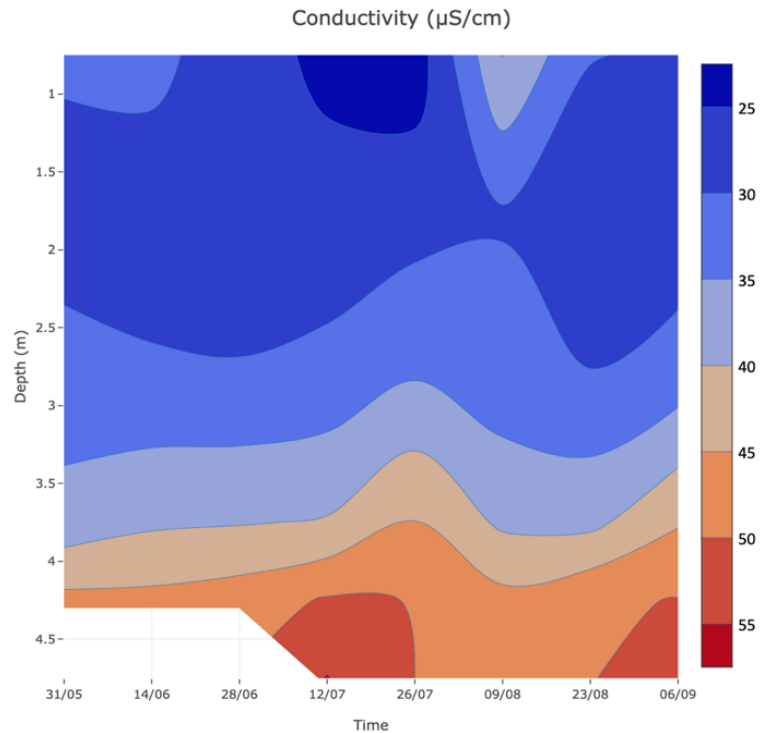


Figure 10. Contour plot of the seasonal variation in conductivity ($\mu\text{S/cm}$) at different depths (0.75m, 1.75m, 2.75m, 3.75m, 4.25m, 4.75m) in Lake Solbergvann on sampling days from May to September.

3.1.5 Secchi depth

The Secchi depth (Figure 11) ranged from 1.33m (6 September) to 1.70m (26 July). Both 9 August and 23 August recorded very similar Secchi depths, measured at 1.67m and 1.68m, respectively.

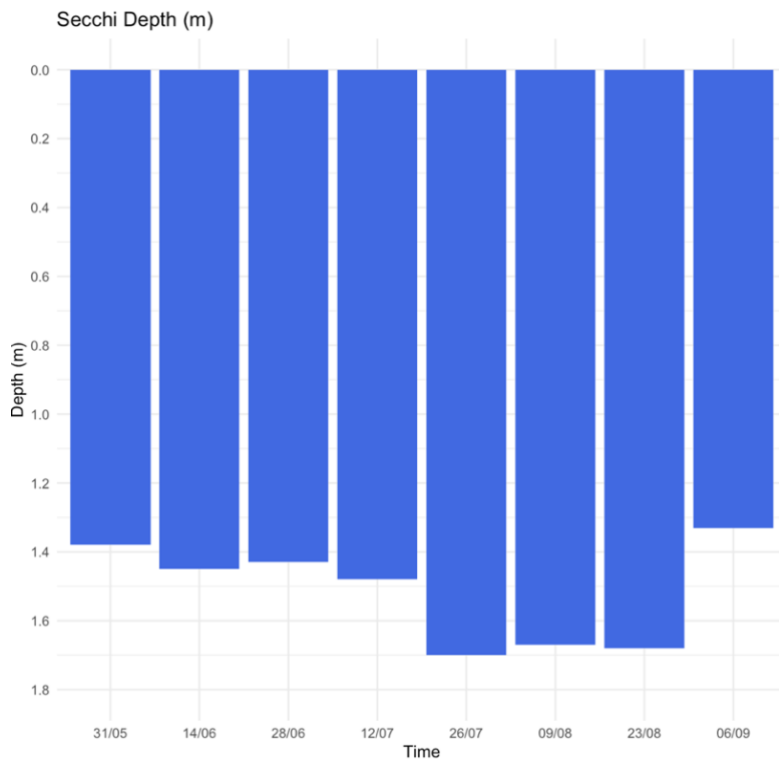


Figure 11. Bar plot of the seasonal variation in Secchi depth (m) in Lake Solbergvann on sampling days from May to September.

3.1.6 Phosphorus

Phosphorus (P) levels were measured in both dissolved and total forms. The dissolved P concentrations (Figure 12) ranged from 0.0035mg/L (0.75m on 9 August) to 0.0283mg/L (4.25m on 14 June). Although the dissolved P concentration exhibited fluctuation, they showed an overall decreasing trend until August. Generally, deeper water layers contained higher concentrations of dissolved P. An exception occurred on 9 August, where dissolved P was more abundant at 1.75m than at 2.75m and 3.75m.

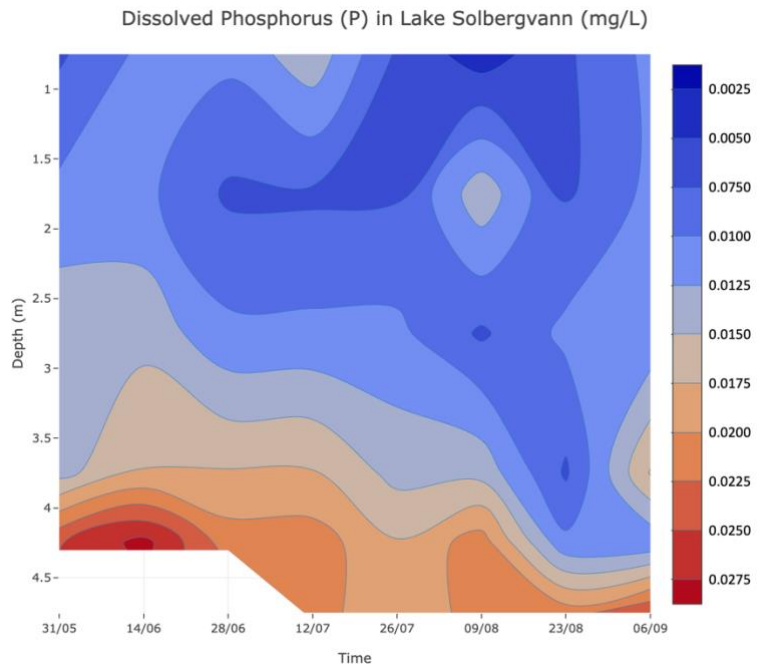


Figure 12. Contour plot of the seasonal variation in dissolved phosphorus (mg/L) at different depths (0.75m, 1.75m, 2.75m, 3.75m, 4.25m, 4.75m) in Lake Solbergvann on sampling days from May to September.

Total P concentrations (Figure 13) ranged from 0.0034mg/L (0.75m on 6 September) to 0.1149mg/L (4.25m on 31 May). The Total P fluctuated throughout the sampling period, sharply decreasing from 31 May to 28 June in water layers shallower than 3m. In general, the deeper water layers show higher concentrations of Total P. The exception for this occurred again on 9 August, where there was relatively more Total P present at 1.75m compared to 2.75m and 3.75m.

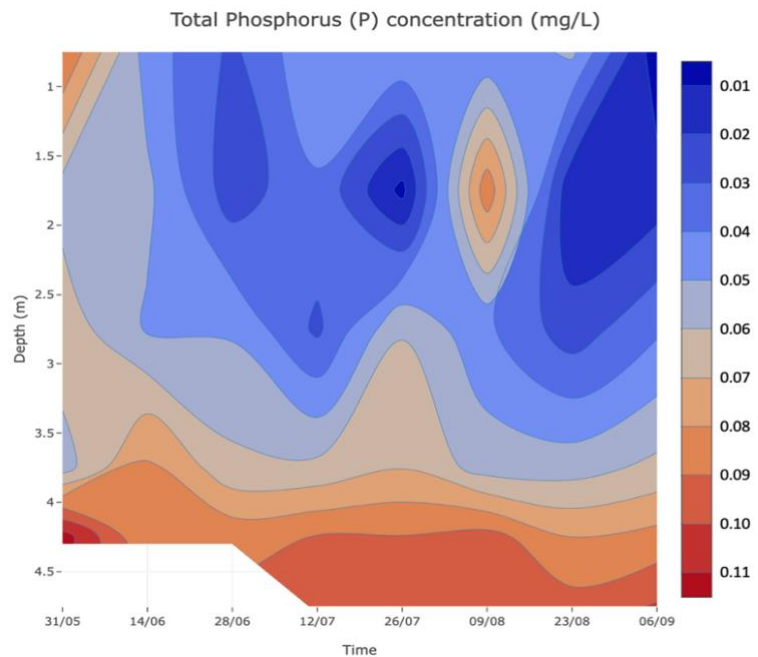


Figure 13. Contour plot of the seasonal variation in total phosphorus (mg/L) at different depths (0.75m, 1.75m, 2.75m, 3.75m, 4.25m, 4.75m) in Lake Solbergvann on sampling days from May to September.

3.1.7 Iron

Iron (Fe) concentrations (Figure 14) ranged from 0.06 mg/L (0.75m on 28 June) to 1.00 mg/L (4.75m on 6 September). The overall Fe concentrations were at their lowest at the beginning of the sampling period, then showed a continuous increase. A clear depth-related pattern can be observed with higher Fe concentrations in the bottom water layers.

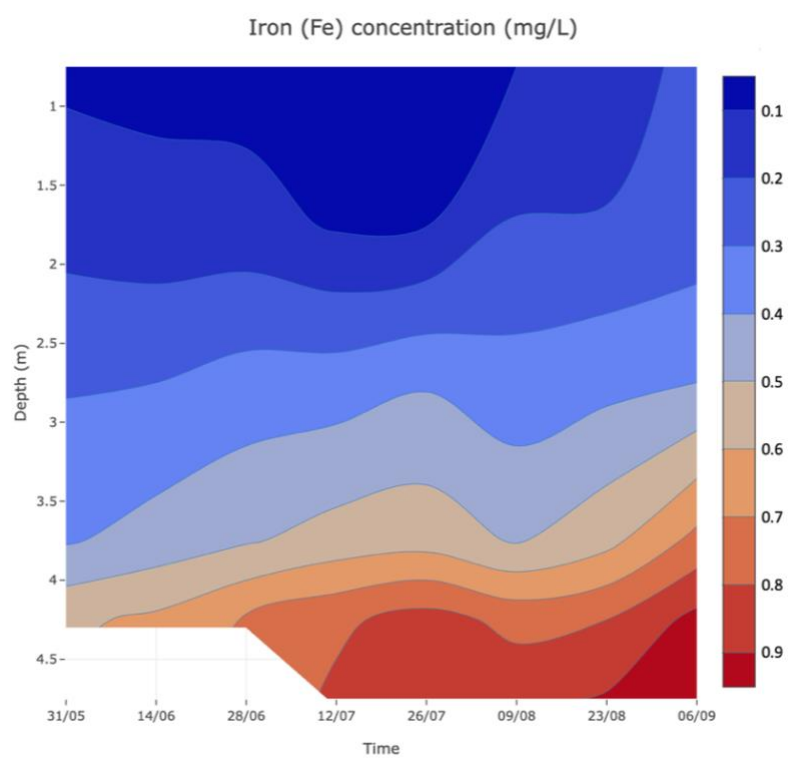


Figure 14. Contour plot of the seasonal variation in iron (Fe) (mg/L) at different depths (0.75m, 1.75m, 2.75m, 3.75m, 4.25m, 4.75m) in Lake Solbergvann on sampling days from May to September.

3.1.8 Manganese

The Manganese (Mn) concentrations (Figure 15) ranged from 0.01 mg/L (0.75m on 12 July and 9 August, 1.75m on 26 July and 9 August) to 0.05 mg/L (4.75m on 23 August). The Mn concentrations slightly increased until 23 August and slightly dropped in September. A depth-related pattern was observed; bottom water layers contained higher concentrations of Mn.

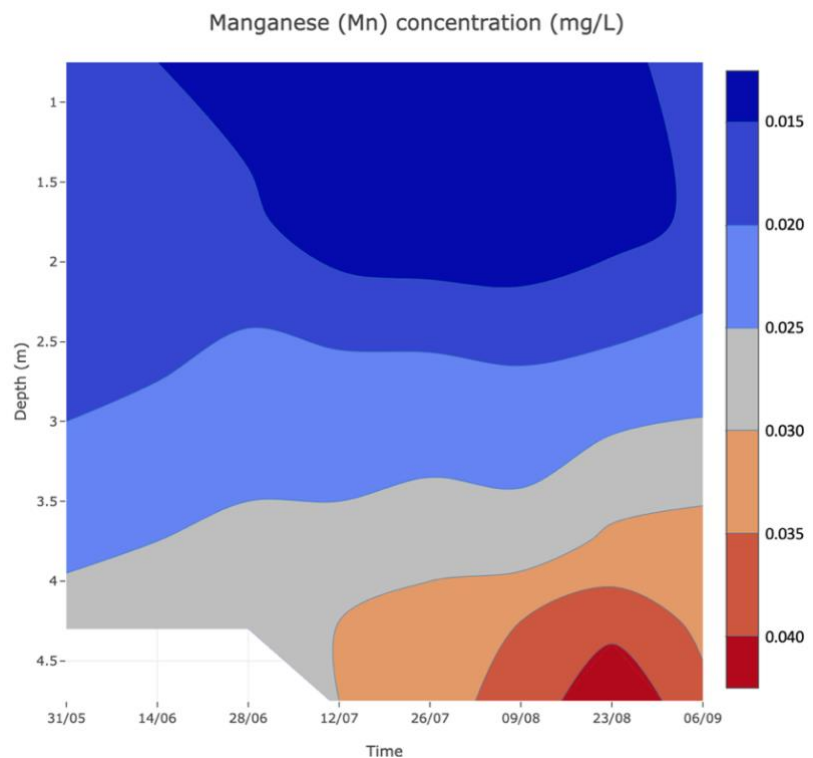


Figure 15. Contour plot of the seasonal variation in manganese (Mn) (mg/L) at different depths (0.75m, 1.75m, 2.75m, 3.75m, 4.25m, 4.75m) in Lake Solbergvann on sampling days from May to September.

3.1.9 Sulfur and Sulfate

The Sulfur (S) concentrations (Figure 16) ranged from 0.58mg/L (0.75m on 9 August) to 1.10mg/L (3.75m on both 31 May and 23 August). The S concentrations generally decreased in both the surface and bottom layers from May to September. A depth-related pattern could be observed, with the lowest concentrations in the surface water layers and the highest concentrations between 2.75 and 3.75m.

Sulfate (SO_4^{2-} -S) concentrations (Figure 17) ranged from 0.28 mg/L (4.75m on 6 September) to 0.81 mg/L (3.75m on 9 August). SO_4^{2-} -S concentrations approximately mirrored the same seasonal and depth pattern as S. However, it can be observed that the highest SO_4^{2-} -S relative to S was found around 2.75m.

3.1.10 Additional

measurements

Besides the previously discussed measurements, measurements were also taken for ammonium (NH_4^+), total nitrogen (N), aluminum (Al), dissolved chloride (Cl^-), bacteriochlorophyll concentrations, and chlorophyll a concentrations. These contour plots can be found in Appendix B.

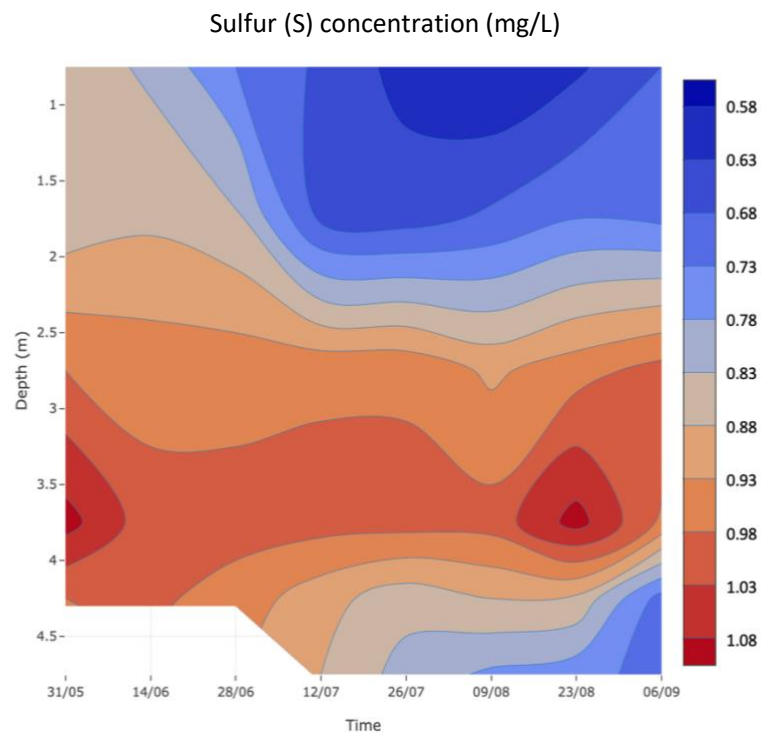


Figure 16. Contour plot of the seasonal variation in sulfur (S) (mg/L) at different depths (0.75m, 1.75m, 2.75m, 3.75m, 4.25m, 4.75m) in Lake Solbergvann on sampling days from May to September.

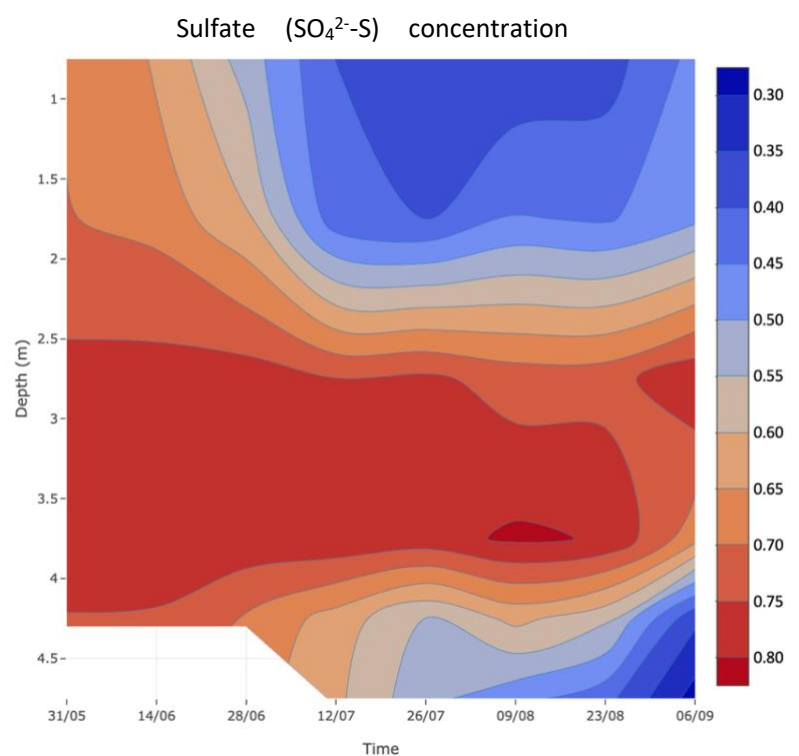


Figure 17. Contour plot of the seasonal variation in sulfate (SO_4^{2-}) (mg/L) at different depths (0.75m, 1.75m, 2.75m, 3.75m, 4.25m, 4.75m) in Lake Solbergvann on sampling days from May to September.

3.2 Dissolved organic matter

Dissolved organic matter (DOM) was measured both as dissolved organic carbon (DOC) concentrations and chromophoric dissolved organic carbon (CDOM) signal. The molecular weight of CDOM was also measured using size-exclusion chromatography.

3.2.1 Dissolved Organic Carbon

DOC concentrations (Figure 18) ranged from 12.83 mg/L (1.75m on 26 July) to 22.42 mg/L (1.75m on 6 September). The DOC concentrations notably increased at 0.75m and 1.75m throughout the sampling season. They slightly decreased at 2.75m and 3.75m, while fluctuations occurred at 4.25m. Interestingly, the DOC concentrations slightly increased at 4.75m.

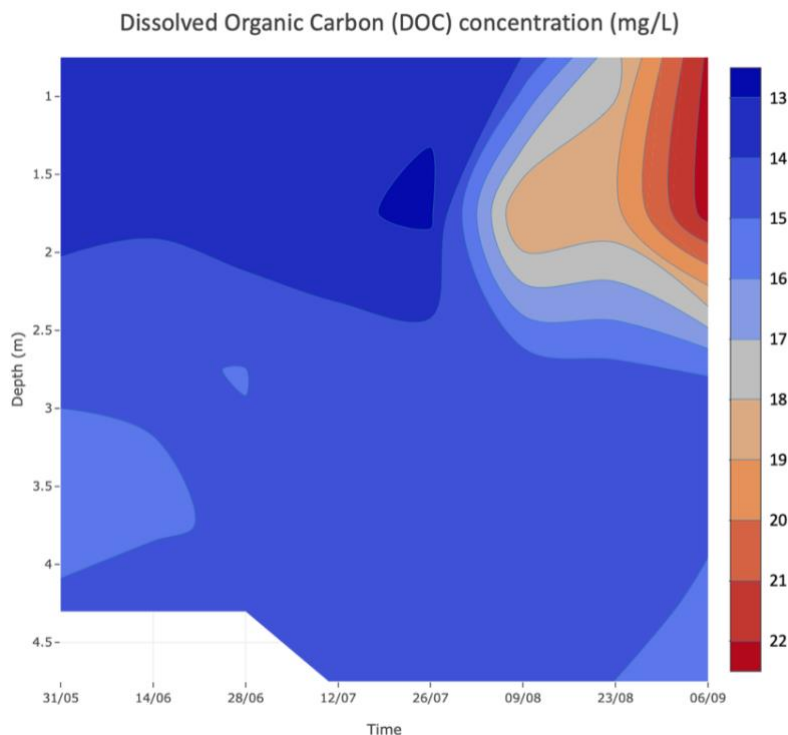


Figure 18. Contour plot of the seasonal variation dissolved organic carbon (DOC) (mg/L) at different depths (0.75m, 1.75m, 2.75m, 3.75m, 4.25m, 4.75m) in Lake Solbergvann on sampling days from May to September.

3.2.2 Chromophoric Dissolved Organic Matter

CDOM was measured using spectroscopy measuring at a wavelength of 254 nm. Figure 19 displays the relationship between CDOM signal [mAU]*Dalton across different depths. This signal serves as an indicator of CDOM abundance. Note that the analysis of CDOM below 4.25m was not conducted.

The CDOM signal ranged from 8409 mAU (0.75m on 14 June) to 16,725 (0.75m on 6 September). The surface layers initially contained the lowest CDOM signal compared to deeper layers. However, a marked increase in CDOM signal occurred during the second half of the sampling season at 0.75m and 1.75m. CDOM remained relatively stable at 2.75m. Nevertheless, at both 3.75m and 4.25m, the CDOM signal increased throughout the sampling season, with a more pronounced increase in the deepest layer of the lake.

The molecular weight of CDOM

The molecular weight of CDOM was estimated using size exclusion chromatography (SEC). Figure 20 illustrates the CDOM size distribution (ranging from 200 to 50,000 Da) from May to September, revealing substantial temporal and depth variation in CDOM size distribution.

Until late July, the chromatograms show a similar CDOM size distribution pattern across all depths. The signal peak (mAU), as shown on the y-axis, corresponds with a molecular weight (MW) of approximately 5

kDa to 6 kDa. Two smaller peaks

also occurred around 2 and 4 kDa. Deeper water layers generally contained more CDOM of higher MW than surface layers. They also showed more stability in the distribution of CDOM signal and MW. On the contrary, the CDOM signal and its corresponding MW showed a large increase in the surface layers towards the end of the sampling season.

Appendix C provides details on the exact Da values that correspond with the signal peaks for each measurement. These results demonstrate a depth-related pattern before September. The depths of 2.75m and 3.75m consistently exhibited the highest MW until 23 August, with only a limited difference between the two depths. However, this pattern shifted in September when the MW in the surface layers showed a notable increase compared to the previous sampling days. Across all depths on 12 July, the peak of the MW was approximately 700 Da lower than the preceding and subsequent sampling days. A seasonal profile emerged where the highest MW corresponding to its peak for 0.75m, 1.75m, and 2.75m was observed on the last sampling day. In contrast, for the depths of 3.75m and 4.25m, this peak in MW occurred much earlier, namely on 26 July.

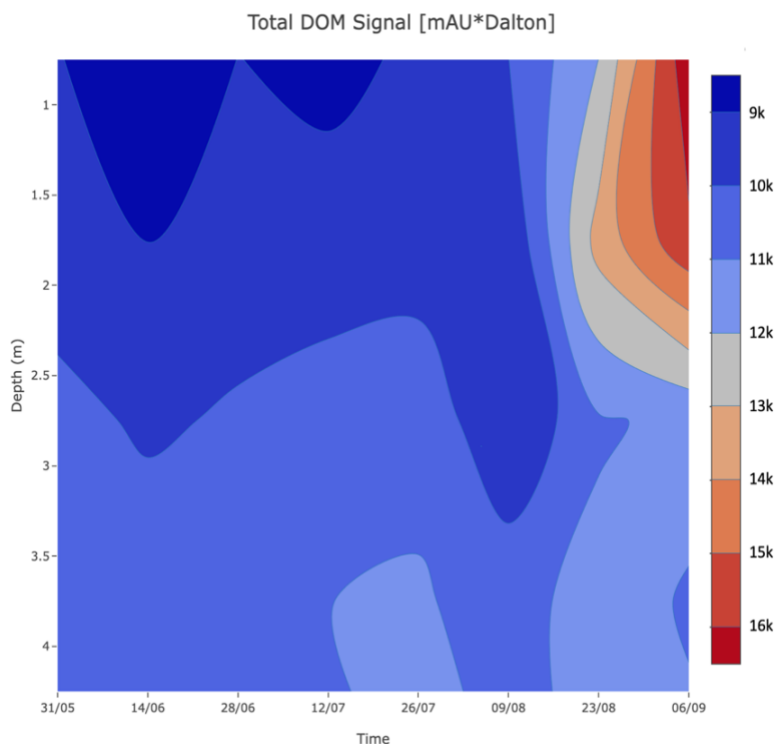


Figure 19. Contour plot of chromophoric dissolved organic matter (CDOM) signal (mAU*Dalton) at different depths (0.75m, 1.75m, 2.75m, 3.75m, 4.25m) in Lake Solbergvann on sampling days from May to September.

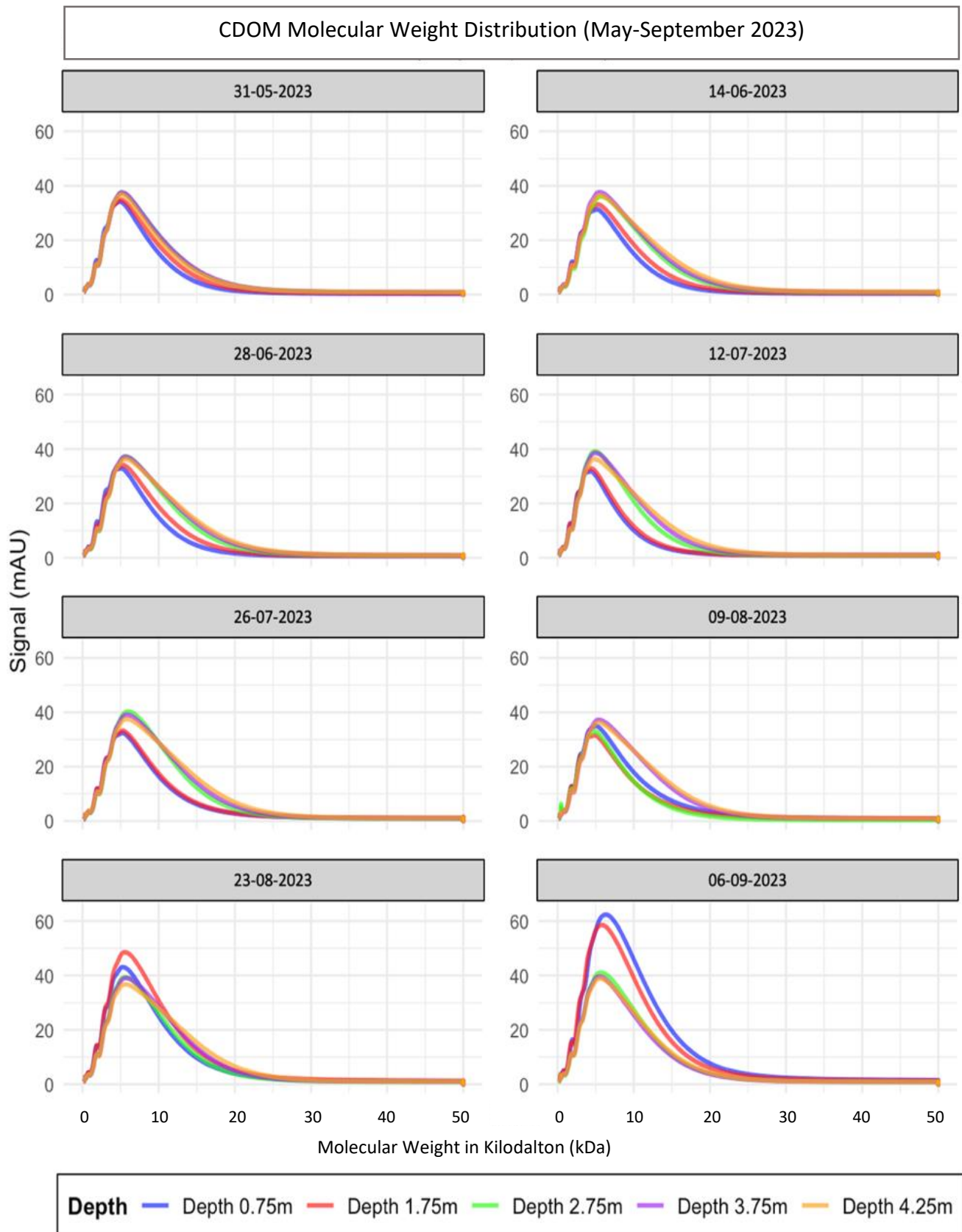


Figure 20. Graph CDOM molecular weight distribution with molecular weight in kilodalton (kDa) and signal (mAU) at different depths (0.75m, 1.75m, 2.75m, 3.75m, 4.25m) in Lake Solbergvann on sampling days from May to September.

3.3 Statistical Analysis

3.3.1 Fractioning of CDOM

The extensive dataset of CDOM was divided into multiple subsets for analysis using the kmeans function in R. This analysis suggested that the optimal number of subsets is four, which was based on their similarity of molecular size distribution and signal. This resulted in four fractions based on their molecular weight (MW): CDOM1 (< 1 kDa), CDOM2 (1 – 3 kDa), CDOM3 (3 – 10 kDa), and CDOM4 (> 10 kDa).

Figure 21 presents the fractions across different depths in Lake Solbergvann. The relative contribution of these fractions compared to the total CDOM of that sampling day is as follows: CDOM1 ranged from 5,0% to 9,3%, CDOM2 from 13,8% to 26,3%, CDOM3 from 54,1 to 60,7%, and CDOM4 from 10,0% to 24,3%. This makes CDOM1 the least abundant and CDOM3 the most abundant in Lake Solbergvann.

Throughout the year, a notable increase in the fractions of CDOM3 and CDOM4 size compounds at 0.75m was observed from May to September, with an increase of 84% and 290%, respectively. CDOM1 and CDOM2 slightly increased but remained relatively stable at this depth. A similar composition change was found at 1.75m, but less pronounced changes in the proportion of each fraction. In general, these shallower depths contained a relatively higher share of lower MW (6.6%) compared to 2.75m (6.1%) and the deepest water layers (5.9%)

At 2.75m, there was little variation in its CDOM abundance and distribution throughout the sampling period. The total CDOM slightly increased at this depth, but with a drop on 9 August. On this day, there was a relatively higher proportion of CDOM1 and CDOM2 compared to the other sampling dates. This phenomenon was also observed at 3.75m and 4.25m but with substantially less change compared to 2.75m.

At 3.75m and 4.25m, CDOM3 and CDOM4 showed a slight increase until the end of August, followed by a drop in September. These depths usually contained a higher percentage of higher MW compared to the surface layers.

Signal Strength [mAU] of CDOM per Molecular Weight Fraction (May-September 2023)

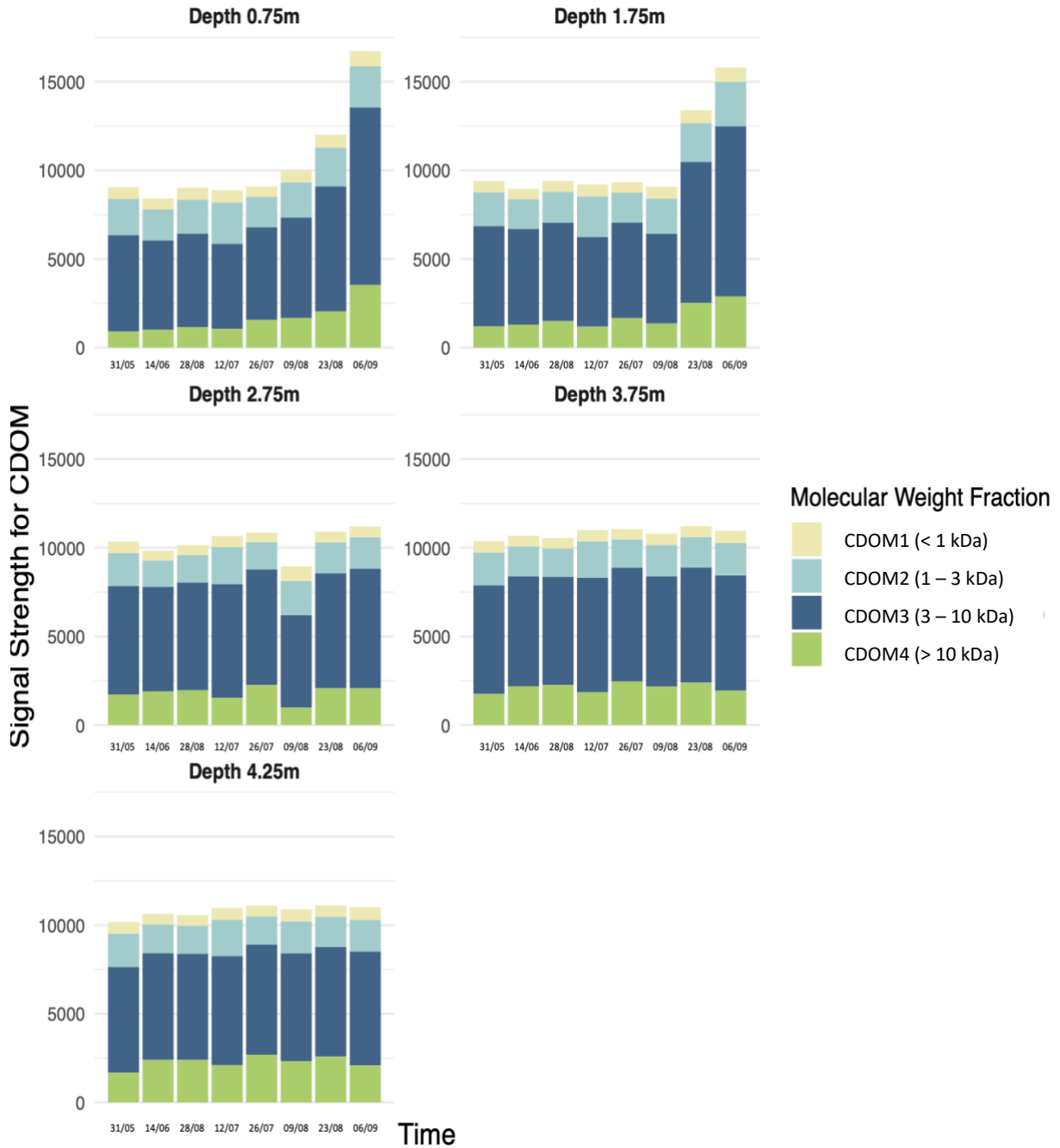


Figure 21. Bar chart of the distribution of CDOM of four molecular weight fractions (in kDa). Measured by using signal strength [mAU] of each DOM fractions at different depths (0.75m, 1.75m, 2.75m, 3.75m, 4.25m) in Lake Solbergvann on sampling days from May to September.

3.3.2 Principal Component Analysis and Pearson's Correlation Coefficient

This section used the principal component analysis (PCA) and Pearson correlation coefficient (PCC) to integrate all variables for analysis. This approach aims to provide a greater understanding of depth-specific relationships between variables. Key variables were selected for the PCA, while the PCC included all measured variables. Detailed coefficients and p-values can be found in appendices II-VI.

0.75m

At 0.75m, the PCA analysis showed that PC1 explained 46.0% and PC2 22.7% of the variability (Figure 22a). The positive correlations in PC1 were mainly explained by the DOC, various CDOM fractions, and Fe, while the negative correlations for PC1 mainly included pH, P (Tot), and O₂ (%). PC2 showed positive correlations with S, SO₄²⁻, and P (Tot) while negative correlations were observed with O₂ (%), water temperature, air temperature, and precipitation.

The PCC showed that there was a significant correlation between air temperature and water temperature (p-value <0.001, coefficient 0.949) (Appendix D). Precipitation was negatively correlated with SO₄²⁻ (p-value = 0.002, coefficient -0.901).

DOC and all CDOM fractions were positively correlated with each other, except for CDOM2, which was only positively correlated with CDOM1 (p-value = 0.017, coefficient = 0.799). DOC, Total CDOM, CDOM1, CDOM3, and CDOM4 were strongly positively correlated with both Fe, with stronger and more significant correlations for Total CDOM, CDOM3, and CDOM4 (p < 0.001). pH was negatively correlated with DOC, total CDOM, CDOM3, CDOM4, and Fe. On the other hand, pH exhibited a positive correlation with Total P (p-value = 0.008, coefficient 0.844).

A significant positive correlation was observed between air/water temperature and O₂ saturation (%). Precipitation was not significantly correlated with O₂ saturation. O₂ saturation was negatively correlated with Fe. O₂ saturation did not show significant correlations with DOC or any CDOM fractions, but the p-values trended toward significance with a negative coefficient. Interestingly, O₂ (mg/L) had a significant negative correlation with DOC, Total CDOM, CDOM1, and CDOM3.

1.75m

At 1.75m, PC1 and PC2 explained 46.8% and 29.8% of the variability (Figure 22b). This PCA plot has a similar distribution of variables as the PCA plot at 0.75m. DOC, CDOM,

Fe, and precipitation were positively correlated with PC1, while pH and P (Tot) were negatively correlated. For PC2, the behavior O₂ (%) begins to differ from 0.75m by showing a (weak) positive correlation with PC2. Other positive correlations with PC2 included P (Tot), SO₄²⁻, S, Mn, and P (Dis). A negative correlation with PC2 was displayed by air temperature, Secchi depth, water temperature, and precipitation.

The PCC showed that there was no longer a significant correlation between air temperature and water temperature (Appendix E). Precipitation was positively correlated with water temperature (p-value = 0.007, coefficient 0.856) and negatively with SO₄²⁻ and S.

DOC and all CDOM fractions were positively correlated with each other at this depth, except for CDOM2, which was only positively correlated with CDOM1 and Total CDOM. No significant correlation was found between Total CDOM and DOC. DOC, CDOM1, CDOM3, and CDOM4 showed significant positive correlations with Fe. On the other hand, DOC, CDOM3, CDOM4, and Fe were negatively correlated with pH.

O₂ (%) was negatively correlated with Total CDOM, but not with any CDOM fractions or DOC. Besides positive correlations with P (Dis), P (Tot), and conductivity, O₂ was not significantly correlated with other variables.

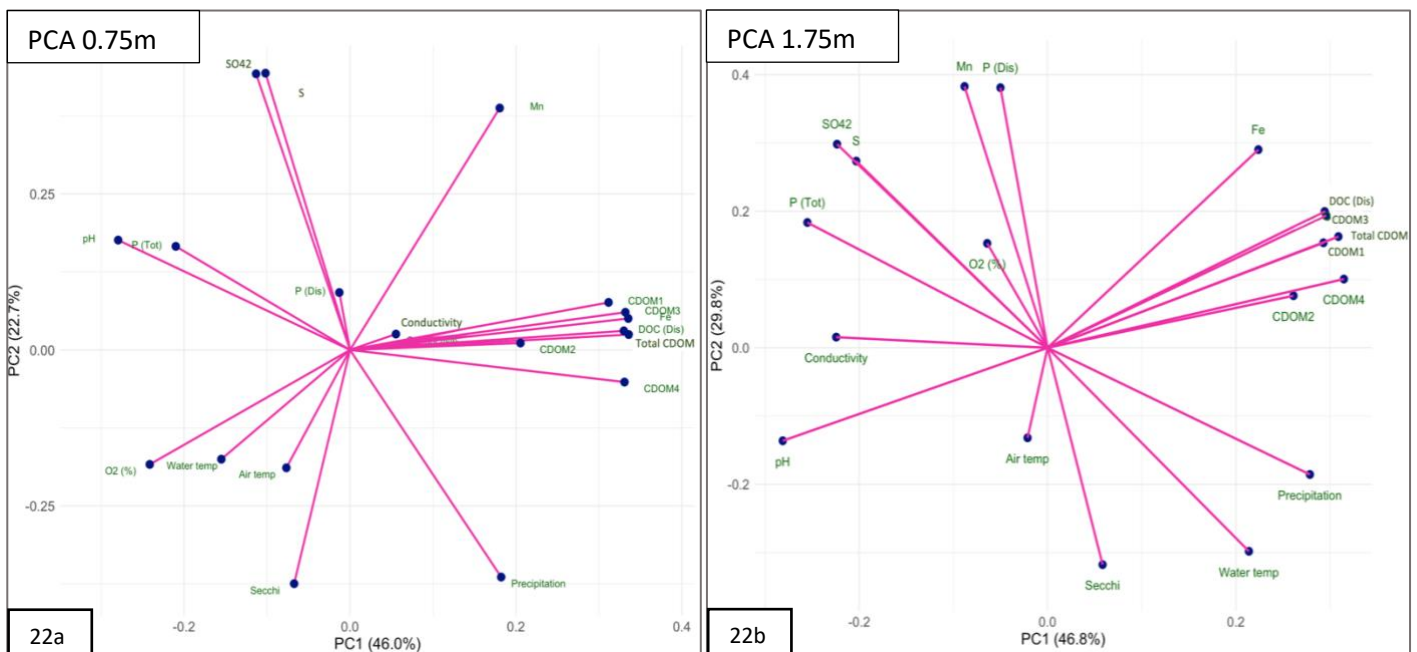


Figure 22. Principal component analysis for 0.75m (23a) and 1.75m (23b). Including the following variables: dissolved organic carbon (DOC), total chromophoric dissolved organic matter (Total CDOM), CDOM of <1 kDa (CDOM1), CDOM of 1 – 3 kDa (CDOM2), CDOM of 3 – 10 kDa (CDOM3), CDOM >10 kDa, manganese (Mn), iron (Fe), total phosphorus (P (Tot)), dissolved phosphorus (P (Dis)), sulfur (S), sulfate (SO₄²⁻), oxygen saturation (O₂ (%)), pH, conductivity, Secchi depth (Secchi), water temperature (Water temp), air temperature (Air temp), and precipitation.

2.75m

At 2.75m, PC1 accounted for 36.0% and PC2 for 30.4% of the variability (Figure 23). It is clearly visible that this PCA plot differs from PCA plots at 0.75m and 1.75m. The positive correlations in PC1 were primarily from CDOM1, CDOM2, Secchi depth, precipitation, and water temperature. In contrast, P (Dis), DOC (Dis), SO_4^{2-} , S, CDOM4, Total CDOM, and CDOM3 were negatively associated with PC1. PC2 had positive correlations with pH, P (Tot), O_2 , CDOM1, and CDOM2, while it showed negative correlations with Mn and Fe.

The PCC (Appendix F) shows that air temperature was no longer significantly correlated with any variables. Precipitation was positively correlated with water temperature and Fe.

Total CDOM was positively correlated with CDOM3 and CDOM4. These variables were also positively correlated with each other, thus displaying minimal variation in their relationship compared to shallower depths. Significant negative correlations between CDOM1 and CDOM4 were observed (p-value 0.002, coefficient -0.900). Fe was no longer significantly

correlated with DOC or any CDOM variables. Total CDOM and CDOM3 were positively correlated with S, while only DOC was positively correlated with SO_4^{2-} .

O_2 was positively correlated with pH (p-value 0.04, coefficient 0.73) and negatively with Mn (p-value = 0.009, coefficient -0.838), and it trended toward significance with Fe (p-value = 0.057, coefficient -0.692).

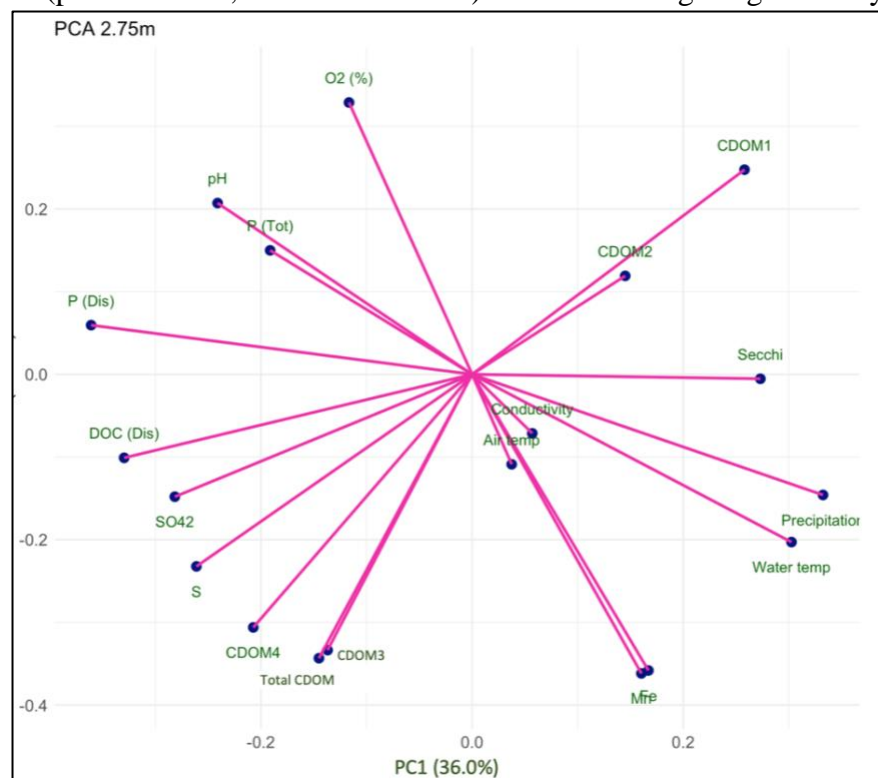


Figure 23. Principal component analysis at a depth of 2.75m. Including the following variables: dissolved organic carbon (DOC), total chromophoric dissolved organic matter (Total CDOM), CDOM of <1 kDa (CDOM1), CDOM of 1 – 3 kDa (CDOM2), CDOM of 3 – 10 kDa (CDOM3), CDOM >10 kDa, manganese (Mn), iron (Fe), total phosphorus (P (Tot)), dissolved phosphorus (P (Dis)), sulfur (S), sulfate (SO_4^{2-}), oxygen saturation (O_2 (%)), pH, conductivity, Secchi depth (Secchi), water temperature (Water temp), air temperature (Air temp), and precipitation.

3.75m

At 3.75m, the distributions of variables underwent a substantial change (Figure 24). PC1 explained 39.3% of the variability and PC2 23.2%. Positive correlations for PC1 were mainly found for water temperature, precipitation, Total CDOM, CDOM3, Fe, Mn, and conductivity. Negative correlations in PC1 included pH, DOC (Dis), and SO_4^{2-} . Positive correlations in PC2 mainly stem from CDOM1, CDOM2, and P (Dis), while PC2 was negatively correlated with air temperature, Secchi depth, CDOM4, and SO_4^{2-} .

The PCC (Appendix G) shows that air temperature was not significantly correlated with any variables. Precipitation was positively correlated with water temperature and negatively with pH. Precipitation was negatively correlated with DOC (p-value = 0.007, coefficient -0.85).

Total CDOM was positively correlated with CDOM3 (p-value = 0.001, coefficient 0.918). CDOM2 was negatively correlated with CDOM4 (p-value = 0.016, coefficient -0.807). DOC was positively correlated with pH (p-value = 0.014, coefficient 0.814). CDOM4 was negatively correlated with pH (p-value 0.015, coefficient -0.808). Total CDOM was positively

correlated with Mn (p-value = 0.033, coefficient 0.748) and trended toward significance with Fe (p-value = 0.06). CDOM3 positively correlated with Mn (p-value = 0.025, coefficient 0.77) and Fe (p-value = 0.014, coefficient 0.811). Fe was also negatively correlated with SO_4^{2-} (p-value = 0.009, coefficient -0.838). Furthermore, O_2 was no longer present at this depth.

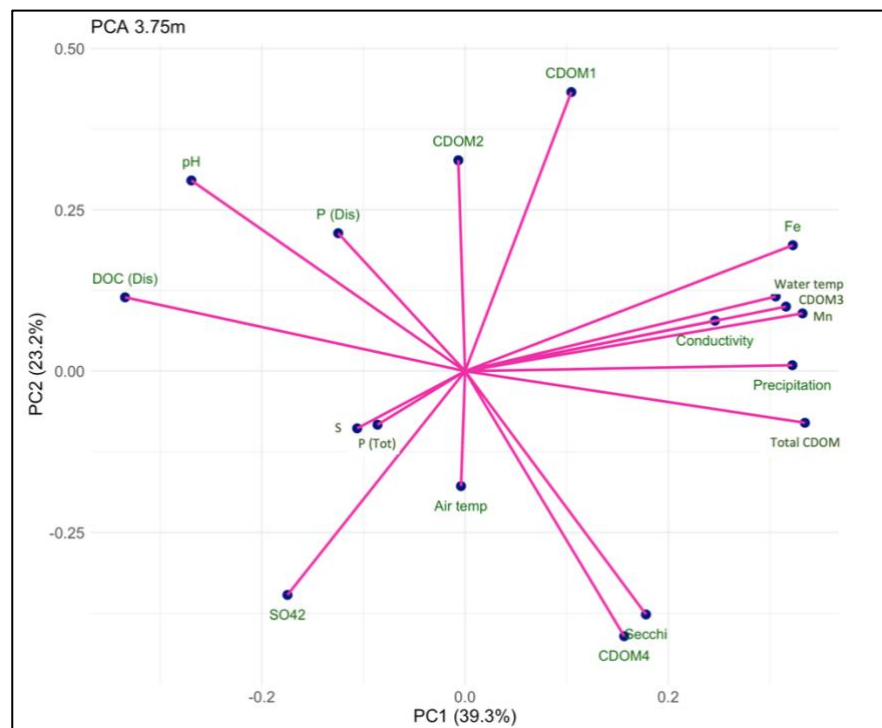


Figure 24. Principal component analysis at a depth of 3.75m. Including the following variables: dissolved organic carbon (DOC), total chromophoric dissolved organic matter (Total CDOM), CDOM of <1 kDa (CDOM1), CDOM of 1 – 3 kDa (CDOM2), CDOM of 3 – 10 kDa (CDOM3), CDOM >10 kDa, manganese (Mn), iron (Fe), total phosphorus (P (Tot)), dissolved phosphorus (P (Dis)), sulfur (S), sulfate (SO_4^{2-}), oxygen saturation (O_2 (%)), pH, conductivity, Secchi depth (Secchi), water temperature (Water temp), air temperature (Air temp), and precipitation.

4.25m

At 4.25m, PC1 explained 48.7% and PC2 explained 24.3% of the variability (Figure 25). PC1 was still positively dominated by water temperature, precipitation, Total CDOM, CDOM3, Fe, and Mn. On the other side of PC1, negative correlations were found with P (Dis), S, and SO_4^{2-} . PC2 was negatively correlated with air temperature, Secchi depth, and CDOM, and positively with pH, DOC, CDOM1, CDOM2, and P (Tot).

The PCC (Appendix H) shows that the air temperature was not correlated with any variables. Precipitation was positively correlated with water temperature (p-value = 0.036, coefficient 0.741). It was also positively correlated with Fe and Mn, and negatively with S and SO_4^{2-} . Water temperature displayed similar trends as precipitation in terms of correlations and positively correlated with CDOM1 (p-value = 0.015, coefficient 0.811).

Only Total CDOM and CDOM3 were positively correlated with each other (p-value = 0.028, coefficient 0.761). pH was negatively correlated with CDOM4 (p-value = 0.009, coefficient -0.841). Total CDOM and CDOM3 were positively correlated with Fe and conductivity, and Total CDOM was also positively correlated with Mn. SO_4^{2-} and S were negatively correlated with Fe and trended toward significance with Mn.

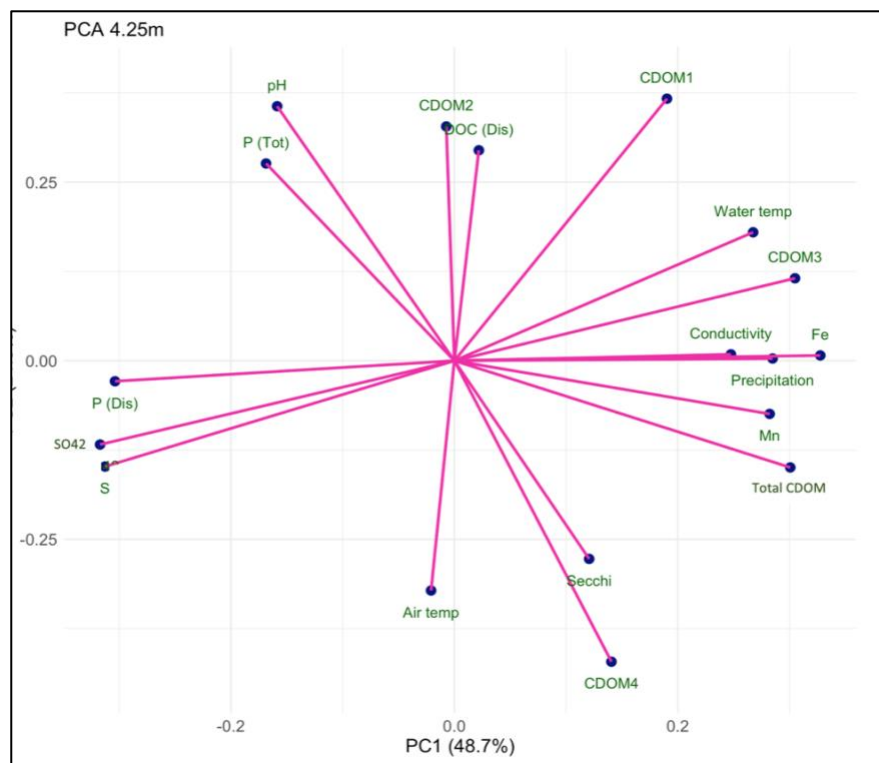


Figure 25. Principal component analysis at a depth of 4.25m. Including the following variables: dissolved organic carbon (DOC), total chromophoric dissolved organic matter (Total CDOM), CDOM of <1 kDa (CDOM1), CDOM of 1 – 3 kDa (CDOM2), CDOM of 3 – 10 kDa (CDOM3), CDOM >10 kDa, manganese (Mn), iron (Fe), total phosphorus (P (Tot)), dissolved phosphorus (P (Dis)), sulfur (S), sulfate (SO_4^{2-}), oxygen saturation (O_2 (%)), pH, conductivity, Secchi depth (Secchi), water temperature (Water temp), air temperature (Air temp), and precipitation.

4.75m

At a depth of 4.75m, I only collected samples from 12 July until 6 September. Thus, I only have five sampling measurements for this day. In addition, I did not have any measurements for CDOM at this depth. Thus, this PCA includes limited variables.

At 4.75m, PC1 explained 49.1% of the variability, and PC2 explained 30.1% (Figure 26). PC1 was positively dominated by water temperature, DOC (Dis), Fe, Mn, P (Dis), and P (Tot). Negative correlations in PC1 stem from S and SO_4^{2-} . PC2 was positively correlated with air temperature, pH, conductivity, and to a certain extent P (Tot), P (Dis), S, and SO_4^{2-} . It was negatively correlated with precipitation, Secchi depth, and Mn.

The PCC (Appendix I) shows that DOC (Dis) only was positively correlated with Fe (p-value = 0.04, coefficient 0.895). Fe was also significantly positively correlated with water temperature (p-value = 0.017, coefficient 0.94). Fe was negatively correlated with SO_4^{2-} and S.

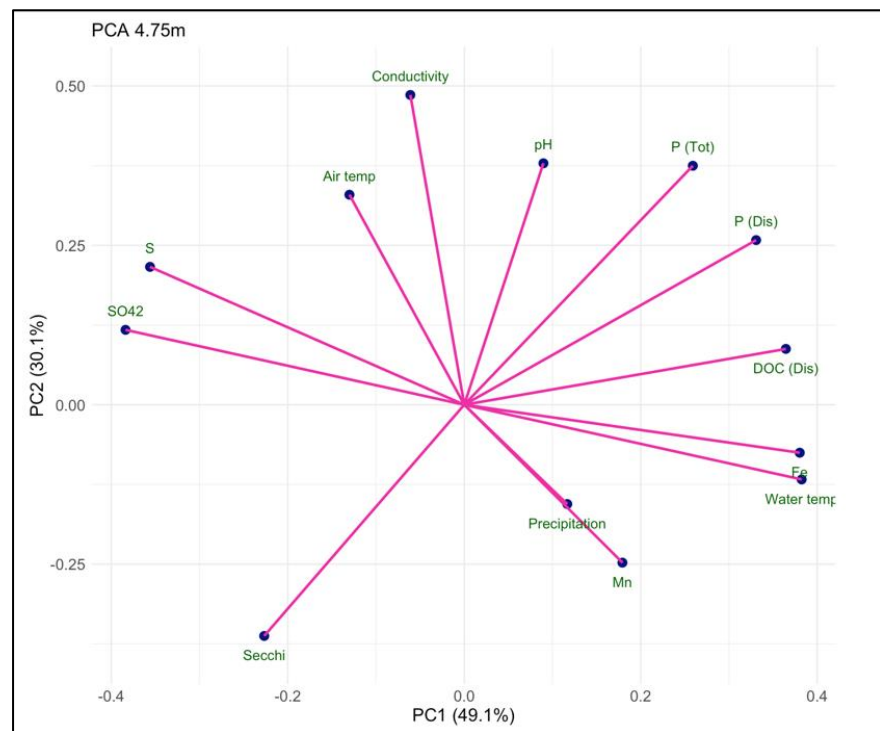


Figure 26. Principal component analysis at a depth of 4.75m. Including the following variables: dissolved organic carbon (DOC), manganese (Mn), iron (Fe), total phosphorus (P (Tot)), dissolved phosphorus (P (Dis)), sulfur (S), sulfate (SO_4^{2-}), oxygen saturation ($\text{O}_2\%$), pH, conductivity, Secchi depth (Secchi), water temperature (Water temp), air temperature (Air temp), and precipitation.

4. Discussion

The discussion is divided based on the oxygen conditions in Lake Solbergvann. This division includes oxic conditions, a transition zone between oxic and anoxic conditions, and fully anoxic conditions. First, the drivers of the changing DOM concentrations and DOM dynamics are discussed, followed by a thorough explanation of the role of oxygen that interacts with these dynamics. The following abbreviations are used to describe the fractions of the molecular weight of CDOM: CDOM1 (< 1 kDa), CDOM2 (1 – 3 kDa), CDOM3 (3 - 10 kDa), and CDOM4 (> 10 kDa).

4.1 Oxic conditions

4.1.1 Weather changes impacting DOM dynamics

The great variability in dissolved organic matter (DOM) in Lake Solbergvann is most likely attributed to changes in weather conditions in the oxic part of the lake (0.75-1.75m), such as temperature and precipitation. The CDOM signal (Figure 19) and DOC concentrations (Figure 18) substantially increased throughout the sampling period. The CDOM and DOC levels were initially relatively low, but they nearly doubled.

In 2023, there was a strong deviation from the long-term trends (1991-2020) in both air temperature (Table 1) and precipitation (Table 2). In the spring, the air temperatures were high with little precipitation, followed by a shift to relatively lower air temperatures and higher precipitation in the summer, including several extreme rainfall events. Studies have indicated that external DOM sources account for a greater proportion of DOM in forest lakes than internal production, and weather conditions significantly impact external DOM sources (Meili, 1992; Pace & Cole, 2002; Warner & Saros, 2019). However, in-lake processes are also affected by weather conditions, such as the decomposition rate. The relatively cold climate in Norway restricts the decomposition of DOM (Evans et al., 2006; Jennings et al., 2010). The high temperatures in the spring could have increased the decomposition rate of DOM, followed by a slower rate in the relatively colder months. This observation aligns with the findings in Lake Solbergvann, where DOM concentrations were lower during periods of higher temperatures and vice versa.

Furthermore, higher DOM concentrations were observed during periods of higher precipitation in the lake throughout the study period, although no statistically significant correlation was found between these variables. Precipitation facilitates DOM inflow to water bodies by generating runoff that act as a transportation agent. Thus, low DOM concentrations

are commonly observed during periods of low precipitation because there is less DOM inflow from terrestrial sources (Laudon et al., 2011; Pace & Cole, 2002). Precipitation can also affect the pH in the soil, thus impacting runoff conditions. During dry periods, the soil may oxidize, which can oxidize sulfur to sulfate.; This process creates more acidic soils, reducing the solubility of DOM due to protonation effects (Clark et al., 2005). Consequently, the reduced solubility of DOM reduces the mobility of terrestrial DOM to water bodies.

The extreme rainfall events that occurred on 8 August (49mm), 20 August (42mm), and 27 August (73mm) had varying effects on the DOM concentrations in Lake Solbergvann. It was observed that the CDOM signal increased on all the subsequent sampling occasions (9 August, 23 August, 6 September). Yet, despite comparable precipitation events, the CDOM signal on 9 August did not increase to the same degree as on 23 August and 6 September. A plausible explanation can be through variations in the amount of contact that was established with soil organic matter (Worrall et al., 2002). On 9 August, the heavy rainfall occurred less than 24 hours before sampling, possibly resulting in less contact with soil organic matter compared to other sampling days. In addition, the soil in Lake Solbergvann's catchment could have been wetter after periods of high precipitation. Wetter soils also promote increased runoff conditions by activating subsurface flow resulting from an increased water table that triggers additional runoff (Penna et al., 2011). The increase in the carbon-to-nitrogen ratio on 23 August and 6 September, but just a slight increase on 9 August, further supports this fluctuation in runoff. Allochthonous material generally contains less nitrogen compared to autochthonous material (Royer & Minshall, 1997). An increase in the C:N ratio suggests a notable inflow of allochthonous material on 23 August and 6 September, and to a lesser extent on 9 August. Earlier studies have demonstrated that heavy precipitation can have mixed effects on the DOM concentrations in lakes (Warner & Saros, 2019). For instance, precipitation can result in dilution effects (Wang et al., 2019) or changes in water retention time (Wetzel, 2001). This directly influences the degradation and sedimentation rates of DOM, while also affecting redox reactions, which may affect DOM dynamics (Hongve et al., 2004; Stanley et al., 2012).

The DOM dynamics in this oxic part of the lake were characterized by significant positive correlations between all CDOM fractions with DOC, except for CDOM2 at 1.75m. These findings closely align with the observations made by Griffin et al. (2018) and Lau et al. (2024), who reported that lakes that mainly receive allochthonous DOM generally show significant positive correlations between CDOM and DOC as well as display less diversity in their molecular composition.

Changes in the DOM dynamics were observed after the heavy rainfall events. The molecular weight (MW) of CDOM increased compared to drier periods. CDOM3 was the most abundant (58.5%), followed by CDOM2 (19.6%), CDOM4 (15.3%), and CDOM1 (6.6%). Even though no significant correlations were found between any of the CDOM fractions and precipitation, the correlation coefficient increased as the MW rose, suggesting a possible association between precipitation and the MW of CDOM. DOM compounds of a MW > 1 kDa usually consist of humic substances, soluble proteins, and carbohydrates, while low MW (<1 kDa) contains fatty acids, free sugars, and amino acids (O'Loughlin & Chin, 2004). It is worth noting that DOM consists of many overlapping groups, so attempting to classify each fraction into distinct functional groups would not be feasible or accurate (O'Loughlin & Chin, 2004; Yan et al., 2012). Given the large proportion of high MW, humic compounds most likely make up a sizable portion of Lake Solbergvann's DOM.

Previous studies have verified that high-flow conditions usually result in CDOM of high MW (> 10 kDa) (Riise et al., 1994). High-flow conditions impact the hydrological pathway of water, affecting the kind of terrestrial DOM carried with it and ultimately influencing the properties of DOM found in water bodies (Hongve et al., 2004). This size fraction of > 10 kDa is also associated with the increased inflow of Fe (Riise et al., 1994). In Lake Solbergvann, Fe held significant positive correlations with CDOM3 and CDOM4. These higher MW compounds are usually aromatic substances and are known to bind more to metals due to their higher electrostatic potential and ligands (Zhou et al., 2000). This relationship between MW and Fe is particularly important for lakes surrounded by coniferous forests, like Lake Solbergvann (Riise et al., 2023). These forest soils usually contain higher DOM and Fe concentrations (Björnerås et al., 2017). Increasing concentrations in DOM and Fe may contribute to the browning of water (Björnerås et al., 2017; Kritzberg & Ekström, 2012), which was a phenomenon that was also reported in a long-term study in Lake Solbergvann (Riise et al., 2023). It was also found that CDOM of higher MW contributes more to lake color than CDOM of lower MW (Lau et al., 2024; Riise et al., 2023). Although lake color was not measured directly in Lake Solbergvann, the Secchi depth – a measure of water transparency – was not significantly correlated with any CDOM fractions.

Apart from the processes mentioned earlier that affect the correlation between precipitation and DOM, the analysis was probably affected by the small sample size, irregular sampling intervals (every 14 days), and highly variable precipitation. These factors prevented the analysis from capturing the initial and subsequent effects of the runoff rates on CDOM export, leading to insignificant correlations between the variables (Jennings et al., 2010).

4.1.2 Other potential drivers impacting DOM dynamics

DOM can also derive from primary production (Bertilsson & Jones, 2003; Stedmon & Markager, 2005). In Lake Solbergvann, chlorophyll a was found in the entire water column, with an average of 3.6 $\mu\text{g/L}$ across all samples. The highest average concentrations of chlorophyll a were found in these oxic water layers (with an average of 4.8 $\mu\text{g/L}$). Here, CDOM₂ was the only fraction that exhibited a positive, although insignificant, correlation with chlorophyll a. This observation hints at the potential influence of autochthonous material on DOM dynamics as the relative proportion of CDOM of lower MW increased closer to the surface waters. Due to its high susceptibility to degradation, autochthonous material is typically of lower MW (Lepane et al., 2004; M. Li et al., 2022). However, primary production can be restricted due to high DOM concentrations through increased respiration, shading, and reduced mixing of nutrients from deeper water layers (Brothers et al., 2014).

In the upper strata of Lake Solbergvann, the DOM dynamics are likely also influenced by photobleaching. Photobleaching, where sunlight degrades CDOM, alters the CDOM properties, such as molecular weight distribution (Maizel & Remucal, 2017). These authors found that photochemical degradation of CDOM is more efficient for CDOM of lower MW, and this degradation leads to the creation of even smaller compounds. Although UV exposure had not been measured in Lake Solbergvann, the idea that photodegradation affected the DOM dynamics would seem plausible.

4.1.3 Isolation of Oxic Waters by Thermal Stratification

The pronounced variations in air temperature and precipitation might also have impacted the thermal stratification in Lake Solbergvann, as shown from other lakes (Caplanne & Laurion, 2008; Elçi, 2008; Holgerson et al., 2022; Liu et al., 2020; Tate et al., 2007). Lake Solbergvann was already thermally stratified before the start of the sampling period (Figure 7). The thermal stratification reached its peak by the end of June, and the lake remained thermally stratified until the end of the sampling period. Most of the seasonal variation of DOM was observed in these oxic water layers, indicating that the lake was strongly impacted by barriers that prevented DOM transportation to deeper waters.

Water temperature was shown to be impacted by air temperature and precipitation. At 0.75m, there was a significant positive correlation between air and water temperatures, but not at 1.75m. Precipitation appeared to have influenced water temperature, as a positive significant

correlation arose at 1.75m, but it showed a negative insignificant correlation at 0.75m. These contrasting correlations may suggest a decrease in the stability of the thermal stratification.

High concentrations of DOM have been shown to enhance the intensity of thermal stratification (Caplanne & Laurion, 2008). In Lake Solbergvann, the period of the strongest thermal stratification did not correspond with the period of the highest DOM concentrations. The spring of 2023 was exceptionally warm and had minimal precipitation. This can result in high DOM decomposition rates due to warmer temperatures (Gudas et al., 2015) and limited inflow of terrestrial DOM (Laudon et al., 2011; Pace & Cole, 2002), resulting in relatively low DOM concentrations while the thermal stratification intensified.

Thermal stratification probably obstructed DOM movement as these waters became rather isolated. The DOM accumulated in these oxic layers, which affected the pH. Between 31 May and 6 September, the pH dropped from 6.8 to 4.6, and it was generally lower during periods of high precipitation. The pH exhibited significant negative correlations with all DOM measurements, except for CDOM1 and CDOM2. The increased DOM concentrations at these surface layers may have contributed to a decreasing pH by increasing concentrations of humic and fulvic acids that are mainly present in larger DOM compounds ($kDa > 1$) (O'Loughlin & Chin, 2004). These compounds are weak acids, thus decreasing the pH. Other factors that could have affected the pH are increased CO₂ concentrations due to intensified DOM decomposition and primary production, (Monteith et al., 2007; Wetzel, 2001). However, this research on Lake Solbergvann did not measure all the variables needed to provide statistical evidence for these relationships.

4.1.4 Oxygen Dynamics

Oxygen (O₂) was primarily restricted to the surface layers in Lake Solbergvann as a result of the barriers created by thermal stratification, which was also found in other lakes by Elçi (2008).

The O₂ saturation slightly decreased towards the end of the sampling period, and significant negative correlations between O₂ saturation and DOM were found at these depths. This correlation can be explained through increased O₂ demand by increased microbial activity (Köhler et al., 2013; Wetzel, 2001). While decomposing DOM, these microbial organisms consume O₂ in the process, thus leading to a decrease in O₂ under elevated DOM concentrations.

Furthermore, O₂ saturation showed a significant positive relationship with water temperature at 0.75m. A plausible explanation can be that warmer temperatures increase photosynthetic activity by promoting enzyme activity and metabolism (Coles & Jones, 2000). No statistical significance was found between chlorophyll a concentrations and O₂ saturation. However, phytoplankton can move through the water column to reach optimal light and nutrient availability conditions, especially under poorly mixed conditions (Klausmeier & Litchman, 2001). These moving algae could have resulted in localized variations in chlorophyll a and O₂ that had not been captured with the methods used in this study. Moreover, the relationship between chlorophyll a and O₂ is not straightforward as phytoplankton can both produce and consume oxygen, depending on the environmental conditions

The results also showed a slight decrease in O₂ saturation at 0.75m, while an increase occurred at 1.75m during periods of increased precipitation. Precipitation can induce mixing of water layers and facilitate the transportation of O₂ to deeper water layers (Liu et al., 2020). However, the observed fluctuations in O₂ and precipitation in Lake Solbergvann were not significantly correlated. It has been observed that after heavy rainfall, microbial organisms consume O₂ at an accelerated rate (Ma et al., 2015). This phenomenon might not have been captured in Lake Solbergvann due to the low sampling frequency.

4.2 Transition Zone

4.2.1 A Complex Interplay of Processes as a Source for DOM Variability

The Total CDOM (Figure 19) remained relatively stable during the entire sampling period in this transition zone between oxic and anoxic water (2.75m), while the DOC concentrations (Figure 18) slightly decreased until the beginning of August, followed by a minor increase. It was also observed that this depth contained more DOM than the oxic waters until early August but less DOM than the anoxic waters. The dynamics between CDOM and DOC changed at this depth compared to the oxic waters. Only CDOM₃, CDOM₄, and Total CDOM showed a significant positive correlation with each other. CDOM₁ and CDOM₄ exhibited a negative significant correlation instead of a positive one, as observed in the oxic waters (Figure 23-24). This negative correlation could have been the result of the breakdown of larger CDOM compounds. DOC was not correlated with any CDOM fractions.

These DOM dynamics are possibly influenced by several processes that occur simultaneously. A positive significant correlation between precipitation and water temperature was observed in this transition zone, which decreased the temperature difference between the

surface and deeper water layers, thus decreasing the stability of the thermal stratification. Previous studies have suggested that weakened thermal stratification enhances the mixing of water layers (Holgerson et al., 2022) and diminishes the barrier of DOM transportation from surface layers to deeper waters (Bach et al., 2012). Eventually, this results in enhanced DOM fluxes and an accumulation of DOM in deeper water layers (Bach et al., 2012). This was particularly evident on 9 August, when the water temperature in the upper layers of the lake showed a large decrease after an extreme rainfall event. This heavy rainfall event likely impacted the DOM transportation from oxic waters to this transition zone, as more CDOM of lower molecular weight was present on this date compared to the overall trend. Other processes mentioned in section 4.1 may also be relevant for the DOM dynamics in this transition zone.

It has been reported that DOM can also leach out the sediment under anoxic conditions (Brothers et al., 2014; Peter et al., 2016). The diffusion of DOM from anoxic water to this transition zone might have occurred slowly due to stratification barriers. However, the distinct set of variable distribution (Figure 23) at this depth compared to the oxic water layers makes it likely that this transition zone is also influenced by processes in anoxic waters, creating greater variability.

Moreover, it had been observed that bacteriochlorophyll started to be present at this depth (Appendix B), along with significant positive correlations between S and DOM. These bacteria reduce sulfate to hydrogen sulfide (H_2S) or result in the oxidation of S (see section 4.2.2) for this. Primary producers can use H_2S through chemosynthesis to produce organic compounds; thereby, H_2S can indirectly contribute to the DOM pool (Yacobi et al., 2014).

4.2.2 Oxygen Dynamics

Oxygen (O_2) was present at this depth on all the sampling days, but its O_2 saturation was always below 3.5%. Unexpectedly, O_2 saturation or concentration was not significantly correlated with any of the DOM measurements. Previous studies suggested that the influx of DOM may exceed the O_2 inflow due to stratification barriers (Hajizadeh, 2007), and the relatively higher temperatures at this depth compared to deeper water layers can accelerate the DOM decomposition rates, potentially leading to a complete depletion of O_2 at this depth (Brothers et al., 2014; Wetzel, 2001). The relatively low sampling frequency and resolution may not have captured these variations accurately, thus resulting in insignificant correlations.

The O_2 conditions also indirectly impacted the pH, with significant positive correlations for both O_2 concentration and O_2 saturation and pH found in Lake Solbergvann. The pH was

generally lower in this transition zone compared to oxic and anoxic waters. This relationship can be explained by the oxidation process of sulfur (S) and the formation of sulfuric acid (H₂SO₄) (Kellogg et al., 1972), which is a process that decreases the pH. This concept of S oxidization was supported by the fact that this transition zone generally contained the highest relative share of SO₄²⁻ compared to S, thus impacting the pH in Lake Solbergvann. On the other hand, sulfate-reducing bacteria started to be present at this depth, but were not as abundant compared to deeper water layers. Nevertheless, none of these correlations between O₂, pH, SO₄, and S were statistically significant. This could have resulted from the complex interplay between sulfate-reducing conditions versus sulfur-oxidizing conditions and other variables influencing the O₂ conditions and pH in Lake Solbergvann.

Furthermore, a negative significance correlation was observed between O₂ and manganese (Mn), and trended towards significance with iron (Fe) (p-value 0.057). The O₂ conditions are of great importance for the speciation of Fe and Mn (Knorr, 2013; Kritzberg & Ekström, 2012; Peter et al., 2016; Skoog & Arias-Esquivel, 2009), which will be discussed in greater detail in section 4.3.2. In the presence of O₂, these substances tend to aggregate and settle after oxidization, thus removing them from this part of the water column (Lidman et al., 2017; Martin, 2005), while the released DOM remains in the water column (Lau et al., 2024). This ties nicely with the findings in Lake Solbergvann, where Fe and Mn concentrations exhibit a strong vertical gradient across the water column, with higher concentrations observed in the deeper water layers, but DOM concentrations did not show a similar pattern. These substances are derived from terrestrial sources, and increased export is expected due to higher temperatures and increased rainfall (Björnerås et al., 2017), which could have large implications for DOM dynamics in lakes with varying O₂ conditions.

4.3 Anoxic conditions

4.3.1 Isolated anoxic waters, yet increasing DOM concentrations

The Total CDOM showed a gradual increase at the depths of 3.75m and 4.25m (Figure 19), but no measurements of CDOM were taken at 4.75m. The DOC concentrations decreased at 3.75m, and fluctuated at 4.25m, but showed a stable increase at 4.75m (Figure 18). This resulted in significant negative correlations between DOC and CDOM₃, and DOC and Total CDOM at 3.75m. Other significant correlations included a negative correlation between CDOM₂ and CDOM₄, and a positive correlation between CDOM₃ and Total CDOM at 3.75m. Only CDOM₃ and Total CDOM were significantly positively correlated at 4.25m. These

findings demonstrate different DOM dynamics compared to shallower water layers. A recent study also observed greater heterogeneity in the molecular composition of DOM under anoxic conditions (Lau et al., 2024).

In Lake Solbergvann, these depths showed stable water temperatures, conductivity, and O₂ concentrations. These stable conditions suggest a limited mixing of water layers, resulting in an isolated water layer that excludes inflow from above (El Kateb et al., 2018; Peter et al., 2016). In addition, there was no indication of a dilution effect on DOM at these depths. This is supported by the high stable conductivity, a measurement of dissolved ions, in the deeper water layers while the DOM concentrations only slightly increased, suggesting that inflowing water is not the primary source of these dissolved ions. In the case of inflowing water, the conductivity would have decreased due to dilution, while the DOM concentrations would have increased. Since conductivity is influenced by the concentrations of dissolved ions, such as salts and minerals, the high conductivity in the deeper layers implies that these may originate from sources other than inflowing waters. At 3.75m and 4.25m, conductivity was significantly positively correlated with iron (Fe), which can be released with DOM from the sediment under anoxic conditions (Björnerås et al., 2019; Brothers et al., 2014; Peter et al., 2016).

Despite the fact that these water layers had been isolated, the Total CDOM increased. Increases in CDOM₃ and CDOM₄ mostly drove this increase. By linking the findings of DOM leaching out of the sediment under anoxic conditions (Björnerås et al., 2019; Brothers et al., 2014; Peter et al., 2016) with research on the molecular weight (MW) of DOM within sediment cores in lakes (O'Loughlin & Chin, 2004), a plausible explanation for the increase in CDOM₃ and CDOM₄ emerges. O'Loughlin and Chin (2004) demonstrated that the upper layer of the sediment core in lakes usually contains DOM of higher MW compounds compared to deeper sediment layers. The DOM in deeper sediment layers is exposed for a prolonged time to microbial and abiotic degradation, thus resulting in lower MW compounds due to degradation (O'Loughlin & Chin, 2004).

In addition, a relationship between the MW of CDOM and pH emerged at these depths in Lake Solbergvann. CDOM was at its overall highest MW at the end of July, which occurred simultaneously with the lowest pH. A significant negative correlation between CDOM₄ and pH statistically supported this relationship. The initial decrease in pH might result from the intensive decomposition of DOM, which increases CO₂ concentrations while consuming hydrogen ions (Wetzel, 2001). Lau et al. (2024) reported that DOM leached out of the sediment consists of highly photo- and biolability compounds. This DOM appeared to be less stable, making it more easily metabolized because of its distinct molecular composition. This DOM

was also no longer shielded by Fe, which typically protects DOM from decomposition. Linking these observations by O'Loughlin and Chin (2004) and Lau et al. (2024) to the findings in Lake Solbergvann, it is reasonable to hypothesize that following the initial release of larger and more reactive DOM compounds, subsequent DOM releases may include less reactive and more recalcitrant compounds. This could restrict DOM decomposition, and thus contribute to a stagnant pH, while other processes like dissimilatory reduction, which raises the pH (Grybos et al., 2009), likely continued.

In addition, previous studies observed that DOM and Fe can be co-released from the sediment under anoxic conditions (Björnerås et al., 2019; Kritzberg & Ekström, 2012; Lau et al., 2024). The results of Lake Solbergvann go beyond those previous reports, showing that Fe concentrations increased simultaneously with CDOM of higher MW (CDOM₃). Previous studies have shown that the MW of DOM influences the binding capacity to inorganic substances (Y. Li et al., 2022). Fe preferably binds to humic substances of higher MW due to their higher density of carboxylic and phenolic groups, which enhances the strength and speed of the Fe-OM complexes (Avena & Koopal, 1999; Y. Li et al., 2022). These humic substances can act as electron donors that incite microbial iron reduction (Johnson et al., 2012; Stumm & Sulzberger, 1992), thus further supporting Fe release from the sediment under anoxic conditions. This interplay between Fe and DOM dynamics, coupled with the potential for microbial iron reduction stimulated by humic substances, suggests the possibility of a positive feedback loop. The release of Fe from sediment leads to increased DOM concentrations, which, in turn, enhance Fe release through complexation and microbial processes. This feedback loop could further increase Fe and DOM concentrations under anoxic conditions.

4.3.2 Oxygen Dynamics

No oxygen (O₂) was present on any of the sampling dates at depths below 3.75m. In anoxic waters, the metabolism is mainly driven by heterotrophic and bacterial processes that further deplete O₂ at this depth (Brothers et al., 2014; Wetzel, 2001). As briefly mentioned in section 4.2.2, O₂ conditions play a central role in the speciation of iron (Fe) and manganese (Mn), especially in humic boreal lakes (Peter et al., 2016), thereby influencing the internal dynamics of DOM.

A large increase in Fe concentrations was observed in Lake Solbergvann's anoxic waters. Significant positive correlations were found between Fe and CDOM₃ at depths of 3.75m and 4.25m and with Total CDOM at 4.25m. Interestingly, Fe was only significantly correlated with DOC at 4.75m, but not at the other depths. These inconsistencies of significant

or insignificant correlations between DOM and Fe align with the studies by Xiao and Riise (2021) and Riise et al. (2023). Xiao and Riise (2021) reported that lakes with short water retention times, such as Lake Solbergvann with 0.5 years, are more prone to changing flow conditions due to the rapid response of these systems, thus showing higher variability in Fe concentrations. In addition, Riise et al. (2023) observed that elevated Fe concentrations may not necessarily lead to increased DOM concentrations, as specific interactions between Fe and DOM, influenced by factors like redox conditions, and the presence of nitrate (NO_3^-) and sulfate (SO_4^{2-}), and pH may play a significant role.

Anoxic conditions may trigger the release of DOM from the sediment (Brothers et al., 2014; Peter et al., 2016; Skoog & Arias-Esquivel, 2009). The mobilization of DOM is facilitated by the redox reaction from Fe(III) to Fe(II) under anoxic conditions (O'Loughlin & Chin, 2004). In oxic water, Fe is present as Fe(III). Fe(III) functions as a chemical trap for DOM in the sediment, and the reduction of Fe releases the associated DOM (Riedel et al., 2013). The redox dynamics of Fe are also influenced by the presence of compounds such as NO_3^- and SO_4^{2-} (Knorr, 2013; Musolff et al., 2017). The NO_3^- concentrations were below the detection limit, while the SO_4^{2-} concentrations declined throughout the sampling period. An inverse relationship between $\text{NO}_3^-/\text{SO}_4^{2-}$ and Fe(III) reduction can occur due to competition of alternative oxygen electron acceptors under anoxic conditions (Musolff et al., 2017). The NO_3^- concentrations were below the detection limit in Lake Solbergvann, which makes this competition less likely and favors the reduction of Fe(III). Fe and SO_4^{2-} showed a significant negative correlation. The increasing Fe and decreasing SO_4^{2-} concentrations may indicate a transition in anaerobic respiration from SO_4^{2-} to Fe(III), which promotes Fe(III) reduction. Previous studies have demonstrated that this shift in anaerobic respiration can occur more frequently due to decreases in atmospheric sulfur deposition (Knorr, 2013). Further evidence for this idea includes the decreasing relative share of SO_4^{2-} compared to S in the deepest layer of Lake Solbergvann (Figures 16 and 17). These conditions that favor Fe(III) reduction likely also contributed to an increase in CDOM3, making anoxic waters a major contributor to the DOM pool.

Furthermore, simultaneous increases in Mn and DOM were also observed in Lake Solbergvann, where Mn had a significant positive correlation with Total CDOM. Similarly to Fe, Mn also binds to DOM (Tipping & Heaton, 1983), responds to redox conditions, and is influenced by pH (Brüggenwirth et al., 2024). Previous studies reported positive correlations between Fe, Mn, and DOM, supporting the interconnected nature of these variables (Grybos et al., 2009; Skoog & Arias-Esquivel, 2009).

4.3.3 pH as a mediator for Fe, DOM and P release

Fluctuations in pH were observed, with an initial decrease until July, followed by a gradual increase until the last sampling day (Figure 9). The PCA plots (Figure 2-26) revealed a positive association between pH and CDOM1 and CDOM2, but a negative association between those variables and Total CDOM, CDOM3, CDOM4, and Fe. Fluctuations in pH directly and indirectly affect DOM mobility (Clark et al., 2005; Grybos et al., 2009; Stumm & Morgan, 1996), making them crucial factors for explaining DOM variability (Figure 27).

The initial decrease in pH could have been caused by the intense decomposition of DOM (see section 4.3.1), but the pH slightly increased during the second half of the sampling period. An increase in pH in anoxic water can be the result of dissimilatory reduction that triggers proton consumption when microorganisms utilize alternative electrons, such as SO_4^{2-} , NO_3^- , Fe, and Mn, instead of O_2 (Grybos et al., 2009). The proton consumption by microorganisms leads to a decrease in free hydrogen ions in the water, thus increasing the pH of the water (Grybos et al., 2009). However, the measurements in Lake Solbergvann did not include a detailed speciation of these substances, thus accurate correlations between pH and these substances cannot be established. It is worth noting that some substances, such as SO_4^{2-} and NO_3^- , can influence the Fe dynamics in multiple ways. For example, their presence may hinder the reduction of Fe(III) to Fe(II), while the reduction of $\text{SO}_4^{2-}/\text{NO}_3^-$ increases the pH (Grybos et al., 2009). Thus, it interacts with the reduction potential of Fe directly through its presence of alternative electron acceptors and indirectly through changing the pH. Since the pH was relatively low during the entire sampling period, the reduction of Fe was most likely hindered by the initial high presence of SO_4^{2-} .

The changes in pH impact the dynamics of organic and inorganic substances (Figure 27). Long-term studies have shown that the pH in Lake Solbergvann has decreased during autumn circulation periods in the past 40 years while total organic carbon concentrations increased (Riise et al., 2023). This may seem contradictory, as it has been observed that an elevated pH may drive DOM release as it weakens the overall adsorption of DOM to particulate organic matter, making DOM more soluble (Clark et al., 2005; Grybos et al., 2009). It has also been found that a higher pH weakens the mineral-DOM adsorption interactions, consequently, DOM is being released from Fe (Grybos et al., 2009). For inorganic substances such as Fe, the pH affects the speciation of this substance (Küsel et al., 2002). A higher pH favors the presence of Fe(III) over Fe(II), which is less soluble compared to Fe(II) (Grybos et al., 2009; Lau et al., 2024; Stumm & Sulzberger, 1992). Meanwhile, a low pH can facilitate the release of Fe from

sediments into the water column (Lau et al., 2024). In line with previous studies (Lau et al., 2024; O'Loughlin & Chin, 2004), this Fe from the sediment co-releases CDOM. In Lake Solbergvann, this co-release of CDOM consisted of a molecular weight between 3 kDa and 10 kDa. Thus, the DOM dynamics are also highly dependent on the mechanisms that are being triggered under specific environmental conditions. Figure 27 summarizes the different processes in the anoxic waters that trigger DOM release. Although research has documented this internal DOM release from aquatic environments under anoxic conditions, it is often overlooked in calculations concerning the carbon cycle (Mendonça et al., 2016; Sobek et al., 2009). It has been found that oxygen-depleted waters usually have high DOM burial efficiency due to less efficient DOM mineralization and respiration (Isidorova et al., 2016; Sobek et al., 2009). However, not accounting for internal DOM release overestimates the carbon burial and does not fully represent the carbon cycle. As can be observed in Figure 27, internal DOM release can be triggered through different mechanisms. This may have cascading effects on ecosystems as increased DOM concentrations are associated with increased watercolor (Solomon et al., 2015).

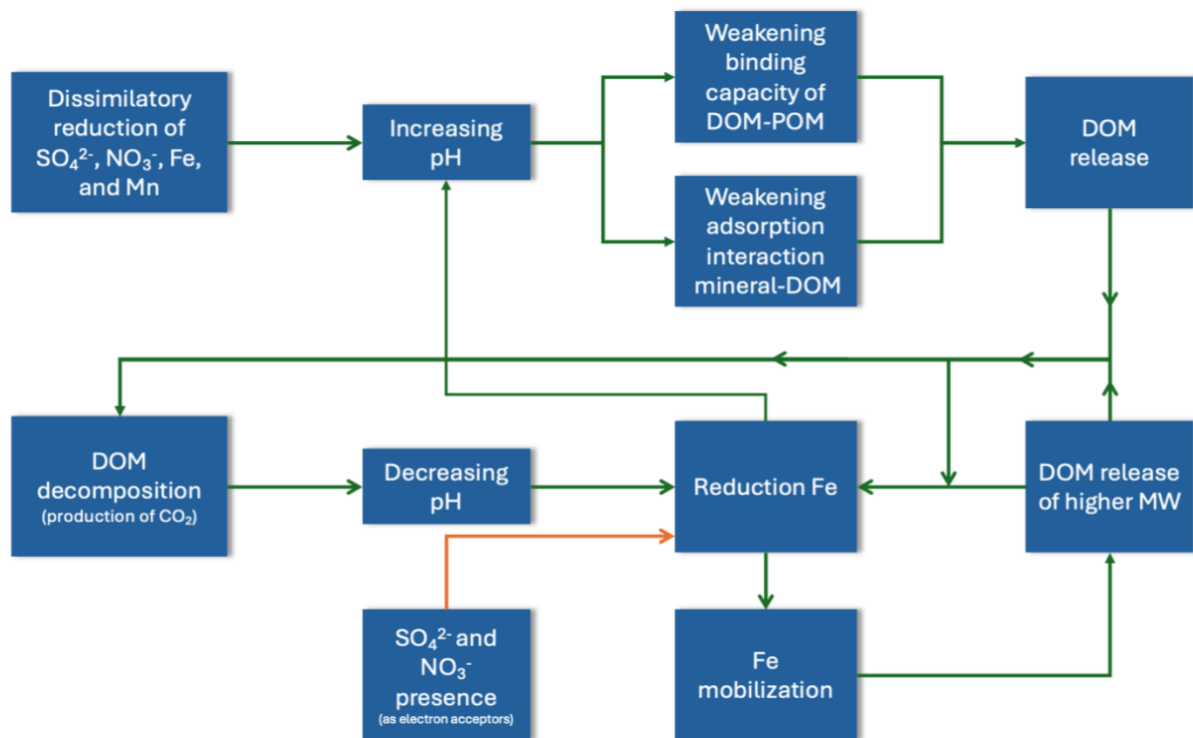


Figure 27. Key mechanisms behind internal DOM release. Dissimilatory reduction (using alternative electron acceptors by microbes) increases the pH. An elevated pH weakens the binding capacity of DOM to POM and weakens the adsorption interaction of mineral-DOM, which results in DOM release. The decomposition of DOM releases CO₂ thus decreasing the pH. A decreasing pH increases the reduction potential of Fe, but this process can be hindered (indicated by the red line) by the presence of other substance (SO₄²⁻ and NO₃⁻) that can act as electron acceptors. The reduction of Fe, results in a mobilization of Fe from the sediment. This Fe releases the associated DOM of 3-10 kDa. The release of DOM can also result in a positive feedback loop with Fe reduction as DOM can increase the potential for microbial Fe reduction.

Contrary to findings from previous studies (Brothers et al., 2014; Peter et al., 2016; Skoog & Arias-Esquivel, 2009), statistically significant support for increased internal phosphorus (P) release coupled with DOM/Fe release was not found in Lake Solbergvann. Despite observing a strong gradient for dissolved and Total P, with higher concentrations in deeper water layers, neither exhibited a significant positive correlation with Fe or CDOM/DOC. At 4.75m, a slight gradual increase of dissolved and Total P was noted. At this depth, DOC was positively associated with dissolved P (coefficient 0.80) and Total P (coefficient 0.69), though these correlations were not statistically significant. This P increase could be attributed to P leaching from the sediment under anoxic conditions (Brothers et al., 2014; Skoog & Arias-Esquivel, 2009). The lack of significant findings may be attributed to suboptimal pH conditions for P to leach out of the sediment. Under optimal conditions, P leaches out of the sediment at a pH of 6-7 (Wetzel, 2001), but the average pH across these depths in Lake Solbergvann was only 5.5. While higher pH levels were commonly reported in previous field observations or laboratory experiments (Brothers et al., 2014; Peter et al., 2016).

Furthermore, it was observed that dissolved P concentrations declined at 3.75m and 4.25m. One statistically significant negative correlation between dissolved P and Fe was found at these depths, suggesting a potential interaction between these variables. One possible explanation for the decline in dissolved P concentrations at these depths could be the precipitation or binding of phosphorus with Fe compounds when the pH is lower than 6.2 (Ping et al., 2023). The low pH and the abundant Fe in Lake Solbergvann possibly resulted in the formation of Fe-P complexes, reducing the concentration of dissolved P in the water column.

5. Conclusion

This study aimed to examine the dynamics of internal dissolved organic matter (DOM) by focusing on the role of stratification and the prevalence of oxygen on these dynamics across different depths in Lake Solbergvann. Although attempts were made to clarify the interactions between DOM and other variables based on the oxygen conditions to enhance the understanding of DOM dynamics, it is important to note that these interactions do not always result in linear relationships. However, the result of this research demonstrated that stratification and oxygen play a major role in shaping the DOM dynamics in a lake.

Firstly, there was nearly a twofold increase in chromophoric dissolved organic matter (CDOM) and dissolved organic carbon (DOC) concentrations in the oxic water layers during the sampling period (May – September 2023). This increase is likely the result of weather fluctuations affecting this surface layer in Lake Solbergvann. Lower air temperatures and more precipitation were associated with higher DOM concentrations. Air temperature significantly affected the water temperature, triggering strong thermal stratification, which created barriers for oxygen diffusion and DOM transport to deeper layers. Consequently, most of the seasonal variation was observed in these oxic layers. Extreme rainfall had varying effects on the DOM concentrations in the lake, possibly the result of different terrestrial conditions that impacted the amount of runoff under heavy precipitation. Furthermore, the molecular weight fractions of CDOM exhibited strong positive significant correlations with DOC, except for CDOM₂ (1 – 3 kDa). Lakes largely supplied with terrestrial DOM generally have little variation in their molecular composition and are frequently shown to exhibit strong correlations between CDOM and DOC (Griffin et al., 2018; Lau et al., 2024). The overall molecular weight of CDOM increased after heavy precipitation events, concomitant with an increase in iron (Fe), suggesting a coupling of CDOM of higher molecular weight and Fe. These higher molecular weight DOM compounds also contribute relatively more to lake browning by absorbing more UV light and fluorescing more intensely (Lau et al., 2024).

Secondly, the transition zone between oxic and anoxic water displayed the greatest variability in DOM dynamics, but contained relatively stable CDOM and DOC concentrations. This water layer is influenced by DOM sedimentation from oxic waters and DOM leaching from the sediment from anoxic waters. Oxygen was present at a very low saturation. The pH variations caused by sulfur oxidation, lowered the pH. These variations were most noticeable in the transition zone, which also contained the largest proportion of sulfate to sulfur. Moreover, a negative significant relationship was observed between CDOM₁ (kDa < 1) and

CDOM4 (kDa > 10), indicating the breakdown of larger CDOM compounds leading to an increase in smaller CDOM compounds. The large variety of mechanisms that occur simultaneously likely increased the diversity in DOM dynamics in this zone.

Thirdly, under persistent anoxic conditions, CDOM, DOC, Fe, manganese, and phosphorus concentrations increased throughout the sampling period. These DOM dynamics differed from the other water layers, particularly by demonstrating the release of iron-bound DOM from the sediment, identified as CDOM3 (kDa 3 - 10). This CDOM3 exhibited a strong positive significant correlation with Fe. This relatively high molecular weight of CDOM might have resulted from the release of organic compounds in the sediment that had not undergone extensive decomposition and the preferred binding of Fe to humic substances of higher molecular weight. This released DOM impacts the internal DOM dynamics of a lake since it is easily metabolized. On the contrary, the high presence of sulfate, which increases the competition for alternative electron acceptors, and thus decreases the Fe reduction potential, was found to be one of the major factors limiting the release of Fe-bound DOM from the sediment. The pH was also an important mediator for DOM release by affecting DOM mobility, the binding capacity of DOM to POM, and the overall reduction potential of Fe. However, this study demonstrated that a low pH promotes increased Fe dissolution, thus influencing Fe reduction, which is the primary mechanism that results in increased DOM release under anoxic conditions.

This research provides insights into the interactions and mechanisms that govern DOM dynamics. While efforts were made to clarify these dynamics, it is important to acknowledge that the interactions between variables do not always conform to linear relationships. More research is needed to comprehensively understand the DOM dynamics in a boreal forest lake that capture non-linear relationships. Future research could also include other important factors, such as microbial activity, CO₂, and the exact speciation of Fe. Lastly, this study focused on the DOM dynamics during a summer stratification period; however, long-term monitoring is also necessary to comprehend seasonal and interannual variation in DOM dynamics. In conclusion, this study has shown thermal stratification and the development of hypolimnic anoxia might impact internal DOM dynamics.

6. References

- Avena, M. J., & Koopal, L. K. (1999). Kinetics of humic acid adsorption at solid-water interfaces. *Environmental science & technology*, 33(16), 2739-2744.
<https://doi.org/10.1021/es981236u>
- Bach, L. T., Riebesell, U., Sett, S., Febiri, S., Rzepka, P., & Schulz, K. G. (2012). An approach for particle sinking velocity measurements in the 3-400 µm size range and considerations on the effect of temperature on sinking rates. *Marine Biology*, 159(8), 1853-1864. <https://doi.org/10.1007/s00227-012-1945-2>
- Benedetti, M., Ranville, J. F., Ponthieu, M., & Pinheiro, J. P. (2002). Field-flow fractionation characterization and binding properties of particulate and colloidal organic matter from the Rio Amazon and Rio Negro. *Organic Geochemistry*, 33(3), 269-279.
[http://dx.doi.org/10.1016/S0146-6380\(01\)00159-0](http://dx.doi.org/10.1016/S0146-6380(01)00159-0)
- Benner, R., & Amon, R. M. W. (2015). The size-reactivity continuum of major bioelements in the ocean. *Annual Review of Marine Science*, 7(1), 185-205.
<https://doi.org/10.1146/annurev-marine-010213-135126>
- Bertilsson, S., & Jones, J. B. (2003). Supply of dissolved organic matter to aquatic ecosystems: autochthonous sources. *Aquatic ecosystems* (pp. 3-24). Academic Press.
<https://doi.org/10.1016/B978-012256371-3/50002-0>
- Björnerås, C., Škerlep, M., Floudas, D., Persson, P., & Kritzberg, E. S. (2019). High sulfate concentration enhances iron mobilization from organic soil to water. *Biogeochemistry*, 144(3), 245-259. <https://doi.org/10.1007/s10533-019-00581-6>
- Björnerås, C., Weyhenmeyer, G. A., Evans, C. D., Gessner, M. O., Grossart, H.-P., Kangur, K., Kokorite, I., Kortelainen, P., Laudon, H., Lehtoranta, J., Lottig, N., Monteith, D. T., Nöges, P., Nöges, T., Oulehle, F., Riise, G., Rusak, J. A., Räike, A., Sire, J., . . . Kritzberg, E. S. (2017). Widespread increases in iron concentration in European and North American freshwaters. *Global Biogeochemical Cycles*, 31(10), 1488-1500.
<https://doi.org/10.1002/2017GB005749>
- Blanchet, C. C., Arzel, C., Davranche, A., Kahilainen, K. K., Secondi, J., Taipale, S., Lindberg, H., Loehr, J., Manninen-Johansen, S., Sundell, J., Maanan, M., & Nummi, P. (2022). Ecology and extent of freshwater browning - What we know and what should be studied next in the context of global change. *Science of The Total Environment*, 812, 152420. <https://doi.org/10.1016/j.scitotenv.2021.152420>
- Brothers, S., Köhler, J., Attermeyer, K., Grossart, H. P., Mehner, T., Meyer, N., Scharnweber, K., & Hilt, S. (2014). A feedback loop links brownification and anoxia in a temperate, shallow lake. *Limnology and Oceanography*, 59(4), 1388-1398.
<https://doi.org/10.4319/lo.2014.59.4.1388>
- Brüggenwirth, L., Behrens, R., Schnee, L. S., Sauheith, L., Mikutta, R., & Mikutta, C. (2024). Interactions of manganese oxides with natural dissolved organic matter: Implications for soil organic carbon cycling. *Geochimica et Cosmochimica Acta*, 366, 182-200.
<https://doi.org/10.1016/j.gca.2023.12.016>
- Caplanne, S., & Laurion, I. (2008). Effect of chromophoric dissolved organic matter on epilimnetic stratification in lakes. *Aquatic Sciences*, 70(2), 123-133.
<https://doi.org/10.1007/s00027-007-7006-0>

- Chmiel, H. E., Niggemann, J., Kokic, J., Ferland, M.-È., Dittmar, T., & Sobek, S. (2015). Uncoupled organic matter burial and quality in boreal lake sediments over the Holocene. *Journal of Geophysical Research: Biogeosciences*, 120(9), 1751-1763. <https://doi.org/10.1002/2015JG002987>
- Clark, J. M., Chapman, P. J., Adamson, J. K., & Lane, S. N. (2005). Influence of drought-induced acidification on the mobility of dissolved organic carbon in peat soils. *Global Change Biology*, 11(5), 791-809. <https://doi.org/10.1111/j.1365-2486.2005.00937.x>
- Climate.data.org. (n.d.). *KLIMA: OSLO*. Retrieved on 16th of October 2023, from: <https://no.climate-data.org/europa/norge/oslo-1190/>
- Coles, J. F., & Jones, R. C. (2000). Effect of temperature on photosynthesis-light response and growth of four phytoplankton species isolated from a tidal freshwater river. *Journal of Phycology*, 36(1), 7-16. <https://doi.org/10.1046/j.1529-8817.2000.98219.x>
- Cooper, W. J., Zika, R. G., Petasne, R. G., & Fischer, A. M. (1989). *Sunlight-induced photochemistry of humic substances in natural waters: major reactive species*. American Chemical Society.
- de Wit, H. A., Valinia, S., Weyhenmeyer, G. A., Futter, M. N., Kortelainen, P., Austnes, K., Hessen, D. O., Råike, A., Laudon, H., & Vuorenmaa, J. (2016). Current browning of surface waters will be further promoted by wetter climate. *Environmental Science & Technology Letters*, 3(12), 430-435. <https://doi.org/10.1021/acs.estlett.6b00396>
- El Kateb, A., Rüggeberg, A., Stalder, C., Neururer, C., & Spezzaferri, S. (2018). High-resolution monitoring of water temperature and oxygen concentration in Lake Murten (Switzerland). *Swiss Journal of Geosciences*, 111(3), 501-510. <https://doi.org/10.1007/s00015-018-0316-5>
- Elçi, Ş. (2008). Effects of thermal stratification and mixing on reservoir water quality. *Limnology*, 9(2), 135-142. <https://doi.org/10.1007/s10201-008-0240-x>
- Evans, C. D., Chapman, P. J., Clark, J. M., Monteith, D. T., & Cresser, M. S. (2006). Alternative explanations for rising dissolved organic carbon export from organic soils. *Global Change Biology*, 12(11), 2044-2053. <https://doi.org/10.1111/j.1365-2486.2006.01241.x>
- Fasching, C., Behounek, B., Singer, G. A., & Battin, T. J. (2014). Microbial degradation of terrigenous dissolved organic matter and potential consequences for carbon cycling in brown-water streams. *Scientific reports*, 4(1), 4981. <https://doi.org/10.1038/srep04981>
- Fee, E., Hecky, R., Kasian, S., & Cruikshank, D. (1996). Effects of lake size, water clarity, and climatic variability on mixing depths in Canadian Shield lakes. *Limnology and Oceanography*, 41(5), 912-920. <https://doi.org/10.4319/lo.1996.41.5.0912>
- Finstad, A. G., Andersen, T., Larsen, S., Tominaga, K., Blumentrath, S., De Wit, H. A., Tømmervik, H., & Hessen, D. O. (2016). From greening to browning: Catchment vegetation development and reduced S-deposition promote organic carbon load on decadal time scales in Nordic lakes. *Scientific reports*, 6(1), 31944. <https://doi.org/10.1038/srep31944>
- Griffin, C. G., Finlay, J. C., Brezonik, P. L., Olmanson, L., & Hozalski, R. M. (2018). Limitations on using CDOM as a proxy for DOC in temperate lakes. *Water Research*, 144, 719-727. <https://doi.org/10.1016/j.watres.2018.08.007>

- Grybos, M., Davranche, M., Gruau, G., Petitjean, P., & Pédrot, M. (2009). Increasing pH drives organic matter solubilization from wetland soils under reducing conditions. *Geoderma*, 154(1-2), 13-19. <https://doi.org/10.1016/j.geoderma.2009.09.001>
- Gudasz, C., Sobek, S., Bastviken, D., Koehler, B., & Tranvik, L. J. (2015). Temperature sensitivity of organic carbon mineralization in contrasting lake sediments. *Journal of Geophysical Research: Biogeosciences*, 120(7), 1215-1225. <https://doi.org/10.1002/2015JG002928>
- Hajizadeh, Z. N. (2007). Characteristics and seasonal variations of dissolved oxygen. *International Environmental Resources*, 1(4), 296-301. https://www.researchgate.net/publication/27794348_Characteristics_and_Seasonal_Variations_of_Dissolved_Oxygen
- Holgerson, M. A., Richardson, D. C., Roith, J., Bortolotti, L. E., Finlay, K., Hornbach, D. J., Gurung, K., Ness, A., Andersen, M. R., & Bansal, S. (2022). Classifying mixing regimes in ponds and shallow lakes. *Water Resources Research*, 58(7). <http://doi.org/10.1029/2022WR032522>
- Hongve, D., Riise, G., & Kristiansen, J. F. (2004). Increased colour and organic acid concentrations in Norwegian forest lakes and drinking water—a result of increased precipitation? *Aquatic Sciences*, 66, 231-238. <https://doi.org/10.1007/s00027-004-0708-7>
- Isidorova, A., Bravo, A. G., Riise, G., Bouchet, S., Björn, E., & Sobek, S. (2016). The effect of lake browning and respiration mode on the burial and fate of carbon and mercury in the sediment of two boreal lakes. *Journal of Geophysical Research: Biogeosciences*, 121(1), 233-245. <https://doi.org/10.1002/2015JG003086>
- Jaffé, R., McKnight, D., Maie, N., Cory, R., McDowell, W. H., & Campbell, J. L. (2008). Spatial and temporal variations in DOM composition in ecosystems: The importance of long-term monitoring of optical properties. *Journal of Geophysical Research: Biogeosciences*, 113(G4). <https://doi.org/10.1029/2008JG000683>
- Jennings, E., Järvinen, M., Allott, N., Arvola, L., Moore, K., Naden, P., Aonghusa, C. N., Nöges, T., & Weyhenmeyer, G. A. (2010). Impacts of climate on the flux of dissolved organic carbon from catchments. *The impact of climate change on European lakes*, 199-220. Aquatic Ecology Series.
- Johnson, D. B., Kanao, T., & Hedrich, S. (2012). Redox transformations of iron at extremely low pH: fundamental and applied aspects. *Frontiers in microbiology*, 3, 96. <https://doi.org/10.3389/fmicb.2012.00096>
- Jones, R. I. (1992). The influence of humic substances on lacustrine planktonic food chains. *Hydrobiologia*, 229, 73-91. <https://doi.org/10.1007/BF00006992>
- Juetten, K., Strecker, A. L., Harrison, A., Landram, Z., De Bruyn, W. J., & Clark, C. D. (2022). Chromophoric dissolved organic matter and dissolved organic carbon in lakes across an elevational gradient from the mountains to the sea. *Earth and Space Science*, 9(12). <https://doi.org/10.1029/2022EA002503>
- Kellogg, W. W., Cadle, R. D., Allen, E. R., Lazrus, A. L., & Martell, E. A. (1972). The Sulfur Cycle: Man's contributions are compared to natural sources of sulfur compounds in the atmosphere and oceans. *Science*, 175(4022), 587-596. <https://doi.org/10.1126/science.175.4022.587>

- Klausmeier, C. A., & Litchman, E. (2001). Algal games: The vertical distribution of phytoplankton in poorly mixed water columns. *Limnology and Oceanography*, 46(8), 1998-2007. <https://doi.org/10.4319/lo.2001.46.8.1998>
- Knorr, K.-H. (2013). DOC-dynamics in a small headwater catchment as driven by redox fluctuations and hydrological flow paths—are DOC exports mediated by iron reduction/oxidation cycles? *Biogeosciences*, 10(2), 891-904. <https://doi.org/10.5194/bg-10-891-2013>
- Köhler, S. J., Kothawala, D., Futter, M. N., Liungman, O., & Tranvik, L. (2013). In-lake processes offset increased terrestrial inputs of dissolved organic carbon and color to lakes. *PLoS One*, 8(8). <https://doi.org/10.1371/journal.pone.0070598>
- Kritzberg, E. S. (2017). Centennial-long trends of lake browning show major effect of afforestation. *Limnology and Oceanography Letters*, 2(4), 105-112. <https://doi.org/10.1002/lol2.10041>
- Kritzberg, E. S., & Ekström, S. M. (2012). Increasing iron concentrations in surface waters - a factor behind brownification? *Biogeosciences*, 9(4), 1465-1478. <https://doi.org/10.5194/bg-9-1465-2012>
- Kritzberg, E. S., Hasselquist, E. M., Škerlep, M., Löfgren, S., Olsson, O., Stadmark, J., Valinia, S., Hansson, L.-A., & Laudon, H. (2020). Browning of freshwaters: Consequences to ecosystem services, underlying drivers, and potential mitigation measures. *Ambio*, 49, 375-390. <https://doi.org/10.1007/s13280-019-01227-5>
- Küsel, K., Roth, U., & Drake, H. L. (2002). Microbial reduction of Fe(III) in the presence of oxygen under low pH conditions. *Environ Microbiol*, 4(7), 414-421. <https://doi.org/10.1046/j.1462-2920.2002.00314.x>
- Lanxiu, Y., Fengchang, W., Congqiang, L., Wen, L., Jing, W., & Yi, M. (2004). Molecular weight distribution of dissolved organic matter in Lake Hongfeng determined by high performance size exclusion chromatography (HPSEC) with on-line UV-vis absorbance and fluorescence detection. *Chinese Journal of Geochemistry*, 23(3), 275-283. <https://doi.org/10.1007/BF02842075>
- Lau, M. P., Hutchins, R. H. S., Tank, S. E., & A. del Giorgio, P. (2024). The chemical succession in anoxic lake waters as source of molecular diversity of organic matter. *Scientific reports*, 14(1), 3831. <https://doi.org/10.1038/s41598-024-54387-0>
- Laudon, H., Berggren, M., Ågren, A., Buffam, I., Bishop, K., Grabs, T., Jansson, M., & Köhler, S. (2011). Patterns and dynamics of dissolved organic carbon (DOC) in boreal streams: The role of processes, connectivity, and scaling. *Ecosystems*, 14(6), 880-893. <https://doi.org/10.1007/s10021-011-9452-8>
- Leenheer, J., & Croue, J. (2003). Characterizing dissolved aquatic organic matter. *Environ. Sci. Technol*, 37(1), 19-26. <https://doi.org/10.1021/es032333c>
- Lepane, V., Leeben, A., & Malashenko, O. (2004). Characterization of sediment pore-water dissolved organic matter of lakes by high-performance size exclusion chromatography. *Aquatic Sciences*, 66, 185-194. <https://doi.org/10.1007/s00027-004-0703-z>
- Lepane, V., Persson, T., & Wedborg, M. (2003). Effects of UV-B radiation on molecular weight distribution and fluorescence from humic substances in riverine and low

- salinity water. *Estuarine, Coastal and Shelf Science*, 56(1), 161-173.
[https://doi.org/10.1016/S0272-7714\(02\)00154-3](https://doi.org/10.1016/S0272-7714(02)00154-3)
- Li, M., Song, G., & Xie, H. (2022). Bio-and photo-lability of dissolved organic matter in the Pearl River (Zhujiang) estuary. *Marine Pollution Bulletin*, 174.
<https://doi.org/10.1016/j.marpolbul.2021.113300>
- Li, Y., Gong, X., Sun, Y., Shu, Y., Niu, D., & Ye, H. (2022). High molecular weight fractions of dissolved organic matter (DOM) determined the adsorption and electron transfer capacity of DOM on iron minerals. *Chemical Geology*, 604.
<https://doi.org/10.1016/j.chemgeo.2022.120907>
- Lidman, F., Boily, Å., Laudon, H., & Köhler, S. J. (2017). From soil water to surface water—how the riparian zone controls element transport from a boreal forest to a stream. *Biogeosciences*, 14(12), 3001-3014. <https://doi.org/10.5194/bg-14-3001-2017>
- Liu, M., Zhang, Y., Shi, K., Zhang, Y., Zhou, Y., Zhu, M., Zhu, G., Wu, Z., & Liu, M. (2020). Effects of rainfall on thermal stratification and dissolved oxygen in a deep drinking water reservoir. *Hydrological Processes*, 34(15), 3387-3399.
<https://doi.org/10.1002/hyp.13826>
- Lutz, J., Hanssen-Bauer, I., & Einar, O. (2024). *Precipitation variability in Norway 1961-2020*. Norwegian Meteorological Institute.
- Ma, W.-X., Huang, T.-L., Li, X., Zhang, H.-H., & Ju, T. (2015). Impact of short-term climate variation and hydrology change on thermal structure and water quality of a canyon-shaped, stratified reservoir. *Environmental Science and Pollution Research*, 22(23), 18372-18380. <https://doi.org/10.1007/s11356-015-4764-4>
- Maizel, A. C., & Remucal, C. K. (2017). Molecular composition and photochemical reactivity of size-fractionated dissolved organic matter. *Environ Sci Technol*, 51(4), 2113-2123. <https://doi.org/10.1021/acs.est.6b05140>
- Martin, S. T. (2005). Precipitation and dissolution of iron and manganese oxides. *Environmental catalysis*, 1, 61-82.
- McKnight, D. M., & Aiken, G. R. (1998). Sources and age of aquatic humus. In: Hessen, D.O., Tranvik, L.J. (eds) *Aquatic humic substances: Ecological studies*, vol 133. Springer, Berlin, Heidelberg. https://doi.org/10.1007/978-3-662-03736-2_2
- McKnight, D. M., Boyer, E. W., Westerhoff, P. K., Doran, P. T., Kulbe, T., & Andersen, D. T. (2001). Spectrofluorometric characterization of dissolved organic matter for indication of precursor organic material and aromaticity. *Limnology and Oceanography*, 46(1), 38-48. <https://doi.org/10.4319/lo.2001.46.1.0038>
- Meili, M. (1992). Sources, concentrations and characteristics of organic matter in softwater lakes and streams of the Swedish forest region. *Hydrobiologia*, 229(1), 23-41.
<https://doi.org/10.1007/BF00006988>
- Mendonça, R., Kosten, S., Sobek, S., Cardoso, S. J., Figueiredo-Barros, M. P., Estrada, C. H. D., & Roland, F. (2016). Organic carbon burial efficiency in a subtropical hydroelectric reservoir. *Biogeosciences*, 13(11), 3331-3342.
<https://doi.org/10.5194/bg-13-3331-2016>
- Monteith, D. T., Stoddard, J. L., Evans, C. D., de Wit, H. A., Forsius, M., Høgåsen, T., Wilander, A., Skjelkvåle, B. L., Jeffries, D. S., Vuorenmaa, J., Keller, B., Kopáček, J., & Vesely, J. (2007). Dissolved organic carbon trends resulting from changes in

- atmospheric deposition chemistry. *Nature*, 450(7169), 537-540.
<https://doi.org/10.1038/nature06316>
- Mrkva, M. (1983). Evaluation of correlations between absorbance at 254 nm and COD of river waters. *Water Research*, 17(2), 231-235. [https://doi.org/10.1016/0043-1354\(83\)90104-5](https://doi.org/10.1016/0043-1354(83)90104-5)
- Musolff, A., Selle, B., Büttner, O., Opitz, M., & Tittel, J. (2017). Unexpected release of phosphate and organic carbon to streams linked to declining nitrogen depositions. *Global Change Biology*, 23(5), 1891-1901. <https://doi.org/10.1111/gcb.13498>
- Nikulin, G., Kjellström, M. E., Hansson, U., Strandberg, G., & Ullerstig, A. (2011). Evaluation and future projections of temperature, precipitation and wind extremes over Europe in an ensemble of regional climate simulations. *Tellus A: Dynamic Meteorology and Oceanography*, 63(1), 41-55. <https://doi.org/10.1111/j.1600-0870.2010.00466.x>
- Norwegian Center for Climate Services (n.d.). *Observations and weather statistics*. Retriever on the 6th of December 2023, from <https://seklima.met.no>
- O'Loughlin, E. J., & Chin, Y.-P. (2004). Quantification and characterization of dissolved organic carbon and iron in sedimentary porewater from Green Bay, WI, USA. *Biogeochemistry*, 71(3), 371-386. <https://doi.org/10.1007/s10533-004-0373-x>
- Pace, M. L., & Cole, J. J. (2002). Synchronous variation of dissolved organic carbon and color in lakes. *Limnology and Oceanography*, 47(2), 333-342. <https://doi.org/10.4319/lo.2002.47.2.0333>
- Penna, D., Tromp-van Meerveld, H., Gobbi, A., Borga, M., & Dalla Fontana, G. (2011). The influence of soil moisture on threshold runoff generation processes in an alpine headwater catchment. *Hydrology and earth system sciences*, 15(3), 689-702. <https://doi.org/10.5194/hess-15-689-2011>
- Perminova, I. V., Frimmel, F. H., Kudryavtsev, A. V., Kulikova, N. A., Abbt-Braun, G., Hesse, S., & Petrosyan, V. S. (2003). Molecular weight characteristics of humic substances from different environments as determined by size exclusion chromatography and their statistical evaluation. *Environmental science & technology*, 37(11), 2477-2485. <https://doi.org/10.1021/es0258069>
- Peter, S., Isidorova, A., & Sobek, S. (2016). Enhanced carbon loss from anoxic lake sediment through diffusion of dissolved organic carbon. *Journal of Geophysical Research: Biogeosciences*, 121(7), 1959-1977. <https://doi.org/10.1002/2016JG003425>
- Ping, Q., Zhang, B., Zhang, Z., Lu, K., & Li, Y. (2023). Speciation analysis and formation mechanism of iron-phosphorus compounds during chemical phosphorus removal process. *Chemosphere*, 310, 136852. <https://doi.org/10.1016/j.chemosphere.2022.136852>
- Read, J. S., & Rose, K. C. (2013). Physical responses of small temperate lakes to variation in dissolved organic carbon concentrations. *Limnology and Oceanography*, 58(3), 921-931. <https://doi.org/10.4319/lo.2013.58.3.0921>
- Repeta, D. J., Quan, T. M., Aluwihare, L. I., & Accardi, A. (2002). Chemical characterization of high molecular weight dissolved organic matter in fresh and marine waters. *Geochimica et Cosmochimica Acta*, 66(6), 955-962. [https://doi.org/10.1016/S0016-7037\(01\)00830-4](https://doi.org/10.1016/S0016-7037(01)00830-4)

- Riedel, T., Zak, D., Biester, H., & Dittmar, T. (2013). Iron traps terrestrially derived dissolved organic matter at redox interfaces. *Proceedings of the National Academy of Sciences*, 110(25), 10101-10105. <https://doi.org/10.1073/pnas.1221487110>
- Riise, G., Haaland, S. L., & Xiao, Y. (2023). Coupling of iron and dissolved organic matter in lakes—selective retention of different size fractions. *Aquatic Sciences*, 85(2), 57. <https://doi.org/10.1007/s00027-023-00956-w>
- Riise, G., Salbu, B., Vogt, R. D., Ranneklev, S. B., & Mykkelbost, T. C. (1994). Mobility of humic substances, major and minor elements in lake Skjervatjern and its catchment area. *Environment International*, 20(3), 287-298. [https://doi.org/10.1016/0160-4120\(94\)90112-0](https://doi.org/10.1016/0160-4120(94)90112-0)
- Rostad, C. E., Schmitt, C. J., Schumacher, J. G., & Leiker, T. J. (2011). An exploratory investigation of polar organic compounds in waters from a lead–zinc mine and mill complex. *Water, Air, & Soil Pollution*, 217(1), 431-443. <https://doi.org/10.1007/s11270-010-0598-3>
- Royer, T. V., & Minshall, G. W. (1997). Rapid breakdown of allochthonous and autochthonous plant material in a eutrophic river. *Hydrobiologia*, 344(1), 81-86. <https://doi.org/10.1023/A:1002902327258>
- Skoog, A. C., & Arias-Esquivel, V. A. (2009). The effect of induced anoxia and reoxygenation on benthic fluxes of organic carbon, phosphate, iron, and manganese. *Science of The Total Environment*, 407(23), 6085-6092. <https://doi.org/10.1016/j.scitotenv.2009.08.030>
- Sobek, S., Durisch-Kaiser, E., Zurbrugg, R., Wongfun, N., Wessels, M., Pasche, N., & Wehrl, B. (2009). Organic carbon burial efficiency in lake sediments controlled by oxygen exposure time and sediment source. *Limnology and Oceanography*, 54(6), 2243-2254.
- Solomon, C. T., Jones, S. E., Weidel, B. C., Buffam, I., Fork, M. L., Karlsson, J., Larsen, S., Lennon, J. T., Read, J. S., Sadro, S., & Saros, J. E. (2015). Ecosystem consequences of changing inputs of terrestrial dissolved organic matter to lakes: current knowledge and future challenges. *Ecosystems*, 18(3), 376-389. <https://doi.org/10.1007/s10021-015-9848-y>
- Stanley, E. H., Powers, S. M., Lottig, N. R., Buffam, I., & Crawford, J. T. (2012). Contemporary changes in dissolved organic carbon (DOC) in human-dominated rivers: is there a role for DOC management? *Freshwater Biology*, 57, 26-42. <https://doi.org/10.1111/j.1365-2427.2011.02613.x>
- Stedmon, C. A., & Markager, S. (2005). Tracing the production and degradation of autochthonous fractions of dissolved organic matter by fluorescence analysis. *Limnology and Oceanography*, 50(5), 1415-1426. <https://doi.org/10.4319/lo.2005.50.5.1415>
- Stumm, W., & Morgan, J. J. (2012). *Aquatic chemistry: chemical equilibria and rates in natural waters*. John Wiley & Sons.
- Stumm, W., & Sulzberger, B. (1992). The cycling of iron in natural environments: Considerations based on laboratory studies of heterogeneous redox processes. *Geochimica et Cosmochimica Acta*, 56(8), 3233-3257. [https://doi.org/10.1016/0016-7037\(92\)90301-X](https://doi.org/10.1016/0016-7037(92)90301-X)

- Tate, K. W., Lancaster, D. L., & Lile, D. F. (2007). Assessment of thermal stratification within stream pools as a mechanism to provide refugia for native trout in hot, arid rangelands. *Environmental monitoring and assessment*, 124, 289-300.
<https://doi.org/10.1007/s10661-006-9226-5>
- Tipping, E., & Heaton, M. (1983). The adsorption of aquatic humic substances by two oxides of manganese. *Geochimica et Cosmochimica Acta*, 47(8), 1393-1397.
[https://doi.org/10.1016/0016-7037\(83\)90297-1](https://doi.org/10.1016/0016-7037(83)90297-1)
- Tranvik, L. J., Downing, J. A., Cotner, J. B., Loiselle, S. A., Striegl, R. G., Ballatore, T. J., Dillon, P., Finlay, K., Fortino, K., & Knoll, L. B. (2009). Lakes and reservoirs as regulators of carbon cycling and climate. *Limnology and Oceanography*, 54(6part2), 2298-2314. https://doi.org/10.4319/lo.2009.54.6_part_2.2298
- Verstat.no. (n.d.). *Værstat*. Retrieved on the 11th of April 2024, from <https://verstat.no>
- Wang, L., Yen, H., E, X., Chen, L., & Wang, Y. (2019). Dissolved organic carbon driven by rainfall events from a semi-arid catchment during concentrated rainfall season in the Loess Plateau, China. *Hydrology and Earth System Sciences*, 23(7), 3141-3153.
<https://doi.org/10.5194/hess-23-3141-2019>
- Warner, K. A., & Saros, J. E. (2019). Variable responses of dissolved organic carbon to precipitation events in boreal drinking water lakes. *Water Resources*, 156, 315-326.
<https://doi.org/10.1016/j.watres.2019.03.036>
- Wetzel, R. G. (2001). *Limnology: lake and river ecosystems*. Gulf professional publishing.
- Williamson, C. E., Morris, D. P., Pace, M. L., & Olson, O. G. (1999). Dissolved organic carbon and nutrients as regulators of lake ecosystems: Resurrection of a more integrated paradigm. *Limnology and Oceanography*, 44(3part2), 795-803.
https://doi.org/10.4319/lo.1999.44.3_part_2.0795
- Williamson, C. E., Overholt, E. P., Pilla, R. M., Leach, T. H., Brentrup, J. A., Knoll, L. B., Mette, E. M., & Moeller, R. E. (2015). Ecological consequences of long-term browning in lakes. *Scientific reports*, 5(1). <https://doi.org/10.1038/srep18666>
- Worrall, F., Burt, T., Jaeban, R., Warburton, J., & Shedden, R. (2002). Release of dissolved organic carbon from upland peat. *Hydrological Processes*, 16(17), 3487-3504.
<https://doi.org/10.1002/hyp.1111>
- Xiao, Y., & Riise, G. (2021). Coupling between increased lake color and iron in boreal lakes. *Science of The Total Environment*, 767, 145104.
<https://doi.org/10.1016/j.scitotenv.2021.145104>
- Yacobi, Y., Erez, J., Hadas, O. (2014). Primary Production. In: Zohary, T., Sukenik, A., Berman, T., Nishri, A. (eds) *Lake Kinneret. Aquatic Ecology Series*, vol 6. Springer, Dordrecht. https://doi.org/10.1007/978-94-017-8944-8_24
- Yan, M., Korshin, G., Wang, D., & Cai, Z. (2012). Characterization of dissolved organic matter using high-performance liquid chromatography (HPLC)–size exclusion chromatography (SEC) with a multiple wavelength absorbance detector. *Chemosphere*, 87(8), 879-885. <https://doi.org/10.1016/j.chemosphere.2012.01.029>
- Zhou, Q., Cabaniss, S. E., & Maurice, P. A. (2000). Considerations in the use of high-pressure size exclusion chromatography (HPSEC) for determining molecular weights of aquatic humic substances. *Water Research*, 34(14), 3505-3514.
[https://doi.org/10.1016/S0043-1354\(00\)00115-9](https://doi.org/10.1016/S0043-1354(00)00115-9)

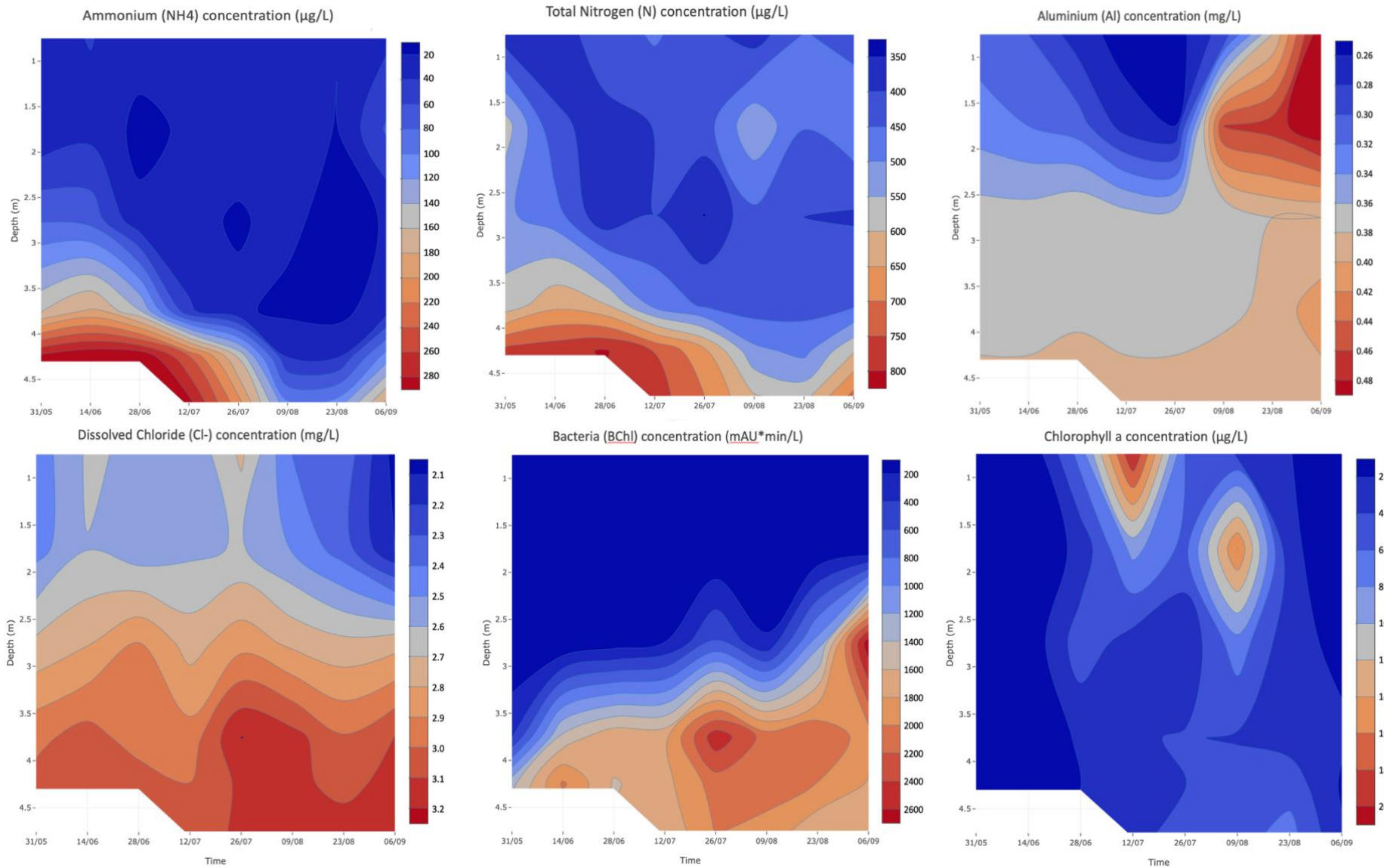
7. Appendices

Appendix A: Raw Data of the Measurements in Lake Solbergvann

Date	Depth	CDOM1	CDOM2	CDOM3	CDOM4	Total CDOM	DOC (Dis)	Air temp	Precipi tation	Water temp	O2 (%)	O2 (ml)	pH	P (Dis)	P (Tot)	Fe	Mn	SO42	S	NH4 (Dis)	N (Tot)	Al	CHL (Dis)	Condu ctivity	Bacteri a	Chloro phylla	Secchi depth
31/05	0,75	669	2035	5442	901	9046	13,20	13,7	1,4	14,1	74,5	7,7	6,8	0,00709	0,09050	0,08	0,016	0,69	0,86	32	370	0,31	2,44	30,9	0,0	0,42	1,38
31/05	1,75	636	1910	5647	1204	9397	13,64	13,7	1,4	9,0	28,9	3,3	5,9	0,01063	0,05569	0,16	0,017	0,70	0,85	23	573	0,33	2,46	27,7	0,0	0,25	1,38
31/05	2,75	648	1863	6118	1716	10345	14,93	13,7	1,4	5,4	3,5	0,4	5,5	0,01417	0,06613	0,29	0,019	0,77	0,98	78	509	0,37	2,72	31,5	0,0	0,00	1,38
31/05	3,75	644	1853	6129	1748	10373	15,21	13,7	1,4	5,6	0,0	0,0	5,6	0,01417	0,05569	0,39	0,023	0,80	1,10	158	572	0,38	2,97	37,0	374	0,00	1,38
31/05	4,25	659	1886	5956	1680	10180	14,90	13,7	1,4	5,5	0,0	0,0	5,8	0,02481	0,11486	0,58	0,028	0,75	0,98	287	768	0,38	3,03	46,3	1342	0,00	1,38
14/06	0,75	624	1747	5044	994	8410	13,40	17,2	0,0	17,8	83,8	8,0	5,8	0,01063	0,04525	0,07	0,015	0,65	0,82	41	379	0,30	2,62	31,2	0,0	0,19	1,45
14/06	1,75	595	1678	5390	1294	8957	13,81	17,2	0,0	11,4	32,2	3,5	5,5	0,01063	0,05221	0,14	0,016	0,68	0,87	33	407	0,32	2,60	27,8	0,0	0,29	1,45
14/06	2,75	543	1496	5888	1900	9828	14,97	17,2	0,0	6,1	1,0	0,1	5,1	0,01417	0,04873	0,30	0,020	0,77	0,96	73	472	0,37	2,79	30,4	0,0	0,43	1,45
14/06	3,75	610	1683	6199	2181	10673	15,04	17,2	0,0	4,9	0,0	0,0	5,5	0,01772	0,08354	0,44	0,025	0,80	1,00	185	637	0,38	3,04	39,2	1464	0,00	1,45
14/06	4,25	602	1619	6022	2394	10637	14,84	17,2	0,0	4,8	0,0	0,0	5,7	0,02835	0,08006	0,62	0,029	0,74	0,99	299	781	0,38	3,10	46,3	2031	0,72	1,45
28/06	0,75	667	1918	5273	1150	9009	13,39	20,7	7,5	20,2	88,8	8,1	5,8	0,01063	0,02785	0,06	0,013	0,53	0,73	28	422	0,27	2,58	27,6	0,0	6,83	1,43
28/06	1,75	621	1734	5549	1495	9398	13,40	20,7	7,5	13,3	20,5	2,1	5,4	0,00709	0,02436	0,14	0,016	0,61	0,84	15	387	0,31	2,53	28,5	0,0	2,58	1,43
28/06	2,75	563	1548	6076	1959	10146	15,01	20,7	7,5	7,3	0,4	0,0	5,0	0,01063	0,04873	0,34	0,022	0,77	0,96	24	359	0,38	2,90	30,1	98	5,14	1,43
28/06	3,75	593	1594	6107	2251	10545	14,95	20,7	7,5	5,4	0,0	0,0	5,4	0,01772	0,06265	0,49	0,026	0,78	1,00	142	606	0,37	2,95	39,7	1754	2,40	1,43
28/06	4,25	609	1582	5989	2394	10574	14,54	20,7	7,5	5,0	0,0	0,0	5,5	0,02126	0,08702	0,71	0,029	0,69	0,96	299	805	0,39	3,05	47,5	1576	1,99	1,43
12/07	0,75	686	2331	4799	1050	8866	13,25	17,5	11,3	18,3	87,1	8,2	6,0	0,01417	0,04873	0,06	0,011	0,40	0,67	36	457	0,25	2,51	23,6	0,0	20,10	1,48
12/07	1,75	675	2296	5054	1179	9204	13,13	17,5	11,3	14,7	20,0	2,0	5,9	0,00709	0,03829	0,09	0,012	0,42	0,67	23	401	0,27	2,58	27,1	0,0	8,67	1,48
12/07	2,75	626	2089	6414	1530	10659	14,65	17,5	11,3	8,5	0,3	0,0	5,2	0,01063	0,02785	0,35	0,022	0,75	0,97	23	400	0,37	2,76	31,1	201	3,05	1,48
12/07	3,75	636	2059	6443	1858	10996	14,64	17,5	11,3	5,9	0,0	0,0	5,5	0,01772	0,06265	0,54	0,026	0,79	1,00	43	486	0,38	2,94	40,4	1745	3,79	1,48
12/07	4,25	656	2054	6147	2105	10963	14,27	17,5	11,3	5,4	0,0	0,0	5,7	0,02126	0,09050	0,78	0,030	0,63	0,90	242	748	0,38	3,00	50,5	1735	3,46	1,48
12/07	4,75	NA	NA	NA	NA	NA	14,45	17,5	11,3	5,2	0,0	0,0	5,7	0,02126	0,09746	0,82	0,030	0,61	0,88	286	774	0,39	3,03	55,2	1644	3,67	1,48
26/07	0,75	585	1713	5233	1555	9086	13,23	15,5	12,7	16,1	84,4	8,3	5,8	0,00709	0,04873	0,07	0,012	0,37	0,61	35	416	0,25	2,72	22,3	0,0	5,93	1,70
26/07	1,75	583	1703	5379	1668	9332	12,83	15,5	12,7	14,9	32,5	3,2	5,5	0,00709	0,00696	0,10	0,011	0,40	0,66	25	427	0,26	2,61	28,0	0,0	5,37	1,70
26/07	2,75	544	1527	6528	2249	10847	14,57	15,5	12,7	9,3	0,2	0,0	4,9	0,01063	0,05917	0,39	0,022	0,76	0,97	19	348	0,37	2,86	34,0	616	2,43	1,70
26/07	3,75	591	1589	6416	2457	11053	14,66	15,5	12,7	6,0	0,0	0,0	5,3	0,01417	0,06961	0,56	0,027	0,78	1,00	23	443	0,37	3,20	45,1	2534	4,16	1,70
26/07	4,25	619	1589	6207	2694	11108	14,58	15,5	12,7	5,6	0,0	0,0	5,5	0,01772	0,09050	0,84	0,033	0,55	0,85	158	660	0,38	3,12	49,9	2090	3,96	1,70
26/07	4,75	NA	NA	NA	NA	NA	14,32	15,5	12,7	5,5	0,0	0,0	5,5	0,01772	0,09050	0,87	0,034	0,51	0,81	207	700	0,39	3,12	50,0	2013	4,38	1,70
09/08	0,75	675	1986	5660	1668	9988	14,01	16,1	18,3	15,6	76,7	7,6	5,7	0,00354	0,04177	0,10	0,011	0,36	0,58	28	374	0,29	2,40	40,1	0,0	3,87	1,67
09/08	1,75	NA	NA	NA	NA	NA	19,17	16,1	18,3	15,0	53,2	5,4	4,9	0,01417	0,08702	0,21	0,011	0,45	0,69	35	540	0,46	2,49	29,6	0,0	16,05	1,67
09/08	2,75	832	1932	5218	974	8956	14,32	16,1	18,3	10,7	1,7	0,2	5,0	0,00709	0,04177	0,34	0,021	0,73	0,92	24	438	0,36	2,78	31,6	224	7,18	1,67

09/08	3,75	641	1771	6212	2168	10792	14,65	16,1	18,3	7,2	0,0	0,0	5,3	0,01417	0,05569	0,49	0,027	0,81	1,00	16	424	0,37	3,14	39,1	2112	3,76	1,67
09/08	4,25	687	1797	6077	2330	10891	14,82	16,1	18,3	6,3	0,0	0,0	5,6	0,02126	0,09398	0,77	0,035	0,61	0,88	39	513	0,39	3,15	46,5	2083	5,36	1,67
09/08	4,75	NA	NA	NA	NA	NA	14,37	16,1	18,3	5,8	0,0	0,0	5,7	0,02126	0,09398	0,87	0,036	0,47	0,77	102	604	0,39	3,13	49,9	1940	5,20	1,67
23/08	0,75	730	2188	7057	2035	12010	17,72	17	11,5	16,9	78,3	7,6	5,2	0,00709	0,05221	0,13	0,013	0,38	0,62	21	453	0,38	2,37	30,3	0,0	2,06	1,68
23/08	1,75	735	2191	7943	2525	13394	18,75	17	11,5	14,7	19,7	2,0	4,9	0,00709	0,01044	0,21	0,013	0,44	0,73	19	453	0,47	2,35	25,6	0,0	2,12	1,68
23/08	2,75	601	1746	6483	2072	10902	14,75	17	11,5	11,0	0,7	0,1	5,1	0,01063	0,02436	0,37	0,022	0,73	0,96	13	398	0,38	2,73	29,9	1101	2,47	1,68
23/08	3,75	625	1715	6495	2386	11221	14,61	17	11,5	7,2	0,0	0,0	5,4	0,00709	0,05569	0,57	0,031	0,80	1,10	13	432	0,39	3,01	38,7	2191	3,15	1,68
23/08	4,25	646	1705	6181	2584	11115	14,30	17	11,5	6,4	0,0	0,0	5,6	0,01063	0,08006	0,80	0,038	0,56	0,87	37	485	0,40	3,04	49,2	1995	5,18	1,68
23/08	4,75	NA	NA	NA	NA	NA	15,01	17	11,5	6,0	0,0	0,0	5,7	0,02126	0,09398	0,91	0,045	0,42	0,75	106	581	0,39	3,19	49,8	1649	6,67	1,68
06/09	0,75	863	2316	10010	3536	16725	22,20	15,7	14,7	14,8	71,5	7,4	4,6	0,01063	0,00348	0,24	0,018	0,47	0,68	35	431	0,50	2,06	29,0	0,0	0,64	1,33
06/09	1,75	813	2506	9587	2892	15797	22,42	15,7	14,7	13,8	30,4	3,3	4,6	0,01063	0,01392	0,24	0,016	0,49	0,72	62	488	0,50	2,09	27,2	0,0	1,61	1,33
06/09	2,75	606	1775	6739	2077	11197	15,01	15,7	14,7	10,7	0,6	0,1	5,0	0,01063	0,03829	0,40	0,023	0,79	1,00	21	394	0,38	2,76	31,6	2742	1,65	1,33
06/09	3,75	692	1828	6497	1935	10952	14,78	15,7	14,7	7,4	0,0	0,0	5,5	0,01772	0,06265	0,73	0,032	0,67	0,97	32	443	0,41	3,11	44,6	1889	2,24	1,33
06/09	4,25	727	1787	6422	2088	11023	15,31	15,7	14,7	6,5	0,0	0,0	5,6	0,01063	0,08354	0,93	0,034	0,36	0,71	109	595	0,40	3,17	50,2	1783	1,75	1,33
06/09	4,75	NA	NA	NA	NA	NA	15,38	15,7	14,7	6,3	0,0	0,0	5,7	0,02481	0,10094	1,00	0,036	0,28	0,71	183	716	0,40	3,14	52,2	1656	2,21	1,33

Appendix B: Contour plots of NH4+, Tot N, Al, Cl-, BChl, and Chl a



Appendix C: Table of Molecular Weight and Signal Peak

Date	0.75m	1.75m	2.75m	3.75m	4.25m
31-05-2023	4923 (34.15)	5015 (34.85)	5173* (37.47)	5173* (37.63)	5046 (36.77)
14-06-2023	5173 (31.31)	5335 (33.13)	5710* (36.02)	5503 (37.71)	5571 (36.42)
28-06-2023	5046 (32.87)	5302 (34.12)	5606* (37.24)	5606* (37.18)	5606 (36.27)
12-07-2023	4324 (31.78)	4432 (32.89)	4923 (39.16)	4984* (38.58)	4833 (36.30)
26-07-2023	5205 (32.38)	5269 (33.20)	5926* (40.24)	5853** (39.04)	5782** (37.48)
09-08-2023	5046 (34.91)	NA	4833 (32.94)	5401* (37.25)	5368 (36.20)
23-08-2023	5269 (43.10)	5537 (48.52)	5571 (39.36)	5675* (39.06)	5606 (36.73)
06-09-2023	6343*&** (62.35)	5853** (58.55)	5710** (41.05)	5435 (39.57)	5537 (38.88)

* highest molecular weight per date (horizontal comparison) – depth profile

** highest molecular weight per depth (vertical comparison) – seasonal profile

Appendix D: P-values and Pearson correlation coefficient at 0.75m

The first values in the table are the p-values, where significance ($p < 0.05$) is highlighted in green. The correlation coefficient is presented between parentheses.

0.75m	CDOM1	CDOM2	CDOM3	CDOM4	Total CDOM	DOC (Dis)	Air temp	Precipitation	Water temp	O ₂ (%)	O ₂ (mg/L)	pH	P (Dis)	P (Tot)	Fe	Mn	SO ₄ ²⁻	S	NH ₄ ⁺ (Dis)	N (Tot)	Al	Cl- (Dis)	Conductivity	Bacteria	Chlorophyll a
CDOM2	0.017 (0.799)																								
CDOM3	0.002 (0.913)	0.164 (0.543)																							
CDOM4	0.009 (0.839)	0.233 (0.476)	0 (0.964)																						
CDOM SUM	0.001 (0.926)	0.12 (0.594)	0 (0.995)	0 (0.976)																					
DOC (Dis)	0.001 (0.919)	0.124 (0.59)	0 (0.988)	0 (0.956)	0 (0.989)																				
Air temp	0.859 (-0.076)	0.89 (-0.059)	0.614 (-0.212)	0.668 (-0.181)	0.643 (-0.195)	0.725 (-0.149)																			
Precipitation	0.368 (0.369)	0.378 (0.362)	0.333 (0.395)	0.125 (0.589)	0.239 (0.471)	0.323 (0.402)	0.979 (-0.011)																		
Water temp	0.473 (-0.298)	0.72 (-0.152)	0.27 (-0.444)	0.313 (-0.41)	0.293 (-0.426)	0.372 (-0.366)	0 (0.949)	0.696 (-0.165)																	
O ₂ (%)	0.095 (-0.629)	0.363 (-0.373)	0.05 (-0.708)	0.096 (-0.627)	0.061 (-0.685)	0.081 (-0.65)	0.043 (0.722)	0.603 (-0.218)	0.004 (0.883)																
O ₂ (mg/L)	0.026 (-0.769)	0.229 (-0.48)	0.029 (-0.759)	0.078 (-0.654)	0.036 (-0.739)	0.037 (-0.738)	0.42 (0.333)	0.594 (-0.224)	0.147 (0.562)	0.004 (0.882)															
pH	0.057 (-0.693)	0.402 (-0.345)	0.016 (-0.806)	0.004 (-0.883)	0.012 (-0.826)	0.007 (-0.85)	0.627 (-0.204)	0.132 (0.58)	0.987 (0.007)	0.477 (-0.296)	0.224 (0.485)														
P (Dis)	0.65 (0.191)	0.393 (0.352)	0.999 (0.001)	0.89 (-0.059)	0.967 (0.018)	0.887 (0.06)	0.274 (0.441)	0.471 (-0.3)	0.174 (0.533)	0.238 (0.472)	0.376 (0.364)	0.912 (-0.047)													
P (Tot)	0.154 (-0.555)	0.615 (-0.212)	0.115 (-0.601)	0.054 (-0.625)	0.097 (-0.615)	0.105 (-0.615)	0.247 (-0.464)	0.203 (-0.504)	0.529 (-0.263)	0.987 (-0.007)	0.633 (0.201)	0.008 (0.844)	0.475 (-0.297)												
Fe	0.002 (0.905)	0.152 (0.557)	0 (0.99)	0 (0.969)	0 (0.991)	0 (0.977)	0.479 (-0.294)	0.267 (0.447)	0.193 (-0.514)	0.032 (-0.751)	0.025 (-0.77)	0.019 (-0.794)	0.938 (-0.033)	0.129 (-0.583)											
Mn	0.129 (0.584)	0.641 (0.197)	0.077 (0.657)	0.234 (0.475)	0.123 (0.59)	0.114 (0.603)	0.425 (-0.33)	0.347 (-0.384)	0.273 (-0.442)	0.114 (-0.603)	0.141 (-0.57)	0.572 (-0.237)	0.671 (0.179)	0.68 (-0.174)	0.098 (0.624)										
SO ₄ ²⁻	0.76 (-0.129)	0.53 (-0.263)	0.701 (-0.162)	0.353 (-0.38)	0.558 (-0.246)	0.6 (-0.22)	0.748 (-0.136)	0.002 (-0.901)	0.854 (-0.078)	0.838 (-0.087)	0.885 (-0.062)	0.199 (0.508)	0.664 (0.183)	0.352 (0.38)	0.632 (-0.202)	0.099 (0.623)									
S	0.765 (-0.126)	0.67 (-0.18)	0.637 (-0.198)	0.298 (-0.422)	0.512 (-0.274)	0.564 (-0.242)	0.806 (-0.104)	0.001 (-0.927)	0.97 (-0.016)	0.979 (-0.011)	0.971 (0.015)	0.165 (0.542)	0.449 (0.314)	0.319 (0.405)	0.569 (-0.239)	0.122 (0.592)	0 (0.986)								
NH ₄ ⁺ (Dis)	0.631 (-0.202)	0.554 (-0.248)	0.696 (-0.165)	0.703 (-0.161)	0.67 (-0.18)	0.654 (-0.189)	0.687 (-0.17)	0.335 (-0.393)	0.973 (-0.014)	0.66 (0.186)	0.344 (0.386)	0.608 (0.215)	0.198 (0.509)	0.865 (-0.072)	0.79 (-0.113)	0.51 (0.275)	0.313 (0.41)	0.268 (0.446)							
N (Tot)	0.346 (0.385)	0.126 (0.587)	0.485 (0.29)	0.411 (0.339)	0.399 (0.347)	0.337 (0.392)	0.328 (0.399)	0.372 (0.366)	0.341 (0.389)	0.505 (0.278)	0.746 (0.137)	0.223 (-0.485)	0.17 (0.537)	0.349 (-0.383)	0.554 (0.248)	0.666 (-0.182)	0.141 (-0.569)	0.257 (-0.455)	0.536 (-0.259)						
Al	0.002 (0.905)	0.172 (0.535)	0 (0.972)	0.003 (0.888)	0 (0.953)	0 (0.968)	0.554 (-0.248)	0.601 (0.22)	0.25 (-0.461)	0.031 (-0.755)	0.011 (-0.831)	0.037 (-0.736)	0.983 (0.009)	0.217 (-0.491)	0 (0.96)	0.031 (0.752)	0.993 (0.004)	0.939 (-0.033)	0.74 (-0.14)	0.629 (0.204)					
Cl- (Dis)	0 (-0.962)	0.032 (-0.751)	0.003 (-0.891)	0.014 (-0.815)	0.002 (-0.9)	0.004 (-0.878)	0.527 (0.264)	0.337 (-0.392)	0.216 (0.492)	0.018 (0.797)	0.003 (0.887)	0.109 (0.609)	0.944 (0.03)	0.296 (0.423)	0.002 (-0.907)	0.13 (-0.582)	0.818 (0.098)	0.772 (0.123)	0.573 (0.237)	0.676 (-0.177)	0.002 (-0.9)				
Conductivity	0.73 (0.146)	0.95 (-0.027)	0.806 (0.104)	0.858 (0.076)	0.832 (0.09)	0.865 (0.072)	0.698 (-0.164)	0.725 (0.149)	0.458 (-0.308)	0.191 (-0.516)	0.076 (-0.659)	0.888 (-0.06)	0.088 (-0.639)	0.92 (0.043)	0.719 (0.152)	0.926 (0.04)	0.847 (0.082)	0.935 (-0.035)	0.451 (-0.312)	0.11 (-0.607)	0.657 (0.187)	0.387 (-0.356)			
Bacteria	NA	NA	NA	NA	NA	NA	NA	NA	NA	NA	NA	NA	NA	NA	NA	NA									
Chlorophyll a	0.696 (-0.165)	0.411 (0.339)	0.307 (-0.414)	0.441 (-0.319)	0.42 (-0.333)	0.391 (0.353)	0.381 (0.36)	0.57 (0.238)	0.207 (0.5)	0.098 (0.624)	0.106 (0.614)	0.615 (0.212)	0.149 (0.56)	0.971 (-0.016)	0.339 (-0.39)	0.103 (-0.618)	0.301 (-0.419)	0.491 (-0.287)	0.755 (0.132)	0.154 (0.555)	0.193 (-0.513)	0.484 (0.291)	0.208 (-0.5)	NA	
Secchi depth	0.268 (-0.446)	0.453 (-0.311)	0.482 (-0.292)	0.806 (-0.104)	0.544 (-0.254)	0.56 (-0.244)	0.932 (-0.037)	0.228 (0.481)	0.968 (0.017)	0.691 (0.168)	0.606 (0.217)	0.863 (-0.073)	0.124 (-0.589)	0.69 (0.169)	0.541 (-0.256)	0.031 (-0.753)	0.053 (-0.7)	0.039 (-0.732)	0.266 (-0.448)	0.818 (0.098)	0.373 (-0.366)	0.358 (0.376)	0.799 (0.108)	NA	0.844 (0.084)

Appendix E: P-values and Pearson correlation coefficient at 1.75m

The first values in the table are the p-values, where significance ($p < 0.05$) is highlighted in green. The correlation coefficient is presented between parentheses.

1.75m	CDOM1	CDOM2	CDOM3	CDOM4	Total CDOM	DOC (Dis)	Air temp	Precipitation	Water temp	O ₂ (%)	O ₂ (mg/L)	pH	P (Dis)	P (Tot)	Fe	Mn	SO ₄ ²⁻	S	NH ₄ ⁺ (Dis)	N (Tot)	Al	Cl- (Dis)	Conductivity	Bacteria	Chlorophyll a	
CDOM2	0.002 (0.93)																									
CDOM3	0.004 (0.912)	0.07 (0.716)																								
CDOM4	0.021 (0.831)	0.134 (0.624)	0.001 (0.961)																							
CDOM SUM	0.002 (0.935)	0.045 (0.764)	0 (0.995)	0 (0.967)																						
DOC (Dis)	0.002 (0.93)	0.052 (0.751)	0 (0.995)	0.001 (0.944)	0.625 (0.205)																					
Air temp	0.773 (-0.135)	0.685 (-0.189)	0.687 (-0.188)	0.834 (-0.098)	0.996 (0.002)	0.634 (-0.2)																				
Precipitation	0.169 (0.584)	0.142 (0.615)	0.221 (0.53)	0.107 (0.66)	0.654 (-0.189)	0.119 (0.596)	0.979 (-0.011)																			
Water temp	0.533 (0.287)	0.462 (0.335)	0.604 (0.24)	0.319 (0.444)	0.139 (-0.102)	0.327 (0.327)	0.429 (0.329)	0.007 (0.856)																		
O ₂ (%)	0.629 (-0.224)	0.517 (-0.298)	0.945 (0.032)	0.999 (0)	0.04 (-0.729)	0.438 (0.321)	0.33 (-0.397)	0.354 (0.379)	0.807 (0.104)																	
O ₂ (mg/L)	0.689 (-0.186)	0.551 (-0.275)	0.912 (0.052)	0.943 (-0.034)	0.061 (-0.684)	0.445 (0.317)	0.255 (-0.457)	0.526 (0.265)	0.922 (-0.041)	0 (0.988)																
pH	0.059 (-0.737)	0.279 (-0.477)	0.003 (-0.924)	0.001 (-0.924)	0.79 (-0.113)	0.001 (-0.924)	0.986 (0.007)	0.097 (-0.626)	0.248 (-0.463)	0.34 (-0.389)	0.383 (-0.359)															
P (Dis)	0.701 (0.179)	0.862 (0.082)	0.546 (0.278)	0.894 (0.062)	0.159 (-0.549)	0.254 (0.458)	0.284 (-0.433)	0.748 (0.136)	0.591 (-0.226)	0.006 (0.864)	0.001 (0.914)	0.336 (-0.393)														
P (Tot)	0.397 (-0.382)	0.566 (-0.265)	0.238 (-0.514)	0.07 (-0.717)	0.012 (-0.824)	0.957 (-0.023)	0.642 (-0.196)	0.861 (-0.074)	0.49 (-0.287)	0.06 (0.687)	0.045 (0.718)	0.821 (0.096)	0.017 (0.799)													
Fe	0.032 (0.798)	0.211 (0.54)	0.003 (0.922)	0.02 (0.833)	0.719 (0.152)	0.001 (0.925)	0.616 (-0.211)	0.397 (0.349)	0.924 (0.04)	0.434 (0.324)	0.386 (0.357)	0.006 (-0.86)	0.162 (0.546)	0.808 (0.103)												
Mn	0.81 (0.112)	0.869 (-0.077)	0.672 (0.197)	0.981 (-0.011)	0.245 (0.465)	0.975 (-0.014)	0.923 (0.041)	0.051 (-0.705)	0.018 (-0.798)	0.418 (-0.334)	0.637 (-0.199)	0.804 (0.105)	0.869 (0.07)	0.9 (-0.053)	0.597 (0.222)											
SO ₄ ²⁻	0.456 (-0.34)	0.299 (-0.46)	0.586 (-0.252)	0.338 (-0.428)	0.962 (0.021)	0.458 (-0.308)	0.998 (-0.001)	0.006 (-0.865)	0.001 (-0.921)	0.853 (-0.079)	0.898 (0.055)	0.406 (0.343)	0.551 (0.25)	0.427 (0.329)	0.989 (0.006)	0.007 (0.856)										
S	0.469 (-0.331)	0.252 (-0.501)	0.643 (-0.215)	0.435 (-0.355)	0.824 (0.094)	0.477 (-0.296)	0.663 (0.184)	0.006 (-0.861)	0.011 (-0.828)	0.638 (-0.198)	0.852 (-0.079)	0.51 (0.275)	0.787 (0.114)	0.628 (0.204)	0.949 (0.027)	0.007 (0.855)	0 (0.969)									
NH ₄ ⁺ (Dis)	0.132 (0.627)	0.203 (0.548)	0.081 (0.699)	0.159 (0.594)	0.547 (0.252)	0.045 (0.719)	0.381 (-0.36)	0.422 (0.332)	0.87 (0.07)	0.337 (0.392)	0.289 (0.429)	0.102 (-0.619)	0.181 (0.525)	0.99 (0.005)	0.139 (0.572)	0.68 (0.174)	0.822 (-0.096)	0.653 (-0.19)								
N (Tot)	0.523 (0.293)	0.593 (0.247)	0.473 (0.327)	0.723 (0.166)	0.537 (-0.258)	0.308 (0.414)	0.027 (-0.766)	0.771 (0.123)	0.371 (-0.367)	0.158 (0.55)	0.105 (0.614)	0.591 (-0.226)	0.051 (0.704)	0.203 (0.504)	0.151 (0.557)	0.809 (0.103)	0.689 (0.169)	0.974 (0.014)	0.487 (0.289)							
Al	0.009 (0.879)	0.108 (0.659)	0.001 (0.962)	0.005 (0.902)	0.737 (0.142)	0 (0.968)	0.666 (-0.182)	0.222 (0.486)	0.599 (0.221)	0.449 (0.314)	0.439 (0.32)	0.002 (-0.901)	0.218 (0.49)	0.876 (0.066)	0 (0.976)	0.912 (0.047)	0.666 (-0.182)	0.724 (-0.15)	0.14 (0.57)	0.226 (0.482)						
Cl- (Dis)	0.002 (-0.932)	0.045 (-0.766)	0 (-0.969)	0.01 (-0.875)	0.132 (-0.58)	0.005 (-0.874)	0.571 (0.237)	0.4 (-0.347)	0.88 (-0.064)	0.914 (0.046)	0.986 (0.008)	0.045 (0.719)	0.63 (-0.203)	0.475 (0.297)	0.011 (-0.831)	0.44 (-0.32)	0.781 (0.118)	0.788 (0.114)	0.052 (-0.703)	0.359 (-0.376)	0.012 (-0.824)					
Conductivity	0.126 (-0.634)	0.128 (-0.632)	0.21 (-0.541)	0.193 (-0.558)	0.018 (-0.796)	0.72 (-0.152)	0.871 (0.069)	0.733 (0.144)	0.954 (-0.024)	0.04 (0.729)	0.046 (0.716)	0.972 (0.015)	0.136 (0.575)	0.087 (0.641)	0.817 (-0.098)	0.762 (-0.128)	0.701 (0.162)	0.87 (0.069)	0.886 (0.061)	0.623 (0.207)	0.691 (-0.168)	0.351 (0.382)				
Bacteria	NA	NA	NA	NA	NA	NA	NA	NA	NA	NA	NA	NA	NA	NA	NA	NA	NA									
Chlorophyll a	0.872 (-0.076)	0.63 (0.223)	0.456 (-0.34)	0.623 (-0.228)	0.021 (-0.785)	0.719 (0.152)	0.987 (0.007)	0.049 (0.71)	0.115 (0.601)	0.089 (0.638)	0.172 (0.535)	0.671 (-0.179)	0.332 (0.396)	0.166 (0.541)	0.994 (-0.003)	0.02 (-0.787)	0.134 (-0.578)	0.089 (-0.638)	0.997 (-0.002)	0.668 (0.181)	0.788 (0.114)	0.565 (0.241)	0.156 (0.552)	NA		
Secchi Depth	0.563 (-0.267)	0.586 (-0.252)	0.724 (-0.165)	0.866 (0.079)	0.302 (-0.418)	0.977 (-0.012)	0.932 (-0.037)	0.228 (0.481)	0.099 (0.623)	0.462 (0.305)	0.651 (0.191)	0.667 (-0.182)	0.817 (-0.098)	0.974 (-0.014)	0.832 (-0.09)	0.008 (-0.846)	0.091 (-0.634)	0.145 (-0.564)	0.355 (-0.378)	0.905 (-0.051)	0.937 (0.033)	0.395 (0.35)	0.933 (0.036)	NA	0.174 (0.533)	

Appendix F: P-values and Pearson correlation coefficient at 2.75m

The first values in the table are the p-values, where significance ($p < 0.05$) is highlighted in green. The correlation coefficient is presented between parentheses.

2.75m	CDOM1	CDOM2	CDOM3	CDOM4	Total CDOM	DOC (Dis)	Air temp	Precipitation	Water temp	O ₂ (%)	O ₂ (mg/L)	pH	P (Dis)	P (Tot)	Fe	Mn	SO ₄ ²⁻	S	NH ₄ ⁺ (Dis)	N (Tot)	Al	Cl- (Dis)	Conductivity	Bacteria	Chlorophyll a
CDOM2	0.077 (0.656)																								
CDOM3	0.059 (-0.689)	0.811 (-0.102)																							
CDOM4	0.002 (-0.9)	0.07 (-0.668)	0.018 (0.798)																						
CDOM SUM	0.086 (-0.642)	0.882 (-0.063)	0 (0.996)	0.022 (0.78)																					
DOC (Dis)	0.073 (-0.663)	0.313 (-0.41)	0.274 (0.441)	0.122 (0.592)	0.301 (0.419)																				
Air temp	0.5 (-0.281)	0.488 (-0.289)	0.864 (-0.073)	0.843 (0.084)	0.772 (-0.123)	0.616 (0.211)																			
Precipitation	0.188 (0.519)	0.361 (0.375)	1 (0)	0.506 (-0.277)	0.959 (0.022)	0.077 (-0.657)	0.979 (-0.011)																		
Water temp	0.398 (0.348)	0.569 (0.239)	0.715 (0.154)	0.885 (-0.061)	0.663 (0.184)	0.192 (-0.515)	0.985 (-0.008)	0.001 (0.916)																	
O ₂ (%)	0.284 (0.433)	0.53 (0.263)	0.309 (-0.413)	0.341 (-0.389)	0.381 (-0.36)	0.892 (0.058)	0.103 (-0.618)	0.32 (-0.405)	0.227 (-0.481)																
O ₂ (mg/L)	0.371 (0.367)	0.548 (0.251)	0.48 (-0.294)	0.472 (-0.299)	0.563 (-0.242)	0.696 (0.165)	0.075 (-0.66)	0.319 (-0.406)	0.239 (-0.471)	0 (0.985)															
pH	0.978 (-0.012)	0.362 (0.373)	0.893 (0.057)	0.798 (-0.108)	0.84 (0.086)	0.334 (0.394)	0.285 (-0.432)	0.072 (-0.664)	0.083 (-0.647)	0.04 (0.73)	0.031 (0.752)														
P (Dis)	0.099 (-0.623)	0.417 (-0.335)	0.499 (0.282)	0.254 (0.458)	0.525 (0.265)	0.046 (0.716)	0.624 (-0.206)	0.001 (-0.934)	0.016 (-0.805)	0.373 (0.366)	0.307 (0.415)	0.05 (0.707)													
P (Tot)	0.747 (-0.137)	0.301 (-0.42)	0.667 (-0.182)	0.753 (0.133)	0.656 (-0.188)	0.67 (0.18)	0.37 (-0.367)	0.237 (-0.472)	0.087 (-0.641)	0.162 (0.545)	0.155 (0.553)	0.572 (0.237)	0.269 (0.445)												
Fe	0.747 (-0.136)	0.946 (-0.029)	0.127 (0.586)	0.33 (0.397)	0.126 (0.587)	0.634 (-0.201)	0.904 (0.051)	0.029 (0.759)	0.013 (0.82)	0.057 (-0.692)	0.1 (-0.622)	0.069 (-0.67)	0.154 (-0.555)	0.301 (-0.419)											
Mn	0.668 (-0.181)	0.998 (-0.001)	0.178 (0.528)	0.431 (0.326)	0.196 (0.511)	0.87 (-0.07)	0.32 (0.404)	0.054 (0.699)	0.035 (0.742)	0.009 (-0.838)	0.023 (-0.777)	0.059 (-0.689)	0.134 (-0.578)	0.123 (-0.591)	0.001 (0.917)										
SO ₄ ²⁻	0.119 (-0.595)	0.312 (-0.41)	0.269 (0.445)	0.173 (0.534)	0.329 (0.398)	0.021 (0.786)	0.881 (0.064)	0.328 (-0.399)	0.28 (-0.436)	0.873 (0.067)	0.874 (0.067)	0.755 (0.132)	0.187 (0.519)	0.301 (0.42)	0.942 (0.031)	0.837 (0.087)									
S	0.101 (-0.62)	0.849 (-0.081)	0.006 (0.859)	0.063 (0.682)	0.007 (0.851)	0.059 (0.689)	0.558 (-0.245)	0.531 (-0.262)	0.675 (-0.177)	0.894 (-0.056)	0.818 (0.098)	0.387 (0.356)	0.167 (0.541)	0.774 (0.122)	0.513 (0.273)	0.605 (0.218)	0.032 (0.751)								
NH ₄ ⁺ (Dis)	0.815 (-0.099)	0.745 (-0.138)	0.49 (-0.287)	0.841 (-0.085)	0.482 (-0.293)	0.304 (0.417)	0.385 (-0.358)	0.007 (-0.851)	0.007 (-0.853)	0.044 (0.721)	0.043 (0.722)	0.035 (0.741)	0.016 (0.805)	0.114 (0.602)	0.006 (-0.86)	0.002 (-0.901)	0.464 (0.304)	0.775 (0.121)							
N (Tot)	0.423 (0.331)	0.539 (0.257)	0.267 (-0.447)	0.292 (-0.426)	0.302 (-0.419)	0.747 (0.137)	0.185 (-0.521)	0.151 (-0.558)	0.165 (-0.542)	0.007 (0.856)	0.009 (0.839)	0.022 (0.782)	0.187 (0.52)	0.456 (0.309)	0.015 (-0.811)	0.004 (-0.88)	0.888 (-0.06)	0.853 (-0.079)	0.006 (0.861)						
Al	0.079 (-0.653)	0.411 (-0.339)	0.043 (0.723)	0.03 (0.755)	0.043 (0.722)	0.042 (0.725)	0.335 (0.394)	0.761 (-0.129)	0.829 (0.092)	0.345 (-0.386)	0.487 (-0.289)	0.935 (-0.035)	0.573 (0.236)	0.52 (-0.269)	0.344 (0.387)	0.203 (0.504)	0.255 (0.457)	0.099 (0.624)	0.52 (-0.269)	0.29 (-0.428)					
Cl- (Dis)	0.371 (-0.367)	0.088 (-0.639)	0.893 (-0.057)	0.5 (0.281)	0.784 (-0.116)	0.898 (0.055)	0.098 (0.624)	0.929 (0.038)	0.799 (-0.108)	0.203 (-0.504)	0.18 (-0.527)	0.084 (-0.645)	0.664 (-0.183)	0.446 (0.316)	0.658 (0.187)	0.46 (0.307)	0.436 (0.322)	0.727 (-0.148)	0.518 (-0.27)	0.087 (-0.641)	0.767 (0.126)				
Conductivity	0.951 (0.026)	0.893 (-0.057)	0.694 (0.166)	0.785 (0.116)	0.701 (0.162)	0.282 (-0.435)	0.156 (-0.552)	0.421 (0.332)	0.719 (0.152)	0.969 (-0.016)	0.983 (0.009)	0.528 (-0.264)	0.691 (-0.168)	0.218 (0.49)	0.348 (0.384)	0.83 (0.091)	0.805 (0.105)	0.73 (0.146)	0.75 (-0.135)	0.57 (-0.238)	0.329 (-0.398)	0.609 (0.215)			
Bacteria	0.802 (-0.106)	0.958 (0.023)	0.114 (0.603)	0.324 (0.402)	0.101 (0.62)	0.58 (0.232)	0.641 (-0.197)	0.233 (0.476)	0.096 (0.628)	0.457 (-0.308)	0.687 (-0.17)	0.542 (-0.255)	0.631 (-0.202)	0.392 (-0.352)	0.031 (0.753)	0.074 (0.662)	0.433 (0.324)	0.143 (0.566)	0.269 (-0.445)	0.42 (-0.333)	0.172 (0.535)	0.615 (-0.211)	0.785 (0.116)		
Chlorophyll a	0.109 (0.609)	0.617 (0.21)	0.156 (-0.552)	0.136 (-0.575)	0.158 (-0.55)	0.106 (-0.613)	0.248 (0.463)	0.065 (0.677)	0.219 (0.489)	0.53 (-0.262)	0.392 (-0.352)	0.089 (-0.637)	0.003 (-0.892)	0.495 (-0.284)	0.611 (0.214)	0.398 (0.348)	0.219 (-0.488)	0.038 (-0.735)	0.113 (-0.604)	0.311 (-0.412)	0.474 (-0.297)	0.338 (0.391)	0.926 (-0.039)	0.709 (-0.158)	
Secchi Depth	0.547 (0.252)	0.898 (-0.055)	0.594 (-0.224)	0.774 (-0.122)	0.633 (-0.201)	0.017 (-0.799)	0.932 (-0.037)	0.228 (0.481)	0.18 (0.527)	0.548 (-0.251)	0.37 (-0.368)	0.174 (-0.533)	0.168 (-0.54)	0.647 (-0.193)	0.469 (0.301)	0.73 (0.146)	0.018 (-0.797)	0.09 (-0.636)	0.226 (-0.483)	0.419 (-0.334)	0.384 (-0.358)	0.801 (0.107)	0.469 (0.301)	0.634 (-0.2)	0.267 (0.447)

Appendix G: P-values and Pearson correlation coefficient at 3.75m

The first values in the table are the p-values, where significance ($p < 0.05$) is highlighted in green. The correlation coefficient is presented between parentheses.

3.75m	CDOM1	CDOM2	CDOM3	CDOM4	Total CDOM	DOC (Dis)	Air temp	Precipitation	Water temp	O ₂ (%)	O ₂ (mg/L)	pH	P (Dis)	P (Tot)	Fe	Mn	SO ₄ ²⁻	S	NH ₄ ⁺ (Dis)	N (Tot)	Al	Cl- (Dis)	Conductivity	Bacteria	Chlorophyll a
CDOM2	0.1 (0.622)																								
CDOM3	0.388 (0.355)	0.504 (0.278)																							
CDOM4	0.076 (-0.658)	0.016 (-0.807)	0.719 (0.152)																						
CDOM SUM	0.859 (0.075)	0.887 (0.06)	0.001 (0.918)	0.243 (0.467)																					
DOC (Dis)	0.929 (-0.038)	0.818 (-0.098)	0.037 (-0.737)	0.264 (-0.449)	0.003 (-0.893)																				
Air temp	0.242 (-0.469)	0.494 (-0.285)	0.677 (-0.176)	0.381 (0.36)	0.984 (0.009)	0.758 (-0.13)																			
Precipitation	0.455 (0.31)	0.82 (0.096)	0.17 (0.537)	0.561 (0.244)	0.099 (0.623)	0.007 (-0.85)	0.979 (-0.011)																		
Water temp	0.101 (0.62)	0.713 (0.155)	0.11 (0.608)	0.829 (0.092)	0.119 (0.596)	0.083 (-0.647)	0.505 (-0.278)	0.013 (0.818)																	
O ₂ (%)	NA	NA	NA	NA	NA	NA	NA	NA	NA	NA	NA	NA	NA	NA	NA	NA									
O ₂ (mg/L)	NA	NA	NA	NA	NA	NA	NA	NA	NA	NA	NA	NA	NA	NA	NA	NA									
pH	0.364 (0.372)	0.268 (0.446)	0.378 (-0.362)	0.015 (-0.808)	0.082 (-0.649)	0.014 (0.814)	0.392 (-0.352)	0.044 (-0.72)	0.334 (-0.394)	NA	NA														
P (Dis)	0.831 (0.091)	0.655 (0.189)	0.464 (-0.304)	0.285 (-0.432)	0.261 (-0.452)	0.406 (0.343)	0.542 (0.255)	0.649 (-0.192)	0.236 (-0.474)	NA	NA	0.547 (0.252)													
P (Tot)	0.347 (-0.385)	0.447 (-0.315)	0.842 (-0.085)	0.568 (0.239)	0.902 (-0.052)	0.58 (0.232)	0.655 (0.188)	0.241 (-0.469)	0.117 (-0.598)	NA	NA	0.996 (-0.002)	0.225 (0.483)												
Fe	0.197 (0.509)	0.836 (0.088)	0.014 (0.811)	0.788 (0.114)	0.06 (0.687)	0.117 (-0.598)	0.971 (0.015)	0.081 (0.649)	0.06 (0.686)	NA	NA	0.345 (-0.386)	0.981 (0.01)	0.816 (-0.099)											
Mn	0.265 (0.448)	0.888 (-0.06)	0.025 (0.77)	0.458 (0.308)	0.033 (0.748)	0.089 (-0.637)	0.893 (0.057)	0.087 (0.641)	0.014 (0.816)	NA	NA	0.252 (-0.46)	0.419 (-0.334)	0.609 (-0.215)	0.002 (0.9)										
SO ₄ ²⁻	0.075 (-0.659)	0.804 (-0.105)	0.224 (-0.484)	0.588 (0.227)	0.608 (-0.216)	0.846 (0.083)	0.797 (0.109)	0.479 (-0.295)	0.286 (-0.431)	NA	NA	0.881 (-0.063)	0.422 (-0.332)	0.953 (-0.025)	0.009 (-0.838)	0.081 (-0.65)									
S	0.883 (-0.062)	0.913 (0.047)	0.817 (-0.098)	0.881 (-0.063)	0.821 (-0.096)	0.547 (0.252)	0.418 (-0.334)	0.38 (-0.361)	0.97 (0.016)	NA	NA	0.349 (0.383)	0.03 (-0.757)	0.241 (-0.469)	0.286 (-0.431)	0.698 (-0.164)	0.255 (0.457)								
NH ₄ ⁺ (Dis)	0.497 (-0.283)	0.688 (-0.17)	0.027 (-0.766)	0.499 (-0.282)	0.011 (-0.829)	0.001 (0.923)	0.691 (0.168)	0.001 (-0.919)	0.011 (-0.831)	NA	NA	0.067 (0.674)	0.293 (0.426)	0.253 (0.459)	0.067 (-0.673)	0.056 (-0.695)	0.569 (0.239)	0.765 (0.127)							
N (Tot)	0.353 (-0.38)	0.656 (-0.188)	0.039 (-0.732)	0.625 (-0.206)	0.028 (-0.761)	0.009 (0.839)	0.409 (0.341)	0.003 (-0.892)	0.004 (-0.879)	NA	NA	0.136 (0.575)	0.233 (0.476)	0.193 (0.514)	0.089 (-0.638)	0.068 (-0.672)	0.538 (0.257)	0.925 (0.04)	0 (0.98)						
Al	0.018 (0.797)	0.426 (0.329)	0.121 (0.594)	0.416 (-0.336)	0.438 (0.321)	0.888 (-0.06)	0.545 (-0.253)	0.769 (0.124)	0.185 (0.522)	NA	NA	0.49 (0.287)	0.952 (-0.025)	0.837 (-0.087)	0.047 (0.714)	0.054 (0.699)	0.013 (-0.816)	0.955 (-0.024)	0.607 (-0.216)	0.525 (-0.266)					
Cl- (Dis)	0.943 (0.03)	0.313 (-0.41)	0.496 (0.284)	0.247 (0.464)	0.378 (0.362)	0.34 (-0.39)	0.305 (-0.416)	0.19 (0.516)	0.309 (0.413)	NA	NA	0.144 (-0.566)	0.816 (-0.099)	0.665 (0.183)	0.368 (0.369)	0.423 (0.331)	0.553 (-0.248)	0.348 (-0.384)	0.22 (-0.488)	0.164 (-0.543)	0.99 (-0.005)				
Conductivity	0.798 (0.109)	0.667 (-0.182)	0.12 (0.594)	0.512 (0.274)	0.199 (0.508)	0.264 (-0.45)	0.874 (-0.068)	0.221 (0.487)	0.501 (0.281)	NA	NA	0.235 (-0.475)	0.523 (0.267)	0.514 (0.272)	0.026 (0.767)	0.195 (0.512)	0.064 (-0.68)	0.081 (-0.649)	0.22 (-0.488)	0.264 (-0.45)	0.474 (0.298)	0.076 (0.659)			
Bacteria	0.585 (-0.229)	0.387 (-0.356)	0.135 (0.576)	0.029 (0.758)	0.018 (0.797)	0.005 (-0.871)	0.457 (0.309)	0.039 (0.732)	0.243 (0.468)	NA	NA	0 (-0.961)	0.596 (-0.223)	0.851 (0.08)	0.125 (0.588)	0.096 (0.628)	0.742 (-0.139)	0.276 (-0.44)	0.037 (-0.737)	0.091 (-0.635)	0.908 (-0.049)	0.132 (0.58)	0.101 (0.619)		
Chlorophyll a	0.784 (-0.116)	0.953 (0.025)	0.16 (0.547)	0.282 (0.435)	0.048 (0.711)	0.001 (-0.923)	0.644 (0.195)	0.006 (0.859)	0.195 (0.512)	NA	NA	0.009 (-0.838)	0.584 (-0.23)	0.422 (-0.332)	0.23 (0.479)	0.275 (0.44)	0.992 (-0.004)	0.484 (-0.291)	0.005 (-0.867)	0.024 (-0.774)	0.663 (-0.184)	0.372 (0.367)	0.238 (0.472)	0.012 (0.826)	
Secchi Depth	0.252 (-0.459)	0.411 (-0.339)	0.533 (0.261)	0.036 (0.739)	0.135 (0.576)	0.066 (-0.675)	0.932 (-0.037)	0.228 (0.481)	0.446 (0.316)	NA	NA	0.024 (-0.774)	0.076 (-0.659)	0.741 (-0.14)	0.942 (-0.031)	0.686 (0.171)	0.198 (0.509)	0.692 (0.168)	0.12 (-0.594)	0.143 (-0.566)	0.248 (-0.463)	0.221 (0.487)	0.869 (0.07)	0.063 (0.681)	0.073 (0.663)

Appendix H: P-values and Pearson correlation coefficient at 4.25m

The first values in the table are the p-values, where significance ($p < 0.05$) is highlighted in green. The correlation coefficient is presented between parentheses.

4.25m	CDOM1	CDOM2	CDOM3	CDOM4	Total CDOM	DOC (Dis)	Air temp	Precipitation	Water temp	O ₂ (%)	O ₂ (mg/L)	pH	P (Dis)	P (Tot)	Fe	Mn	SO ₄ ²⁻	S	NH ₄ ⁺ (Dis)	N (Tot)	Al	Cl- (Dis)	Conductivity	Bacteria	Chlorophyll a
CDOM2	0.168 (0.539)																								
CDOM3	0.1 (0.621)	0.859 (0.076)																							
CDOM4	0.25 (-0.462)	0.058 (-0.691)	0.665 (0.183)																						
CDOM SUM	0.578 (0.233)	0.865 (-0.072)	0.028 (0.761)	0.073 (0.663)																					
DOC (Dis)	0.159 (0.549)	0.861 (-0.075)	0.478 (0.295)	0.292 (-0.426)	0.549 (-0.251)																				
Air temp	0.256 (-0.456)	0.412 (-0.338)	0.641 (-0.196)	0.295 (0.425)	0.817 (0.098)	0.27 (-0.444)																			
Precipitation	0.122 (0.592)	0.737 (0.142)	0.099 (0.622)	0.44 (0.32)	0.032 (0.751)	0.966 (-0.018)	0.979 (-0.011)																		
Water temp	0.015 (0.811)	0.619 (0.209)	0.072 (0.665)	0.997 (0.002)	0.187 (0.52)	0.532 (0.261)	0.324 (-0.402)	0.036 (0.741)																	
O ₂ (%)	NA																								
O ₂ (mg/L)	NA																								
pH	0.571 (0.238)	0.05 (0.707)	0.664 (-0.183)	0.009 (-0.841)	0.179 (-0.527)	0.591 (0.226)	0.169 (-0.538)	0.196 (-0.511)	0.734 (-0.144)	NA	NA														
P (Dis)	0.184 (-0.523)	0.935 (0.035)	0.015 (-0.811)	0.505 (-0.278)	0.053 (-0.7)	0.978 (-0.012)	0.911 (0.048)	0.082 (-0.649)	0.016 (-0.807)	NA	NA	0.358 (0.376)													
P (Tot)	0.721 (0.151)	0.276 (0.439)	0.257 (-0.456)	0.049 (-0.709)	0.07 (-0.669)	0.707 (0.159)	0.142 (-0.568)	0.581 (-0.232)	0.881 (-0.064)	NA	NA	0.164 (0.543)	0.343 (0.387)												
Fe	0.166 (0.541)	0.993 (0.004)	0.001 (0.921)	0.361 (0.374)	0.005 (0.867)	0.845 (0.083)	0.971 (0.015)	0.834 (0.834)	0.067 (0.674)	NA	NA	0.24 (-0.47)	0.009 (-0.842)	0.226 (-0.482)											
Mn	0.313 (0.41)	0.784 (-0.116)	0.121 (0.593)	0.195 (0.511)	0.024 (0.773)	0.821 (-0.096)	0.768 (-0.125)	0.039 (0.732)	0.009 (0.838)	NA	NA	0.231 (-0.478)	0.018 (-0.795)	0.279 (-0.437)	0.062 (0.683)										
SO ₄ ²⁻	0.06 (-0.687)	0.941 (-0.031)	0 (-0.975)	0.668 (-0.181)	0.038 (-0.734)	0.42 (-0.333)	0.672 (0.178)	0.043 (-0.722)	0.028 (-0.762)	NA	NA	0.489 (0.288)	0.005 (0.867)	0.338 (0.391)	0 (-0.948)	0.077 (-0.656)									
S	0.036 (-0.741)	0.832 (-0.09)	0 (-0.965)	0.773 (-0.122)	0.049 (-0.708)	0.363 (-0.373)	0.583 (0.23)	0.034 (-0.745)	0.022 (-0.781)	NA	NA	0.558 (0.245)	0.01 (0.835)	0.427 (0.328)	0.001 (-0.938)	0.087 (-0.64)	0 (0.995)								
NH ₄ ⁺ (Dis)	0.147 (-0.562)	0.977 (-0.012)	0.13 (-0.582)	0.367 (-0.37)	0.047 (-0.713)	0.945 (-0.03)	0.547 (0.252)	0.013 (-0.817)	0.002 (-0.903)	NA	NA	0.326 (0.4)	0.04 (0.73)	0.507 (0.276)	0.064 (-0.678)	0 (-0.966)	0.071 (0.666)	0.067 (0.674)							
N (Tot)	0.167 (-0.54)	0.995 (-0.003)	0.175 (-0.532)	0.399 (-0.347)	0.075 (-0.66)	0.942 (-0.031)	0.511 (0.274)	0.034 (-0.744)	0.002 (-0.899)	NA	NA	0.393 (0.352)	0.049 (0.709)	0.519 (0.269)	0.112 (-0.605)	0 (-0.969)	0.106 (0.612)	0.103 (0.618)	0 (0.992)						
Al	0.178 (0.529)	0.724 (-0.15)	0.151 (0.558)	0.663 (0.184)	0.285 (0.432)	0.649 (0.192)	0.686 (0.171)	0.195 (0.512)	0.03 (0.756)	NA	NA	0.339 (-0.39)	0.013 (-0.818)	0.249 (-0.462)	0.125 (0.588)	0.041 (0.727)	0.076 (-0.659)	0.093 (-0.631)	0.067 (-0.674)	0.059 (-0.689)					
Cl- (Dis)	0.28 (0.436)	0.357 (-0.377)	0.199 (0.507)	0.581 (0.232)	0.426 (0.329)	0.042 (0.726)	0.546 (-0.253)	0.242 (0.468)	0.28 (0.436)	NA	NA	0.362 (-0.374)	0.551 (-0.249)	0.553 (-0.248)	0.225 (0.483)	0.358 (0.376)	0.14 (-0.57)	0.12 (-0.594)	0.236 (-0.473)	0.28 (-0.437)	0.428 (0.328)				
Conductivity	0.5 (0.281)	0.589 (0.227)	0.019 (0.792)	0.573 (0.237)	0.032 (0.75)	0.551 (-0.249)	0.922 (0.042)	0.199 (0.507)	0.395 (0.35)	NA	NA	0.695 (-0.166)	0.053 (-0.701)	0.363 (-0.373)	0.015 (0.81)	0.352 (0.381)	0.04 (-0.729)	0.052 (-0.702)	0.451 (-0.312)	0.559 (-0.245)	0.53 (0.263)	0.947 (-0.029)			
Bacteria	0.833 (-0.09)	0.354 (-0.38)	0.4 (0.347)	0.018 (0.795)	0.035 (0.741)	0.763 (-0.128)	0.948 (0.028)	0.253 (0.459)	0.579 (0.233)	NA	NA	0.17 (-0.537)	0.618 (-0.21)	0.087 (-0.64)	0.291 (0.427)	0.096 (0.628)	0.456 (-0.309)	0.481 (-0.293)	0.125 (-0.589)	0.138 (-0.573)	0.737 (0.142)	0.196 (0.511)	0.688 (0.169)		
Chlorophyll a	0.747 (0.137)	0.987 (0.007)	0.489 (0.288)	0.103 (0.618)	0.027 (0.764)	0.202 (-0.505)	0.772 (0.123)	0.018 (0.796)	0.178 (0.528)	NA	NA	0.128 (-0.584)	0.22 (-0.488)	0.42 (-0.333)	0.156 (0.552)	0.018 (0.798)	0.394 (-0.351)	0.4 (-0.347)	0.019 (-0.794)	0.028 (-0.761)	0.389 (0.355)	0.778 (0.12)	0.382 (0.359)	0.077 (0.656)	
Secchi Depth	0.592 (-0.225)	0.542 (-0.255)	0.971 (0.015)	0.04 (0.729)	0.141 (0.569)	0.17 (-0.537)	0.932 (-0.037)	0.228 (0.481)	0.529 (0.263)	NA	NA	0.147 (-0.562)	0.61 (-0.214)	0.649 (-0.192)	0.563 (0.242)	0.087 (0.64)	0.899 (-0.054)	0.922 (-0.042)	0.108 (-0.611)	0.116 (-0.6)	0.938 (0.033)	0.835 (0.088)	0.798 (0.109)	0.043 (0.723)	0.007 (0.857)

Appendix I: P-values and Pearson correlation coefficient at 4.75m

The first values in the table are the p-values, where significance ($p < 0.05$) is highlighted in green. The correlation coefficient is presented between parentheses.

4.75m	CDOM1	CDOM2	CDOM3	CDOM4	Total CDOM	DOC (Dis)	Air temp	Precipitation	Water temp	O ₂ (%)	O ₂ (mg/L)	pH	P (Dis)	P (Tot)	Fe	Mn	SO ₄ ²⁻	S	NH ₄ ⁺ (Dis)	N (Tot)	Al	Cl- (Dis)	Conductivity	Bacteria	Chlorophyll a
CDOM2	NA																								
CDOM3	NA	NA																							
CDOM4	NA	NA	NA																						
CDOM SUM	NA	NA	NA	NA																					
DOC (Dis)	NA	NA	NA	NA	NA																				
Air temp	NA	NA	NA	NA	NA	0.903 (-0.076)																			
Precipitation	NA	NA	NA	NA	NA	0.878 (-0.096)	0.373 (-0.516)																		
Water temp	NA	NA	NA	NA	NA	0.062 (0.859)	0.516 (-0.391)	0.571 (0.344)																	
O ₂ (%)	NA	NA	NA	NA	NA	NA	NA	NA	NA	NA	NA	NA	NA	NA	NA	NA	NA	NA	NA	NA	NA	NA	NA	NA	NA
O ₂ (mg/L)	NA	NA	NA	NA	NA	NA	NA	NA	NA	NA	NA	NA	NA	NA	NA	NA	NA	NA	NA	NA	NA	NA	NA	NA	NA
pH	NA	NA	NA	NA	NA	0.636 (0.29)	0.157 (0.735)	0.96 (0.031)	0.86 (0.11)	NA	NA	NA	NA	NA	NA	NA	NA	NA	NA	NA	NA	NA	NA	NA	NA
P (Dis)	NA	NA	NA	NA	NA	0.103 (0.802)	0.895 (0.082)	0.69 (0.246)	0.19 (0.698)	NA	NA	0.216 (0.67)													
P (Tot)	NA	NA	NA	NA	NA	0.194 (0.693)	0.78 (0.174)	0.938 (0.048)	0.453 (0.445)	NA	NA	0.227 (0.658)	0.022 (0.93)												
Fe	NA	NA	NA	NA	NA	0.04 (0.895)	0.384 (-0.507)	0.734 (0.21)	0.017 (0.94)	NA	NA	0.953 (-0.037)	0.204 (0.683)	0.361 (0.528)											
Mn	NA	NA	NA	NA	NA	0.401 (0.491)	0.957 (0.034)	0.932 (-0.054)	0.254 (0.631)	NA	NA	0.962 (0.03)	0.837 (0.129)	0.778 (-0.176)	0.47 (0.43)										
SO ₄ ²⁻	NA	NA	NA	NA	NA	0.063 (-0.857)	0.378 (0.512)	0.582 (-0.335)	0.003 (-0.981)	NA	NA	0.995 (0.004)	0.208 (-0.679)	0.427 (-0.468)	0.003 (-0.983)	0.376 (-0.514)									
S	NA	NA	NA	NA	NA	0.148 (-0.745)	0.358 (0.53)	0.472 (-0.428)	0.004 (-0.977)	NA	NA	0.921 (0.062)	0.34 (-0.547)	0.667 (-0.265)	0.034 (-0.907)	0.228 (-0.657)	0.008 (0.964)								
NH ₄ ⁺ (Dis)	NA	NA	NA	NA	NA	0.72 (-0.222)	0.674 (0.259)	0.356 (-0.532)	0.259 (-0.626)	NA	NA	0.975 (0.02)	0.86 (-0.111)	0.671 (0.262)	0.549 (-0.362)	0.102 (-0.803)	0.375 (0.515)	0.171 (0.719)							
N (Tot)	NA	NA	NA	NA	NA	0.898 (-0.08)	0.896 (0.082)	0.548 (-0.363)	0.452 (-0.445)	NA	NA	0.976 (0.019)	0.911 (0.07)	0.476 (0.424)	0.802 (-0.156)	0.074 (-0.841)	0.612 (0.31)	0.345 (0.543)	0.008 (0.963)						
Al	NA	NA	NA	NA	NA	0.1 (0.806)	0.47 (-0.429)	0.752 (0.196)	0.166 (0.725)	NA	NA	0.87 (0.102)	0.111 (0.791)	0.116 (0.784)	0.049 (0.88)	0.974 (-0.02)	0.093 (-0.815)	0.245 (-0.64)	0.941 (0.046)	0.643 (0.284)					
Cl- (Dis)	NA	NA	NA	NA	NA	0.429 (0.466)	0.52 (-0.387)	0.746 (0.201)	0.15 (0.743)	NA	NA	0.664 (-0.267)	0.893 (0.084)	0.694 (-0.243)	0.29 (0.595)	0.033 (-0.908)	0.205 (-0.682)	0.083 (-0.829)	0.055 (-0.871)	0.081 (-0.831)	0.815 (0.146)				
Conductivity	NA	NA	NA	NA	NA	0.964 (0.028)	0.343 (0.545)	0.53 (-0.378)	0.508 (-0.398)	NA	NA	0.34 (0.547)	0.584 (0.333)	0.25 (0.634)	0.695 (-0.242)	0.216 (-0.67)	0.557 (0.355)	0.316 (0.57)	0.074 (0.842)	0.077 (0.837)	0.764 (0.187)	0.063 (-0.858)			
Bacteria	NA	NA	NA	NA	NA	0.201 (-0.686)	0.243 (-0.642)	0.423 (0.471)	0.629 (-0.296)	NA	NA	0.147 (-0.747)	0.191 (-0.697)	0.145 (-0.749)	0.625 (-0.299)	0.737 (-0.208)	0.699 (0.239)	0.882 (0.093)	0.742 (-0.204)	0.744 (-0.202)	0.523 (-0.384)	0.881 (0.094)	0.31 (-0.576)		
Chlorophyll a	NA	NA	NA	NA	NA	0.653 (-0.276)	0.59 (0.328)	0.883 (-0.092)	0.886 (-0.09)	NA	NA	0.981 (-0.015)	0.436 (-0.46)	0.21 (-0.676)	0.554 (-0.358)	0.209 (0.677)	0.696 (0.241)	0.99 (0.008)	0.268 (-0.616)	0.1 (-0.805)	0.15 (-0.743)	0.389 (0.502)	0.286 (-0.598)	0.793 (0.163)	
Secchi Depth	NA	NA	NA	NA	NA	0.26 (-0.625)	0.973 (-0.021)	0.961 (0.031)	0.576 (-0.34)	NA	NA	0.456 (-0.442)	0.098 (-0.809)	0.012 (-0.954)	0.372 (-0.518)	0.556 (0.357)	0.485 (0.417)	0.777 (0.176)	0.439(-0.457)	0.253 (-0.632)	0.078 (-0.836)	0.56 (0.353)	0.198 (-0.689)	0.254 (0.631)	0.068 (0.851)



Norges miljø- og biovitenskapelige universitet
Noregs miljø- og biovitenskapelige universitet
Norwegian University of Life Sciences

Postboks 5003
NO-1432 Ås
Norway